NBSIR 79-1759

Low Velocity Performance of Anemometers

L P Purtell

National Bureau of Standards
Fluid Engineering Division
Washington, D.C. 20234

May 1979

Final Report

on
Contract No. H0166198
Evaluation of the Behavior of Mine Anemometers in the NBS Low Velocity Calibration Facility

Prepared for

United States Department of the Interior
Bureau of Mines

NBS-114A (REV. 9-78)

U.S. DEPT. OF COMM. BIBLIOGRAPHIC DATA SHEET	1. PUBLICATION OR REPORT NO. NBSIR 79-1759	2. Gov't. Accession No.	3. Recipient's Accession No.

4. TITLE AND SUBTITLE

LOW VELOCITY PERFORMANCE OF ANEMOMETERS

5. Publication Date
May 1979

6. Performing Organization Code

7. AUTHOR(S)
L. P. Purtell

8. Performing Organ. Report No.
NBSIR 79-1759

9. PERFORMING ORGANIZATION NAME AND ADDRESS

NATIONAL BUREAU OF STANDARDS
DEPARTMENT OF COMMERCE
WASHINGTON, DC 20234

10. Project/Task/Work Unit No.

11. Contract/Grant No.
H0166198

12. SPONSORING ORGANIZATION NAME AND COMPLETE ADDRESS *(Street, City, State, ZIP)*
Office of the Assistant Director - Mining
Bureau of Mines
United States Department of the Interior
Washington, D. C. 20241

13. Type of Report & Period Covered
-Final-
Dec.1,1976--Nov.30,1978

14. Sponsoring Agency Code

15. SUPPLEMENTARY NOTES

☐ Document describes a computer program; SF-185, FIPS Software Summary, is attached.

16. ABSTRACT *(A 200-word or less factual summary of most significant information. If document includes a significant bibliography or literature survey, mention it here.)*

The performance of ten anemometers of several types has been measured at low air speeds. Multiple calibration runs provided sufficient data for measuring random error about the mean calibration curve in addition to the difference between indicated and true speeds. Measurements were also performed of the minimum operating speeds of the anemometers.

17. KEY WORDS *(six to twelve entries; alphabetical order; capitalize only the first letter of the first key word unless a proper name; separated by semicolons)*

Airflow; anemometer; laser velocimeter; low velocity; mine ventilation; wind tunnel.

18. AVAILABILITY ☐ Unlimited

☒ For Official Distribution. Do Not Release to NTIS

☐ Order From Sup. of Doc., U.S. Government Printing Office, Washington, DC 20402, SD Stock No. SN003-003-

☐ Order From National Technical Information Service (NTIS), Springfield, VA. 22161

19. SECURITY CLASS (THIS REPORT)	21. NO. OF PRINTED PAGES
UNCLASSIFIED	
20. SECURITY CLASS (THIS PAGE)	**22. Price**
UNCLASSIFIED	

USCOMM-DC

- FOREWORD -

This report was prepared by the National Bureau of Standards, Fluid Engineering Division, Washington, D. C. 20234, under USBM Contract Number H0166198. The contract was initiated under the Coal Mine Health and Safety Program. It was administered under the technical direction of PM&SRC, with Dr. George H. Schnakenberg, Jr., acting as the Technical Project Officer. Mr. H. R. Eveland was the contract administrator for the Bureau of Mines. This report is a summary of the work recently completed as part of this contract during the period December 1, 1976, and November 30, 1978. This report was submitted by the author May 1979.

NBSIR 79-1759

LOW VELOCITY PERFORMANCE OF ANEMOMETERS

L. P. Purtell

Fluid Engineering Division
Center for Mechanical Engineering
and Process Technology
National Engineering Laboratory
National Bureau of Standards
Washington, D.C. 20234

May 1979

Final Report

Prepared for
United States Department of the Interior
Bureau of Mines

U.S. DEPARTMENT OF COMMERCE, Juanita M. Kreps, *Secretary*

Jordan J. Baruch, *Assistant Secretary for Science and Technology*

NATIONAL BUREAU OF STANDARDS, Ernest Ambler, *Director*

NOMENCLATURE

U	velocity measured by laser velocimeter standard
U_i	velocity indicated by anemometer under test
f	frequency output from (vortex-shedding) anemometer under test (Hz)
I	current output from (heated foil) anemometer under test (μA)
U_{if}	line segments fitted to (U,U_i), (U,f), or (U,I) data
$\overline{U}$	group mean true velocity
$\overline{U}_i$	group mean indicated velocity
$\overline{f}$	group mean indicated frequency
$\overline{I}$	group mean indicated current
σ_i	standard deviation of U_i data about U_{if}
σ_f	standard deviation of f data about U_{if}
σ_I	standard deviation of I data about U_{if}
σ	σ_i, σ_f, or σ_I divided by dU_{if}/dU
σ_c	σ corrected for known variance in laser velocimeter measurements
R_i	resolution of the instrument under test
R	resolution expressed as true velocity

LOW VELOCITY PERFORMANCE OF ANEMOMETERS

1. INTRODUCTION

The National Bureau of Standards in order to meet the need for a calibration capability with adequate accuracy at low air velocities, i.e., below 2.5 meters per second, undertook the development of a low-velocity calibration facility for wind speed measuring instruments which would provide a capability down to 0.05 meters per second (approximately 10 feet per minute) with an accuracy of plus or minus one percent. It was a natural consequence therefore that when said facility became operational to undertake an evaluation of the state-of-the-art and to provide the information needed as to the reliability and performance of instrumentation for such measurement. Thus various types of instruments for low velocity air measurement have undergone testing at NBS. This report summarizes the results and presents analyses of the instruments' performance.

Performance is measured in terms of a comparison between indicated and true air speed, the variation in repeated measurements, and the minimum operating air speed. Since the indicated air speed may be easily corrected using a chart, for instance, to find the true air speed, the latter two measurements of performance are of primary interest. Thus a detailed handling of random error is presented including the effect of instrument resolution where necessary.

2. THE FACILITY

The data reported here were measured in the Low Velocity Air-flow Facility [1] at the National Bureau of Standards. The facility consists primarily of a low velocity wind tunnel and a laser velocimeter velocity standard. The wind tunnel (Figure 1) is an open return type with the fan pulling the air through the tunnel.

The test section, 6.1 m in length and nominally 0.91 m by 0.91 m in cross-section, is constructed of acrylic panels mounted in a steel frame. The test section is supported from above by I-beams to allow the laser velocimeter traversing gear, mounted on rails on the floor of the room parallel to the test section, to be positioned at any location along the length of the test section.

The performance of the wind tunnel in terms of steadiness, flatness of mean velocity profiles, and turbulence level is extremely satisfactory. No drift in air velocity during a test was detected. The mean velocity profiles outside of the wall boundary layers are flat to within 0.5% even as close as 1 meter from the entrance to the test section. The residual turbulence intensity is less than 0.05%.

A laser velocimeter is used as the velocity standard. It is linear with velocity from first principles and does not suffer a

severe loss of resolution at very low velocities as does, for instance, the Pitot-static tube. Furthermore, it is nonintrusive and has good spatial resolution. Adequate sensitivity is obtained in the facility without the artificial seeding of scattering particles. Thus the difficulties and inconvenience associated with seeding and the possible effect of such seeding on the performance of the device under test are avoided.

3. THE INSTRUMENTS

Instrument A -- Bronze bearing vane anemometer.

All of the vane anemometers tested have flat vanes without camber or twist as opposed to helicoidal types. All but one (instrument E below) are entirely mechanical and require only a timer (stopwatch) for operation.

Instrument A is a commercially available instrument (Davis Instrument Manufacturing Company, Incorporated, 4-Inch Low Speed Anemometer, S/N 22889).[1] It was supplied for test by the U. S. Mining Enforcement and Safety Administration (MESA) at the request of the U. S. Bureau of Mines. The housing is 4 inches (10.2 cm) in diameter and 1-3/4 inches (4.4 cm) deep (Figure 2). Thin metal vanes without camber or twist mounted on arms drive a rotor linked to a dial indicator by a gear train. The bearings in this particular instrument are standard bronze bearings (as opposed to ball bearings). One revolution on the dial represents an indicated passage of 100 feet of air through the instrument. Thus an external timer (not a part of the anemometer) is required to complete a measurement of velocity (an average velocity for the duration of the measurement).

Instrument B -- Ball bearing vane anemometer.

This anemometer is a commercially available instrument (Davis Instrument Manufacturing Company, Incorporated, 4-Inch Low Speed Anemometer, S/N 24323 B). It was supplied for test by the U. S. Mining Enforcement and Safety Administration (MESA) at the request of the U. S. Bureau of Mines. As may be seen in Figure 3, it is identical to instrument A except that the bearings are ball bearings instead of bronze bearings.

Instrument C -- Jewel bearing vane anemometer.

This anemometer is a commercially available instrument (Sybron/ Taylor Corporation, 4-Inch Anemometer, S/N H873). It was supplied for test by the U. S. Mining Enforcement and Safety Administration (MESA) at the request of the U. S. Bureau of Mines. It is very

[1]These particular instruments were selected as being representative of the type of anemometer and their selection does not represent an endorsement.

similar in appearance (Figure 4) to instruments A and B though the dimensions of the hub and shroud are slightly different. The bearings, however, are jewel instead of bronze or ball bearing.

Instrument D — High speed vane anemometer.

This anemometer is a commercially available instrument (Davis Instrument Manufacturing Company, Incorporated, 4-Inch High Speed Anemometer, S/N 31125B). It was supplied for test by the U. S. Mining Enforcement and Safety Administration (MESA) at the request of the U. S. Bureau of Mines. This anemometer (Figure 5) is dimensionally identical to instrument B, including ball bearings, but has four vanes instead of eight, thus permitting operation at higher air speeds.

Instrument E — Magnetic pick-up vane anemometer.

This anemometer is a commercially available instrument (Abbirko Instruments, Limited, Flowmaster, S/N 6184). It was supplied for test by the U. S. Mining Enforcement and Safety Administration at the request of the U. S. Bureau of Mines. The instrument's vane housing is approximately 2.75 inches (7.0 cm) in diameter (see Figure 6) with an attached block for the magnetic pick-up, or proximity transducer, and a handle projecting down from the block. The magnetic pick-up detects the passage of the metal vanes, and the resulting electrical signal is converted to a deflection of a meter connected to the probe by a cable. The meter was located outside the tunnel during the tests and was oriented horizontally. Three ranges of operation are selectable: low - 0 to 300 fpm, medium - 0 to 1000 fpm, and high - 0 to 3000 fpm. The anemometer requires a 9 volt battery for operation.

Instrument F — Full size impact-deflection anemometer.

This type of anemometer operates from the dynamic pressure of the air stream. This pressure is converted to a deflection of a dial indicator by impacting a small vane linked to the meter. The operation is thus entirely mechanical.

Instrument F is a commercially available instrument (Alnor Instrument Company, Velometer, Series 6000-P). It was supplied for test by the U. S. Mining Enforcement and Safety Administration at the request of the U. S. Bureau of Mines. The instrument (Figure 7) consists of a main body meter (approximately 15 x 17 x 6 cm) with connections for one of several probes. The Pitot probe is composed of a cylinder 0.5 inches (1.27 cm) in diameter and 13 inches (33 cm) long which mounts in a range selector unit connected to the main body by hoses. The cylinder has ports to admit the airflow and must be properly oriented in the airstream to obtain a reading. The range selector may be set to one of two ranges, 100-1250 fpm (low range) and 100-2500 fpm (high range). Other range selectors are available,

but were not tested herein.

The diffuser probe (Figure 8) is similar to the Pitot probe except that only impact pressure is utilized in the diffuser probe thus requiring a vent to be opened in the range selector for operation. It operates over the same ranges as the Pitot probe.

The low velocity probe (Figure 9) attaches directly to the main body and operates like the Pitot probe except over a range of 30-300 fpm. Note that all the probes and the main body were mounted entirely within the wind tunnel since the flow is slightly below atmospheric pressure.

Instrument G -- Compact impact-defection anemometer.

This anemometer is a commercially available instrument (Alnor Instrument Company, Velometer Jr., Type 8100). It was supplied for test by the U. S. Mining Enforcement and Safety Administration at the request of the U. S. Bureau of Mines. The instrument is approximately 8.2 x 10.2 x 3.8 cm in size (see Figure 10) and contains entrance and exit ports for the air on the upstream and downstream surfaces, respectively. The entrance port is adjustable (two sizes) providing two ranges of velocity measurement, 50 to 200 fpm and 100 to 800 fpm. The instrument is a one piece, self-contained unit.

Instruments H and I -- Vortex-Shedding Anemometers.

This type of instrument measures velocity by detecting the frequency of a vortex street shed from a bluff, two-dimensional object such as a cylinder. This frequency will be well-defined if the shedding body is properly matched to the air speed.

These anemometers (two units, serial numbers 49 and 48, respectively, are commercially available instruments (J-TEC Associates, Incorporated, VA-216 Air Draft Sensor)[1] supplied for test by the U. S. Bureau of Mines. The instruments are approximately 30 x 10 x 14 cm in size (see Figure 11) and include probe heads and the necessary electronics for operation. The probe head consists of a rod approximately 6.4 mm in diameter and 35 mm in length supported at the ends and oriented normal to the air stream. An ultrasonic transmitter and receiver pair located downstream of the cylinder detect the vortex street shed by the cylinder as an amplitude modulation of the ultrasonic signal. This modulation is converted by the electronics section to a pulse train (approximately a square wave signal) as an output. A frequency-to-voltage converter section also provides an analog output. Since the frequency of shedding of a vortex street is roughly proportional to velocity, the output signals can be used to measure the air velocity. A separate power supply is necessary to operate the instrument.

Instrument J -- Heated foil anemometer.

This anemometer is a prototype instrument (Thermogage, Inc.,

Air Velocity Meter) supplied for test by the U. S. Bureau of Mines. It consists of a tube approximately 9.5 mm in diameter and 10.2 cm in length aligned with the flow, and a 15.9 mm diameter handle attached normal to the tube midway along its length (see Figure 12). A part of the wall of the tube is composed of a heat-conducting foil which has an electrically heated spot flanked upstream and downstream by temperature sensors. As air passes through the tube, the upstream sensor experiences a lower temperature than the downstream sensor, and this difference, converted to an electrical signal, is related to velocity. The instrument thus consists of this thermal transducer and an electronics module containing a line-voltage operated power supply, the necessary circuitry, and a micro-ammeter.

4. THE TESTS

4.1 General Description

Many types of tests can be performed on various aspects of an instrument's performance, such as its response to turbulent flow, shock and vibration, dirt, moisture, or orientation to velocity and gravity vectors, but the results of such tests require comparison with a base level of performance. This base level should be obtained under conditions closely approximating the ideal environment, which, in the case of anemometers is a steady, uniform flow field of large dimensions. The Low Velocity Airflow Facility has been found to provide a good approximation to these conditions for the instruments reported on here.

The performance is measured in terms of the mean error, the random error, and minimum operating air speed. The mean error, for the purposes of this report, is defined simply to be the mean difference between the air speed indicated by the anemometer under test and the air speed indicated by the velocity standard. Random error is defined as usual in terms of a root-mean-square deviation of the indicated air speed from an appropriate mean value (see section 5 for more details). To permit evaluation of these characteristics, multiple calibration tests and minimum operating speed determinations were performed.

4.2 Calibration tests

These tests consisted of measuring the response of the anemometer undergoing testing to an air flow of a speed measured by the laser velocimeter velocity standard. (See tables A-1 through J-5). Each instrument was tested at a number of air speeds over the range of operation below about 4 m/s. Five such tests were conducted for each instrument with an attempt made to repeat the air speeds for each test. (The effects of <u>not</u> exactly repeating the air speeds are discussed in the analysis of section 5). The particular test set-up for the calibrations varied somewhat from instrument to instrument, but in general consisted of mounting the anemometer on or near the centerline of the test-section, 1 m from its upstream end, locating the laser velocimeter probe volume at a position where disturbance of the flow due to the presence of the anemometer is negligible, and measuring the air speed with both the

anemometer under test and the laser velocimeter standard. The details which varied from instrument to instrument are described in the following paragraphs.

Four of the vane anemometers, A, B, C, and D, are so similar in dimension and function that the tests were nearly identical for them. The location of the probe volume (30 cm upstream of the anemometer) was the same for each and was determined from a series of velocity measurements upstream of instrument A. These are presented in Figure 13 as the ratio of the local velocity to the freestream velocity. These measurements were performed at two freestream speeds, 3.6 and 0.36 m/s to verify independence of freestream speed as predicted by potential flow theory. With no anemometer in the tunnel, variation in velocity along the centerline is imperceptible over the distance traversed.

The same four anemometers, A, B, C, and D, also require a timer to determine the indicated airspeed. This was computed from initial and final readings of the dial and of the associated time interval (around two minutes). The anemometer runs continuously in the tunnel since it cannot be accessed while the tunnel is in operation without disturbing the flow. Thus the readings of the anemometer were performed with the anemometer in operation. The laser velocimeter measurement of the air velocity was performed during the time interval for reading the vane anemometer.

The remaining vane anemometer, instrument E, has an electronic read-out, thus not requiring a separate time measurement. It is smaller in dimension than A through D and will disturb the airflow less. Consequently the probe volume could be located as for instruments A through D. As with the others, the laser velocimeter measurement of the air velocity was performed during the time interval for reading the vane anemometer.

The full size impact deflection anemometer, instrument F, has three velocity probes which were tested on all ranges. The Pitot probe and diffuser probes are essentially slender (1.27 cm diameter) cylinders presenting little disturbance to the flow. Thus they were tested with the probe volume located 30 cm upstream of the probe as with the vane anemometers. The meter body and hoses were located downstream of the probes. The low velocity probe, however, attaches directly to the meter body rather than by hoses, thus requiring the meter body and probe to be placed together at the calibration position. Thus the velocity upstream of this combination was measured to again find a location for the probe volume. However, 30 cm upstream was found to be quite sufficient (Figure 14).

The velocity upstream of the compact impact-deflection anemometer, instrument G, was also measured to find a location for the probe volume, and again 30 cm was found to be sufficient.

The vortex-shedding anemometers, instruments H and I, are larger than the others and disturb the flow proportionately more. However, it was found that by placing the measuring head on the centerline (thus with the bulk of the instrument off the centerline) that the laser velocimeter probe volume could be located 35 cm upstream of the instruments. Since the outputs of H and I are an analog voltage and a pulse train, separate instrumentation consisting of a digital volt meter and a frequency counter were required for the tests. These measurements were recorded during the time interval required for measurement by the laser velocimeter standard.

The remaining instrument, the heated foil anemometer, instrument J, has a very small probe head and was thus tested with the probe volume again at 30 cm upstream. The output is an analog meter reading in microamps.

4.3 Minimum Operating Speed

Determination of the minimum air speed at which operation of an instrument is possible varies with the type of instrument under test. The instruments may be separated into two categories for this purpose: instruments that entirely cease to function below some speed, and instruments that lose sufficient resolution in their output (or read zero) below some speed.

The vane anemometers, A through E, all fit in the first category, but here two minimum operating speeds may be defined, a starting speed, the speed at which the instrument starts from rest as the air speed is slowly increased, and a stopping speed, the speed at which the anemometer ceases to turn as the air speed is slowly decreased.

To determine the starting speeds of the instruments, the velocity in the tunnel was increased from below the starting speed at a smooth acceleration of approximately 0.15 m/s/min until movement of the vanes could be detected by eye. At that moment the air velocity would be fixed and the laser velocimeter measurements initiated. If the anemometer continued rotating for at least thirty seconds and did not decelerate, the measurement of velocity by the laser velocimeter was recorded as the starting speed.

Because of the anemometer's angular momentum, stopping speed is more difficult to determine than starting speed. Some preliminary runs indicated that a two minute interval between reductions in air velocity of approximately 1 cm/s was sufficient for the anemometer to come to rest if the stopping speed had been reached.

The only other instruments having minimum speeds of functioning are the vortex-shedding anemometers, instruments H and I. As the air speed is reduced the depth of modulation of the ultrasonic signal is reduced until at some speed it can no longer be detected by the instruments.

Since neither friction nor angular momentum is involved, as opposed to the vane anemometers, the minimum operating speed was easily determined by simply observing the pulse train from the instruments as the air speed was slowly reduced. When the pulses disappeared (which occurred rather abruptly) the air speed was recorded as the minimum operating speed.

The other instruments, the impact pressure anemometers, F and G, and the heated foil anemometer, J, all fit in the second category of instruments which lose sufficient resolution below some speed. This minimum operating speed is defined here to be that at which the anemometer under test indicates a speed of one-half the lowest marked division on the dial above zero. This was chosen because at that indicated speed the resolution is at least as large as the reading.

5. RESULTS AND DISCUSSION

5.1 Methods of data analysis

As may be observed in Figures 16 through 32, the data for the calibration curves are in groups because of attempts to repeat the true air speeds from run to run. The mean calibration data are defined to be the pairs of values consisting of the mean true velocity for a group and the mean indicated velocity (or frequency, etc.) of that group. Plots of these pairs (connected by solid lines in Figures 16 through 32), give an indication of linearity of the instrument's response and serve in determining the random error of that response. Furthermore, the mean data may be used to define calibration curves for correcting an indicated reading in the field. Figures 33 through 59 (odd numbered) are especially valuable in this respect.

Random error is frequently defined as the standard deviation (about the mean) of repeated measurements. This is only useful, however, if the true or reference value is fixed or has negligible variation from measurement to measurement. Precise repetition of wind tunnel speeds, though, is extremely difficult at the low speeds required for these tests. The random error here, then is defined in terms of the root-mean-square deviation of the data in a group from an appropriate curve through that group. This is illustrated in Figure 15 where $\bar{U}$ is the group mean true velocity and $\bar{U}_i$ is the group mean indicated velocity. An ideal calibration curve, $U_i(U)$, is approximated within the group by a straight line segment, U_{if}, passing through $(\bar{U},\bar{U}_i)$. The root-mean-square deviation, curve, $\tilde{U}_i(U)$, is approximated within the group by a straight line segment, U'_{if}, passing through $(\bar{U},\bar{U}_i)$. The root-mean-square deviation, σ_i, of the data, (U_r,U_{ir}) from $\tilde{U}_i(U)$ is thus approximated by the root-mean-square deviation from the line segment, U_{if}. More specifically:

$$\sigma_i^2 \simeq \frac{1}{N} \sum_{r=1}^{N} [U_{ir} - U_{if}(U_{ir})]^2$$

The slope of the line segment, U_{if}, is computed as the average of the slopes of line segments connecting the $(\bar{U},\bar{U}_i)$ of interest with the $(\bar{U},\bar{U}_i)$'s of the neighboring group(s).

The standard deviation, σ_i, is a measure of the scatter in the data in terms of indicated air speed (or frequency, etc., depending on the measurement). To compare instruments, however, this must be converted to an equivalent scatter in true air speed. An approach consistent with the above approximations for σ_i is to divide σ_i by the local slope of U_{if}, namely (dU_{if}/dU). The result, σ, is now taken to be a measure of the random error of the instrument in terms of true velocity, subject to the corrections and limitations discussed below.

Computing σ_i from measurements by an instrument having a scale with a resolution, R_i, much smaller than σ_i is an accepted procedure for determining repeatability of the instrument. However, if the resolution is large (poor) compared to σ_i (where σ_i is presumed known by some means independent of the scale being considered, say by a second scale with better resolution), the indicated σ may be much smaller than it should be. For a Gaussian distribution of errors it is assumed that σ_i may be adequately computed if the resolution is at most approximately twice σ_i.

As with the computed values of σ_i, these values of resolution, R_i, were converted to equivalent values, $\bar{R}$, in terms of true velocity by dividing by the slope (dU_{if}/dU). These latter values, divided by two, were then included in the figures where applicable in units of velocity or as percentage of $\bar{U}$. As will be seen, R/2 does indeed exceed σ for several of the instruments. Thus these particular values of σ should be taken with reservation and perhaps replaced by the values R/2. The performance of the instrument in these instances in terms of random error may exceed the quality of its resolution.

The above analysis presumes that the contribution to the random errors from the laser velocimeter is negligible, and indeed this is true for most of the tests. The random uncertainty of the laser velocimeter (random error) may be estimated from repeated measurements at a particular fan setting, thus also including any unsteadiness in the air speed. The value of this uncertainty was reduced as improvements were made to the laser system and varied from 0.005U for instruments A and B to 0.002U for instrument C to 0.001U for all the others. A corrected standard deviation for the tested instruments, σ_c, may thus be computed from, for instance,

$$\sigma_c^2 = \sigma^2 - (0.001U)^2$$

for any given U. Values of σ_c are included in the figures where they differ perceptibly from the values of σ. Since $\pm 2\sigma_c$ is close to the 95 percent confidence interval for one measurement, curves of $\pm 2\sigma_c$ are also included in the figures of U_i against U.

5.2 Calibration Data

The calibration data is presented in three forms for those instruments (A through G) that read directly in velocity: indicated versus true velocity, the deviation of indicated from true velocity against indicated velocity, and the percent deviation against true

velocity (Figures 16 through 60). Instruments H, I, and J have only plots of indicated output (frequency for H and I; current for J) against true velocity, Figures 30, 31, and 32. The primary function of the figures showing indicated velocity or output against true velocity is to illustrate the overall character of the response and the 95% confidence intervals. The other types of figures detail the features of most interest: the linearity, the range of scatter, and the deviation of indicated from the true velocity.

Vane anemometers A, B, and D are nearly identical in dimension and also have very similar calibration curves (see Figures 16, 18, 19, 33 through 36, 39, and 40). The rapid rise in the curve of Figure 33 as the velocity is reduced below 100 feet per minute (0.5 m/s) is almost certainly due to the appearance of friction effects since this instrument, A, has bronze bearings rather than ball bearings as do instruments B and D.

Instrument C, though a vane anemometer similar in appearance to A, B, and D, does differ somewhat from them, especially in the size and shape of the hub. This may explain the somewhat different character of the calibration data as presented in Figures 18, 37, and 38, though the instruments A, B, C, and D really all have quite similar calibration characteristics.

The magnetic pick-up transducer and associated electronics of instrument E may be the fundamental cause of the somewhat different character of its calibration data (figures 20, 21, 22, and 41 through 46) as compared to A through D. This is evidenced by the change in the data between ranges on the instrument (e.g., Figures 41 and 43). This cannot be caused by the dynamics of the vane since mechanically and aerodynamically the instrument is unchanged when compared at the same speed but on different ranges. The overall character of the calibrations though is not significantly different from those of A through D.

The characteristics of the calibration data for the impact-deflection type instruments, F and G, are determined by the aerodynamic characteristics of the probes and flow passages in the instruments as well as the meter characteristics. The different responses in the data of Figures 23 through 29, and 47 through 60 show the effect of various probes and ranges. The only major conclusion to be drawn at this point is that at the lower velocities it is usually very important because of large errors to use a good calibration correction method (chart or table, etc.) when making a measurement. This is true for <u>all</u> the instruments, A through G.

There is little to comment upon concerning the calibration curves for the vortex-shedding and heated film anemometers (H, I, and J) since the output is not "velocity." Both the principle of vortex street frequency-to-velocity relationship and the temperature-to-velocity relationship have long been known. These particular instruments have utilized these principles so that sufficient

sensitivity to velocity changes is produced. Both the near linearity of the vortex frequency with velocity and the usual non-linearity of the heat transfer to velocity are apparent in the data (Figures 30, 31, and 32).

5.3 Random Error

The random error, defined in Section 5.1, is presented in essentially two forms: in units of velocity, and as percent of group mean true velocity. The exceptions are instruments H, I, and J which do not read out in velocity and thus also have plots of random error in units of their read-out (frequency or current). As was discussed in Section 5.1, the measure of random error, σ, is in terms of true velocity which was produced by dividing σ_i by $(d\bar{U}_i/d\bar{U})$. The random error for the instruments not having direct read-out in velocity was also expressed in this manner by dividing the random error in terms of the readout ($\underline{f}$ or $\underline{I}$) by the group mean slope of the calibration curve ($df/d\bar{U}$ or $d\bar{I}/d\bar{U}$).

The rather small sample size, five runs, causes a sizeable uncertainty in any one value of the random error. This is ameliorated somewhat though by the many values of velocity at which the random error was computed, thus permitting a smoothing of the data and effective reduction in the uncertainty. The data as presented, however, have not been smoothed but are the values computed according to the procedures presented in Section 5.1.

The data for vane anemometers A, B, C, and D (Figures 61 and 62 for A, 63 and 64 for B, 65 and 66 for C, and 67 and 68 for D) all show the same trends of σ and $\sigma/\bar{U}$ with $\bar{U}$ differing only in magnitude. The quite different character of the random error for instrument E, the only one with a magnetic pick-up transducer, Figures 69 and 74, is most likely associated with the effects of resolution as discussed in Section 5.1. As noted in the figures, the computed σ is frequently less than the value R/2. The other vane anemometers did not have random errors the same order as the resolution. For evaluation, as noted in Section 5.1, instrument E should perhaps have σ replaced by R/2 for those values of σ less than R/2.

The impact-deflection type anemometers, instruments F and G, likewise have random errors exceeded by the values R/2 at some air speeds (Figures 75 through 88). None of E, F, or G, however, show any adverse or highly unusual characteristics in the trends of the random error with velocity.

The effect of resolution on the vortex-shedding anemometers, instruments H and I, was eliminated by selecting instrumentation for reading the frequency which had far better resolution than required. This was possible in the laboratory because of the unprocessed signals, a pulse train and a voltage, available from

the instruments under test. The only slightly unusual feature of the results (Figures 89 through 96) was that for instrument H, $\sigma_f/\bar{f}$ or $\sigma/\bar{U}$ were nearly constant with velocity. Instrument I, though, gave values which increased somewhat as velocity was decreased. Since the instruments are nominally identical, no explanation is apparent for the (slight) variation.

The heated foil anemometer, instrument J, showed trends with velocity similar to A through D, but had resolution almost perfectly matched to the random error (Figures 97 through 100).

5.4 Minimum Operating Speed

As discussed in Section 4.3, the minimum operating speed is determined in different ways for different instruments. The vane anemometers and the vortex-shedding anemometers all have minimum operating speeds determined by a complete ceasing of operation. The others simply lose resolution below some air speed. The various minimum operating speeds are summarized in Table K.

The difference in starting and stopping speeds for the vane anemometers, A through E, is due to the difference in static and dynamic friction factors for the bearings. Both speeds, though, are lower for the instruments with the more friction-free bearings, such as B and D. Instrument D, having fewer vanes than B, can operate at higher air speeds, but this advantage is offset somewhat by a decreased torque at lower speeds and thus a higher minimum operating speed.

Since the minimum operating speed of the vortex-shedding anemometers, instruments H and I, depends on the level of detection of the ultrasonic modulation, the difference in the speeds for these two instruments is probably due to slightly differing adjustments of the electronic detection circuits rather than a physical or aerodynamic difference. As noted in Section 4.3, these instruments ceased operating rather abruptly as speed was reduced, thus giving a well-defined minimum operating speed.

For the instruments having a minimum operating speed defined by resolution, namely F, G, and J, the procedure for specifying the speed is defined in Section 4.3, and the results are summarized in Table K. The only comment on the results is that the resolution as discussed in Section 4.3 is R_i, the indicated resolution, whereas the minimum operating speeds (for all the instruments) are true speeds.

6. SUMMARY

Performance of ten anemometers of several different types has been measured at low air speeds in a wind tunnel which provides a steady air flow of low turbulence. Multiple calibration runs on

each instrument provided sufficient data for measuring performance in terms of random error about the mean calibration curve as well as the difference between the indicated and true speeds. Measurements were also performed of the minimum operating speeds of the anemometers.

The results are presented in both tabular and graphical form. A detailed description is included of the tests, the results, and the methods of analysis.

7. REFERENCES

1. L. P. Purtell and P. S. Klebanoff, A Low Velocity Airflow Calibration and Research Facility, NBS TN 989, 1979.

Table A1
Davis Vane Anemometer
Serial No. 22889

Indicated Air Speed, fpm	True Air Speed, fpm
730.0	679.0
730.0	687.0
208.0	208.0
479.0	458.0
67.8	94.2
21.0	76.2
26.4	75.0
28.8	72.0
63.6	94.2
63.0	89.4

T = 18.8 to 20.0 °C
B = 763.1 mm Hg

Table A2
Davis Vane Anemometer
Serial No. 22889

Indicated Air Speed, fpm	True Air Speed, fpm
732.0	679.0
208.0	208.0
478.0	451.0
67.2	91.8
37.8	73.2
37.2	65.4
28.8	64.8
60.0	90.0
63.6	91.2

T = 20.1 to 21.0 °C
B = 763.1 mm Hg

Table A3
Davis Vane Anemometer
Serial No. 22889

Indicated Air Speed, fpm	True Air Speed, fpm
732.0	690.0
211.0	207.0
482.0	458.0
70.2	94.8
39.3	72.0
36.5	73.2
29.6	76.2
69.6	96.0
68.4	96.6

T = 21.0 °C
B = 755.0 mm Hg

Table A4
Davis Vane Anemometer
Serial No. 22889

Indicated Air Speed, fpm	True Air Speed, fpm
735.0	687.0
210.0	214.0
481.0	460.0
69.6	94.2
39.1	75.6
44.0	76.8
45.3	75.6
70.8	96.6
70.8	96.6

T = 21.6 °C
B = 764.0 mm Hg

Table A5
Davis Vane Anemometer
Serial No. 22889

Indicated Air Speed, fpm	True Air Speed, fpm
710.0	688.0
208.0	215.0
479.0	458.0
67.8	95.4
25.8	74.4
39.1	74.4
40.9	75.0
64.8	94.2

T = 21.6 °C
B = 764.0 mm Hg

Table B1
Davis Vane Anemometer
Serial No. 24323 B

Indicated Air Speed, fpm	True Air Speed, fpm
712	692
205	211
466	455
80.4	93.0
56.5	72.0
33.2	50.4
12.4	30.3
23.1	40.8
5.8	24.0

T = 20.9 to 21.0 °C
B = 745.7 mm Hg

Table B2
Davis Vane Anemometer
Serial No. 24323 B

Indicated Air Speed, fpm	True Air Speed, fpm
752	724
218	224
491	484
85.6	99.3
60.8	73.1
37.1	51.1
14.3	29.6
24.8	40.6
6.8	23.0
151	158

T = 21.7 to 21.9 °C
B = 744.8 mm Hg

Table B3
Davis Vane Anemometer
Serial No. 24323 B

Indicated Air Speed, fpm	True Air Speed, fpm
717	690
206	209
468	458
80.5	94.4
57.5	71.1
35.0	51.5
12.2	30.7
22.7	41.7
8.1	26.4
144	150

T = 21.3 °C
B = 747.1 mm Hg

Table B4
Davis Vane Anemometer
Serial No. 24323 B

Indicated Air Speed, fpm	True Air Speed, fpm
715	696
206	215
469	466
80.3	96.0
56.8	72.0
33.1	50.4
12.3	31.2
22.4	41.4
6.4	25.2
142	152

T = 22.1 °C
B = 750.5 mm Hg

Table B5
Davis Vane Anemometer
Serial No. 24323 B

Indicated Air Speed, fpm	True Air Speed, fpm
718	682
207	212
471	461
78.8	97.2
56.0	70.8
33.8	50.4
13.6	32.2
26.9	43.4
11.5	29.5
114	153

T = 22.5 °C
B = 750.5 mm Hg

Table C1
Taylor Vane Anemometer
Serial No. H873

Indicated Air Speed, fpm	True Air Speed, fpm
722	752
589	619
457	494
309	322
190	221
110	145
56.8	100
26.7	76.2
7.1	60.6
27.1	76.2

T = 22.8 °C
B = 751.2 mm Hg

Table C2
Taylor Vane Anemometer
Serial No. H873

Indicated Air Speed, fpm	True Air Speed, fpm
719	746
589	623
454	498
324	360
190	222
109	142
55.8	98.0
25.1	74.6
8.4	64.8
25.7	76.0

T = 22.6 °C
B = 753.5 mm Hg

Table C3
Taylor Vane Anemometer
Serial No. H873

Indicated Air Speed, fpm	True Air Speed, fpm
720	750
588	622
456	495
323	363
190	222
110	143
54.7	96.9
23.4	74.2
3.8	63.0
23.8	74.3

T = 22.6 °C
B = 753.1 mm Hg

Table C4
Taylor Vane Anemometer
Serial No. H873

Indicated Air Speed, fpm	True Air Speed, fpm
723	752
590	622
458	499
324	361
190	221
110	142
54.9	97.1
22.4	73.6
23.0	72.4

T = 22.7 °C
B = 752.9 mm Hg

Table C5
Taylor Vane Anemometer
Serial No. H873

Indicated Air Speed, fpm	True Air Speed, fpm
721	742
588	624
457	496
323	360
190	220
109	141
54.5	96.4
20.0	72.6
8.5	65.5
20.8	72.5
9.8	66.1

T = 22.8 °C
B = 753.0 mm Hg

Table D1
Davis Vane Anemometer
Serial No. 31125B

Indicated Air Speed, fpm	True Air Speed, fpm
785	736
639	606
496	478
359	347
219	217
136.4	141.2
80.2	92.1
53.7	68.2
38.9	56.6
28.6	47.7

T = 23.6 °C
B = 753.8 mm Hg

Table D2
Davis Vane Anemometer
Serial No. 31125B

Indicated Air Speed, fpm	True Air Speed, fpm
786	741
640	608
497	477
358	348
219	218
137.3	141.7
81.8	93.1
56.1	70.2
41.8	58.8
26.4	47.3

T = 23.8 °C
B = 753.8 mm Hg

Table D3
Davis Vane Anemometer
Serial No. 31125B

Indicated Air speed, fpm	True Air Speed, fpm
786	738
641	608
498	477
358	347
218	216
135.5	139.5
81.1	91.5
53.7	68.0
38.9	55.7
24.5	43.4

T = 24.2 °C
B = 753.8 mm Hg

Table D4
Davis Vane Anemometer
Serial No. 31125B

Indicated Air Speed, fpm	True Air Speed, fpm
787	738
641	608
498	477
359	347
220	217
135.6	140.5
80.6	91.4
53.0	67.7
37.8	55.4
24.8	44.6

T = 24.6 °C
B = 753.8 mm Hg

Table D5
Davis Vane Anemometer
Serial No. 31125B

Indicated Air Speed, fpm	True Air Speed, fpm
786	740
641	608
498	476
357	347
219	217
134.6	140.0
81.0	91.4
52.6	67.1
38.3	55.3
27.1	46.3

T = 24.7 °C
B = 753.2 mm Hg

Table E1
Abbirko Flowmaster
S/N 6184
Low Range

Indicated Air Speed, fpm	True Air Speed, fpm
50	59.9
52	64.1
64	74.5
74	86.1
86	97.2
96	108.4
144	157
184	200
228	248
272	300

T = 20.8°C
B = 758.4 mm Hg

Table E2
Abbirko Flowmaster
S/N 6184
Low Range

Indicated Air Speed, fpm	True Air Speed, fpm
50	59.6
54	64.0
64	74.0
76	86.4
86	97.1
98	108.8
144	157
186	200
228	250
274	299

T = 20.8°C
B = 758.4 mm Hg

Table E3
Abbirko Flowmaster
S/N 6184
Low Range

Indicated Air Speed, fpm	True Air Speed, fpm
52	59.8
54	64.1
64	74.3
76	86.2
86	96.7
98	107.8
144	157
184	199
230	249
274	298

T = 20.9°C
B = 758.4 mm Hg

Table E4
Abbirko Flowmaster
S/N 6184
Low Range

Indicated Air Speed, fpm	True Air Speed, fpm
48	54.9
50	60.0
60	72.1
74	82.8
84	94.4
98	106.8
142	155
184	198
228	248
272	299

T = 22.2°C
B = 750.3 mm Hg

Table E5
Abbirko Flowmaster
S/N 6184
Low Range

Indicated Air Speed, fpm	True Air Speed, fpm
50	56.6
52	60.7
60	72.1
76	84.2
84	95.3
98	106.4
142	155
182	199
228	249
272	298

T = 22.3°C
B = 751.1 mm Hg

Table E6
Abbirko Flowmaster
S/N 6184
Medium Range

Indicated Air Speed, fpm	True Air Speed, fpm
30	63.4
55	86.1
75	108.1
170	199
265	299
370	402
475	507
585	611
685	716

T = 20.8°C
B = 758.4 mm Hg

Table E7
Abbirko Flowmaster
S/N 6184
Medium Range

Indicated Air Speed, fpm	True Air Speed, fpm
25	64.4
55	86.1
80	108.2
170	200
270	298
375	401
480	507
585	612
685	716

T = 20.9°C
B = 758.4 mm Hg

Table E8
Abbirko Flowmaster
S/N 6184
Medium Range

Indicated Air Speed, fpm	True Air Speed, fpm
25	59.9
50	82.8
75	106.2
165	199
265	298
370	402
475	506
580	611
685	714

T = 22.2°C
B = 750.0 mm Hg

Table E9
Abbirko Flowmaster
S/N 6184
Medium Range

Indicated Air Speed, fpm	True Air Speed, fpm
25	61.1
50	83.6
80	107.5
170	199
265	299
375	402
485	506
585	611
690	716

T = 22.3°C
B = 750.8 mm Hg

Table E10
Abbirko Flowmaster
S/N 6184
Medium Range

Indicated Air Speed, fpm	True Air Speed, fpm
25	61.2
50	83.0
75	106.8
170	199
265	299
375	402
480	506
585	611
685	717

T = 22.4°C
B = 751.2 mm Hg

Table E11
Abbirko Flowmaster
S/N 6184
High Range

Indicated Air Speed, fpm	True Air Speed, fpm
80	107.4
170	199
270	298
370	401
480	506
580	612
690	711

T = 20.6°C
B = 758.4 mm Hg

Table E12
Abbirko Flowmaster
S/N 6184
High Range

Indicated Air Speed, fpm	True Air Speed, fpm
90	108.6
170	199
270	299
380	403
480	507
590	613
690	716

T = 20.9°C
B = 758.4 mm Hg

Table E13
Abbirko Flowmaster
S/N 6184
High Range

Indicated Air Speed, fpm	True Air Speed, fpm
90	106.3
180	198
280	299
380	401
490	505
590	612
695	712

T = 22.1°C
B = 750.0 mm Hg

Table E14
Abbirko Flowmaster
S/N 6184
High Range

Indicated Air Speed, fpm	True Air Speed, fpm
90	106.7
180	199
280	299
380	403
490	507
590	611
695	715

T = 22.3°C
B = 751.1 mm Hg

Table E15
Abbirko Flowmaster
S/N 6184
High Range

Indicated Air Speed, fpm	True Air Speed, fpm
80	107.9
180	200
280	299
390	403
490	506
590	612
695	715

T = 22.4°C
B = 751.2 mm Hg

Table F1
Alnor Velometer
Series 6000-P
Pitot probe-1250 Scale

Indicated Air Speed, fpm	True Air Speed, fpm
100	102
140	153
190	198
285	297
380	400
468	498
560	603
645	705

T = 21.1 °C
B = 739.5 mm Hg

Table F2
Alnor Velometer
Series 6000-P
Pitot probe-1250 Scale

Indicated Air Speed, fpm	True Air Speed, fpm
100	102
140	154
190	199
280	297
378	400
468	499
558	604
645	705

T = 21.1 °C
B = 739.5 mm Hg

Table F3
Alnor Velometer
Series 6000-P
Pitot probe-1250 Scale

Indicated Air Speed, fpm	True Air Speed, fpm
100	102
140	153
190	198
280	297
380	401
470	498
560	605
645	706

T = 21.8 °C
B = 740.1 mm Hg

Table F4
Alnor Velometer
Series 6000-P
Pitot probe-1250 Scale

Indicated Air Speed, fpm	True Air Speed, fpm
100	102
140	153
188	198
285	297
378	401
468	498
560	603
645	704

T = 21.8 °C
B = 740.1 mm Hg

Table F5
Alnor Velometer
Series 6000-P
Pitot probe-1250 Scale

Indicated Air Speed, fpm	True Air Speed, fpm
100	102
140	153
192	198
285	297
378	402
470	497
560	602
648	709

T = 21.8 °C
B = 741.0 mm Hg

Table F6
Alnor Velometer
Series 6000-P
Pitot probe-2500 Scale

Indicated Air Speed, fpm	True Air Speed, fpm
75	103
125	149
190	201
300	300
410	399
540	502
645	604
760	705

T = 21.1 °C
B = 749.2 mm Hg

Table F7
Alnor Velometer
Series 6000-P
Pitot probe-2500 Scale

Indicated Air Speed, fpm	True Air Speed, fpm
75	103
130	149
190	200
295	299
420	399
540	503
655	604
755	707

T = 21.1 °C
B = 749.2 mm Hg

Table F8
Alnor Velometer
Series 6000-P
Pitot probe-2500 Scale

Indicated Air Speed, fpm	True Air Speed, fpm
80	103
130	149
195	200
300	300
435	399
540	503
650	606
755	706

T = 21.1 °C
B = 749.3 mm Hg

Table F9
Alnor Velometer
Series 6000-P
Pitot probe-2500 Scale

Indicated Air Speed, fpm	True Air Speed, fpm
80	103
135	149
185	200
305	300
425	399
540	503
645	605
750	704

T = 21.1 °C
B = 749.3 mm Hg

Table F10
Alnor Velometer
Series 6000-P
Pitot probe-2500 Scale

Indicated Air Speed, fpm	True Air Speed, fpm
75	103
125	149
190	200
300	300
420	398
540	503
650	605
755	705

T = 21.1 °C
B = 749.3 mm Hg

Table F11
Alnor Velometer
Series 6000-P
Diffuser probe-2500 Scale

Indicated Air Speed, fpm	True Air Speed, fpm
75	101
145	148
230	201
395	301
540	401
675	501
820	602
940	701

T = 21.1 °C
B = 747.8 mm Hg

Table F12
Alnor Velometer
Series 6000-P
Diffuser probe-2500 Scale

Indicated Air Speed, fpm	True Air Speed, fpm
75	101
145	149
240	200
395	301
545	401
680	503
815	602
940	698

T = 21.1 °C
B = 747.8 mm Hg

Table F13
Alnor Velometer
Series 6000-P
Diffuser probe-2500 Scale

Indicated Air Speed, fpm	True Air Speed, fpm
80	101
145	149
245	200
400	301
540	401
680	499
820	601
940	699

T = 21.1 °C
B = 747.5 mm Hg

Table F14
Alnor Velometer
Series 6000-P
Diffuser probe-2500 Scale

Indicated Air Speed, fpm	True Air Speed, fpm
90	101
150	147
240	201
395	301
545	400
675	501
825	600
945	698

T = 21.1 °C
B = 747.5 mm Hg

Table F15
Alnor Velometer
Series 6000-P
Diffuser probe-2500 Scale

Indicated Air Speed, fpm	True Air Speed, fpm
90	101
150	148
245	200
395	301
540	400
680	500
815	599
940	698

T = 21.1 °C
B = 747.3 mm Hg

Table F16
Alnor Velometer
Series 6000-P
Diffuser probe-1250 Scale

Indicated Air Speed, fpm	True Air Speed, fpm
135	101
195	149
280	199
395	300
510	401
620	498
735	601
840	698

T = 21.1 °C
B = 746.0 mm Hg

Table F17
Alnor Velometer
Series 6000-P
Diffuser probe-1250 Scale

Indicated Air Speed, fpm	True Air Speed, fpm
130	101
200	148
278	198
398	299
515	399
620	498
738	599
840	699

T = 21.1 °C
B = 746.0 mm Hg

Table F18
Alnor Velometer
Series 6000-P
Diffuser probe-1250 Scale

Indicated Air Speed, fpm	True Air Speed, fpm
130	102
200	149
278	199
400	300
515	401
620	500
740	602
840	697

T = 21.1 °C
B = 745.4 mm Hg

Table F19
Alnor Velometer
Series 6000-P
Diffuser probe-1250 Scale

Indicated Air Speed, fpm	True Air Speed, fpm
135	101
200	149
278	200
398	301
515	402
618	501
738	601
843	701

T = 21.1 °C
B = 745.4 mm Hg

Table F20
Alnor Velometer
Series 6000-P
Diffuser probe-1250 Scale

Indicated Air Speed, fpm	True Air Speed, fpm
138	101
200	148
275	199
395	301
518	401
620	499
738	603
840	696

T = 20.6 °C
B = 744.3 mm Hg

Table F21
Alnor Velometer
Series 6000-P
Low Velocity probe

Indicated Air Speed, fpm	True Air Speed, fpm
33	43.0
47	56.5
68	77.6
93	102
145	150
207	199
297	271

T = 20.6 °C
B = 742.5 mm Hg

Table F22
Alnor Velometer
Series 6000-P
Low Velocity probe

Indicated Air Speed, fpm	True Air Speed, fpm
33	42.9
45	56.5
66	77.4
94	101
145	150
207	199
296	272

T = 20.6 °C
B = 742.5 mm Hg

Table F23
Alnor Velometer
Series 6000-P
Low Velocity probe

Indicated Air Speed, fpm	True Air Speed, fpm
32	42.6
46	56.1
67	77.6
92	101
146	149
207	199
295	270

T = 20.0 °C
B = 742.0 mm Hg

Table F24
Alnor Velometer
Series 6000-P
Low Velocity probe

Indicated Air Speed, fpm	True Air Speed, fpm
34	42.9
45	55.8
68	77.3
93	101
144	149
208	198
295	271

T = 20.0 °C
B = 742.0 mm Hg

Table F25
Alnor Velometer
Series 6000-P
Low Velocity probe

Indicated Air Speed, fpm	True Air Speed, fpm
33	42.3
48	56.9
68	77.6
94	102
144	149
207	199
296	272

T = 20.0 °C
B = 740.3 mm Hg

Table G1
Alnor Velometer Jr.
Low Range

Indicated Air Speed, fpm	True Air Speed, fpm
205	204.7
172	166.4
148	141.1
122	116.3
100	93.0
80	70.6
62	53.0

T = 26.9 °C
B = 747.5 mm Hg

Table G2
Alnor Velometer Jr.
Low Range

Indicated Air Speed, fpm	True Air Speed, fpm
205	204.6
170	165.8
146	141.6
122	118.0
100	94.9
78	70.3
60	53.2

T = 26.9 °C
B = 747.5 mm Hg

Table G3
Alnor Velometer Jr.
Low Range

Indicated Air Speed, fpm	True Air Speed, fpm
200	204.2
170	166.6
148	142.1
120	117.0
100	92.7
80	70.7
62	53.3

T = 26.9 °C
B = 747.5 mm Hg

Table G4
Alnor Velometer Jr.
Low Range

Indicated Air Speed, fpm	True Air Speed, fpm
205	204.7
170	166.3
146	141.1
120	116.4
100	92.9
80	69.5
62	53.4

T = 26.9 °C
B = 747.5 mm Hg

Table G5
Alnor Velometer Jr.
Low Range

Indicated Air Speed, fpm	True Air Speed, fpm
205	204.6
170	166.2
146	141.3
122	117.5
102	93.6
80	70.1
62	53.4

T = 27.0 °C
B = 747.5 mm Hg

Table G6
Alnor Velometer Jr.
High Range

Indicated Air Speed, fpm	True Air Speed, fpm
775	712.8
600	608.5
525	503.1
480	399.0
420	296.1
300	192.2
230	142.0
195	117.2
160	93.5
100	50.8

T = 26.9 °C
B = 747.5 mm Hg

Table G7
Alnor Velometer Jr.
High Range

Indicated Air Speed, fpm	True Air Speed, fpm
800	714.7
610	608.8
525	504.2
485	400.0
420	296.5
300	192.4
230	141.7
195	117.4
160	93.3
105	52.5

T = 26.9 °C
B = 747.5 mm Hg

Table G8
Alnor Velometer Jr.
High Range

Indicated Air Speed, fpm	True Air Speed, fpm
800	714.2
610	609.7
530	504.9
480	399.3
420	296.9
300	191.8
210	140.3
180	117.4
150	93.0
100	53.3

T = 26.9 °C
B = 747.5 mm Hg

Table G9
Alnor Velometer Jr.
High Range

Indicated Air Speed, fpm	True Air Speed, fpm
800	715.9
610	609.4
530	504.4
480	400.2
415	296.9
300	192.5
230	141.5
195	116.9
160	93.4
100	52.8

T = 26.9 °C
B = 747.5 mm Hg

Table G10
Alnor Velometer Jr.
High Range

Indicated Air Speed, fpm	True Air Speed, fpm
800	715.7
625	610.6
530	504.6
480	399.0
420	296.3
300	191.5
225	141.0
195	115.4
160	92.3
100	54.4

T = 27.0 °C
B = 747.5 mm Hg

Table H1
J-Tec Type VA-216
S/N 49

Instrument Output Frequency Hz	Instrument Output Voltage volts	True Air Speed fpm
8.68	.132	60.3
10.9	.160	72.2
12.6	.182	81.0
14.6	.208	91.4
16.5	.233	100.6
22.7	.312	128
32.5	.44	170
46.9	.62	219
65.4	.88	284
83.2	1.12	374
110	1.48	492
147	1.95	649
187	2.45	835
242	3.20	1103
278	3.70	1290
318	4.20	1495

T = 21.3 to 21.6 °C

B = 752.4 mm Hg

Table H2
J-Tec Type VA-216
S/N 49

Instrument Output Frequency Hz	Instrument Output Voltage volts	True Air Speed fpm
8.63	.126	60.8
10.5	.154	72.5
12.3	.175	81.6
15.0	.209	92.9
16.6	.229	100.8
22.9	.308	130
32.6	.44	172
46.9	.62	220
66.2	.86	284
84.0	1.13	375
112	1.49	492
148	1.95	647
186	2.50	833
245	3.20	1109
276	3.65	1293
320	4.15	1502

T = 22.5 °C

B = 752.7

Table H3
J-Tec Type VA-216
S/N 49

Instrument Output Frequency Hz	Instrument Output Voltage volts	True Air Speed fpm
8.70	.130	61.6
10.8	.154	72.5
12.7	.180	81.6
14.9	.210	92.5
16.3	.226	100.2
23.0	.311	131
32.6	.43	171
47.4	.60	219
65.4	.86	285
84.0	1.13	375
112	1.48	492
147	1.96	648
186	2.47	834
245	3.21	1110
282	3.68	1298
318	4.16	1497

T = 22.5 to 22.8 °C

B = 752.8 mm Hg

Table H4
J-Tec Type VA-216
S/N 49

Instrument Output Frequency Hz	Instrument Output Voltage volts	True Air Speed fpm
8.59	.126	59.8
10.6	.154	71.1
12.6	.175	80.5
14.8	.209	91.9
16.3	.227	100.4
22.7	.308	131
32.7	.43	171
46.7	.60	219
64.9	.86	286
82.6	1.12	374
110	1.48	493
148	1.97	648
189	2.46	835
243	3.20	1106
279	3.65	1286
316	4.19	1505

T = 22.8 to 23.0 °C

B = 752.8 mm Hg

Table H5
J-Tec Type VA-216
S/N 49

Instrument Output Frequency Hz	Instrument Output Voltage volts	True Air Speed fpm
8.50	.126	59.5
10.8	.152	71.5
12.6	.177	80.9
14.9	.207	92.1
16.4	.226	100.2
23.3	.313	130
32.8	.43	172
46.5	.61	220
65.4	.84	284
83.3	1.12	375
110	1.48	490
147	1.96	648
188	2.47	836
244	3.20	1111
279	3.65	1292
320	4.12	1502

T = 23.2 to 23.4 °C

B = 751.3 mm Hg

Table I1
J-Tec Type VA-216
S/N 48

Instrument Output Frequency, Hz	Instrument Output Voltage, volts	True Air Speed, fpm
8.61	.118	59.6
10.8	.146	71.0
12.6	.168	80.4
14.7	.195	92.0
16.3	.216	100.5
22.2	.29	130
30.8	.40	172
46.3	.60	220
59.5	.78	286
82.6	1.09	375
106.8	1.43	494
145.6	1.91	650
185.2	2.44	832

T = 23.1°C
B = 751.0 mm Hg

Table I2
J-Tec Type VA-216
S/N 48

Instrument Output Frequency, Hz	Instrument Output Voltage, volts	True Air Speed, fpm
8.48	.116	58.1
10.7	.144	70.3
12.5	.166	80.2
15.0	.199	93.0
16.2	.215	99.5
22.2	.295	130
29.7	.39	170
46.1	.60	219
57.5	.76	285
82.0	1.09	375
105.7	1.42	494
144.5	1.92	649
186.2	2.45	835

T = 23.4°C
B = 751.2 mm Hg

Table I3
J-Tec Type VA-216
S/N 48

Instrument Output Frequency, Hz	Instrument Output Voltage, volts	True Air Speed, fpm
8.65	.117	59.6
10.9	.147	71.9
12.7	.169	81.0
15.0	.198	92.9
16.4	.218	100.9
23.0	.29	130
29.2	.38	171
45.7	.60	220
57.8	.77	285
80.0	1.07	375
106.4	1.49	492
143.7	1.91	650
184.8	2.45	836

T = 23.7°C
B = 750.8 mm Hg

Table I4
J-Tec Type VA-216
S/N 48

Instrument Output Frequency, Hz	Instrument Output Voltage, volts	True Air Speed, fpm
8.50	.119	63.5
10.6	.142	71.2
12.5	.166	80.1
14.7	.196	91.8
16.3	.217	100.2
21.5	.28	130
28.8	.38	170
45.2	.59	220
59.9	.78	284
78.1	1.04	375
107.0	1.40	492
143.5	1.90	647
186.2	2.44	834

T = 23.9°C
B = 750.2 mm Hg

Table I5
J-Tec Type VA-216
S/N 48

Instrument Output Frequency, Hz	Instrument Output Voltage, volts	True Air Speed, fpm
8.40	.06	63.6
10.6	.142	70.4
12.4	.165	80.0
14.6	.195	91.1
16.2	.215	99.4
22.7	.30	130
27.9	.37	170
44.8	.59	219
60.2	.77	283
78.1	1.04	375
103.7	1.58	489
142.9	1.88	642
184.8	2.43	834

T = 24.2°C
B = 750.2 mm Hg

Table J1

Thermogage Air Velocity Meter

Instrument Output, ua	True Air Speed, fpm
99	138.7
89	119.2
80	101.8
70	85.4
58	70.0
44	54.8
27	39.2
16	27.9
9	22.1
8	17.7

T = 22.2 °C
B = 752.8 mm Hg

Table J2

Thermogage Air Velocity Meter

Instrument Output, ua	True Air Speed, fpm
100	138.7
91	119.1
81	102.7
70	86.4
58	69.8
45	54.7
26	37.5
18	30.4
11	23.4
7	15.8

T = 22.2 °C
B = 752.8 mm Hg

Table J3

Thermogage Air Velocity Meter

Instrument Output, μa	True Air Speed, fpm
99	137.9
90	119.1
81	102.7
70	86.3
58	70.0
44	54.3
26	38.2
18	29.8
11	23.0
9	20.1

T = 22.2 °C
B = 752.8 mm Hg

Table J4

Thermogage Air Velocity Meter

Instrument Output, μa	True Air Speed, fpm
100	138.6
90	118.9
81	101.8
71	86.5
58	69.5
43	53.6
24	35.6
17	28.7
12	23.6
8	19.4

T = 22.2 °C
B = 752.8 mm Hg

Table J5

Thermogage Air Velocity Meter

Instrument Output, ua	True Air Speed, fpm
99	140.0
91	119.1
82	102.2
69	85.0
57	68.4
43	52.9
27	35.7
18	29.9
11	21.7
9	18.6

T = 22.0 °C
B = 752.8 mm Hg

Table K

Minimum Operating Speeds

INSTRUMENT	STOPPING SPEED (fpm)	STARTING SPEED (fpm)
A, vane	54	63.3
B, vane	18.2	23.3
C, vane	60.6	66.6
D, vane	31.7	47.8
E, vane	39.5	59.6
F,* impact-deflection, low and high ranges	100	
F,* impact-deflection, low velocity probe	40	
G,* impact-deflection, low range	53.0	
G,* impact-deflection, high range	50.8	
H, vortex-shedding	54.1	
I, vortex-shedding	58.8	
J,* heated-foil	16	

*Determined by resolution

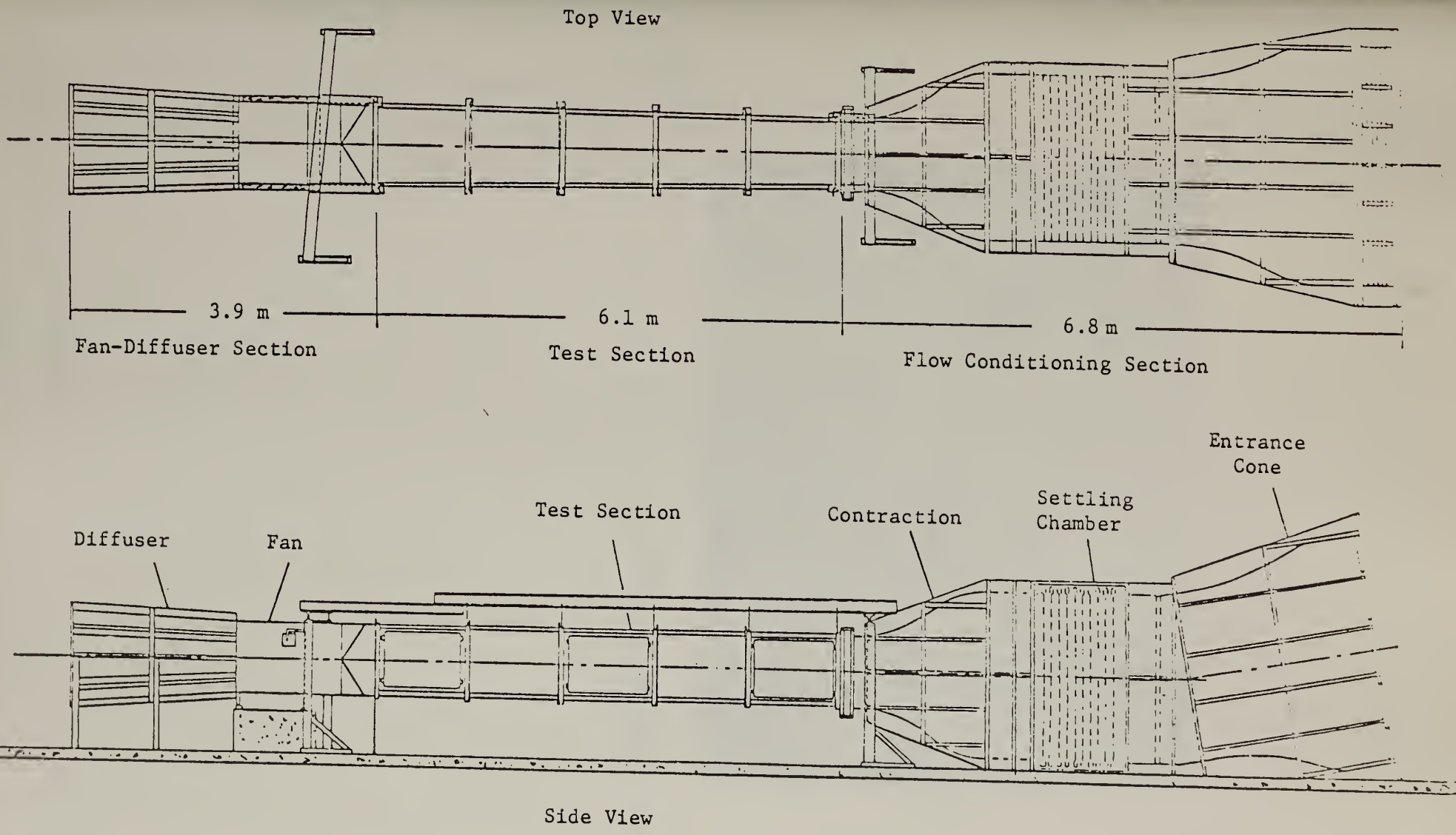

FIGURE 1. SCHEMATIC OF FLOW FACILITY.

FIGURE 2. INSTRUMENT A MOUNTED IN THE TUNNEL, SHOWING METHOD OF SUPPORT.

FIGURE 3. INSTRUMENT B MOUNTED IN THE TUNNEL, SHOWING METHOD OF SUPPORT.

FIGURE 4. INSTRUMENT C MOUNTED IN THE TUNNEL, SHOWING METHOD OF SUPPORT.

FIGURE 5. INSTRUMENT D MOUNTED IN THE TUNNEL, SHOWING METHOD OF SUPPORT.

FIGURE 6. INSTRUMENT E MOUNTED IN THE TUNNEL, SHOWING METHOD OF SUPPORT.

FIGURE 7. INSTRUMENT F, WITH PITOT PROBE MOUNTED IN TUNNEL SHOWING METHOD OF SUPPORT.

FIGURE 8. INSTRUMENT F WITH DIFFUSER PROBE MOUNTED IN TUNNEL SHOWING METHOD OF SUPPORT.

FIGURE 9. INSTRUMENT F WITH LOW-VELOCITY PROBE MOUNTED IN TUNNEL SHOWING METHOD OF SUPPORT.

FIGURE 10. INSTRUMENT G MOUNTED IN THE TUNNEL, SHOWING METHOD OF SUPPORT (VIEWED LOOKING DOWNSTREAM).

FIGURE 11. INSTRUMENTS H AND I MOUNTED IN TUNNEL, SHOWING METHOD OF SUPPORT (VIEWED LOOKING DOWNSTREAM).

FIGURE 12. INSTRUMENT J MOUNTED IN TUNNEL, SHOWING METHOD OF SUPPORT.

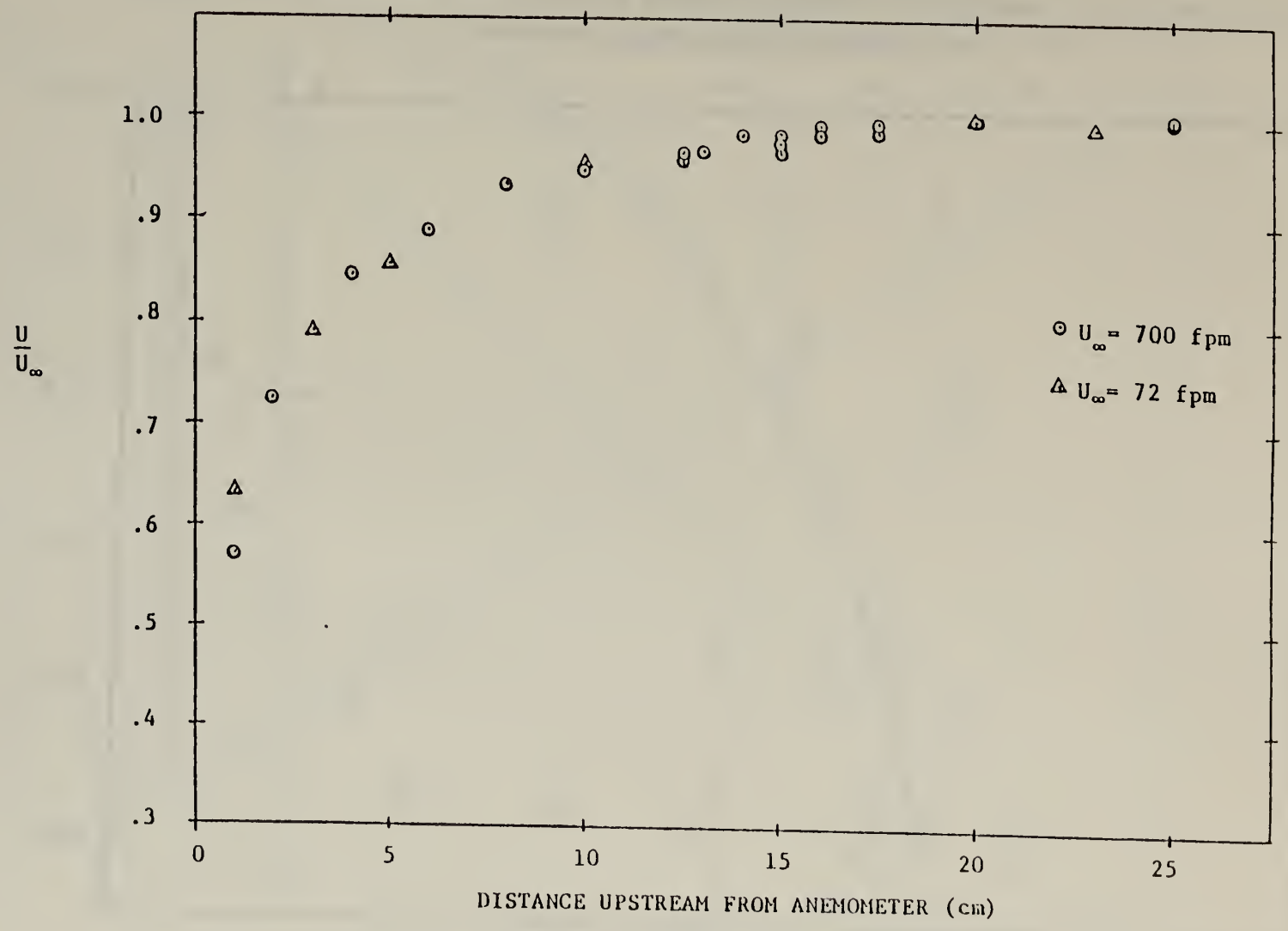

FIGURE 13. VARIATION IN VELOCITY WITH DISTANCE UPSTREAM FROM INSTRUMENT A.

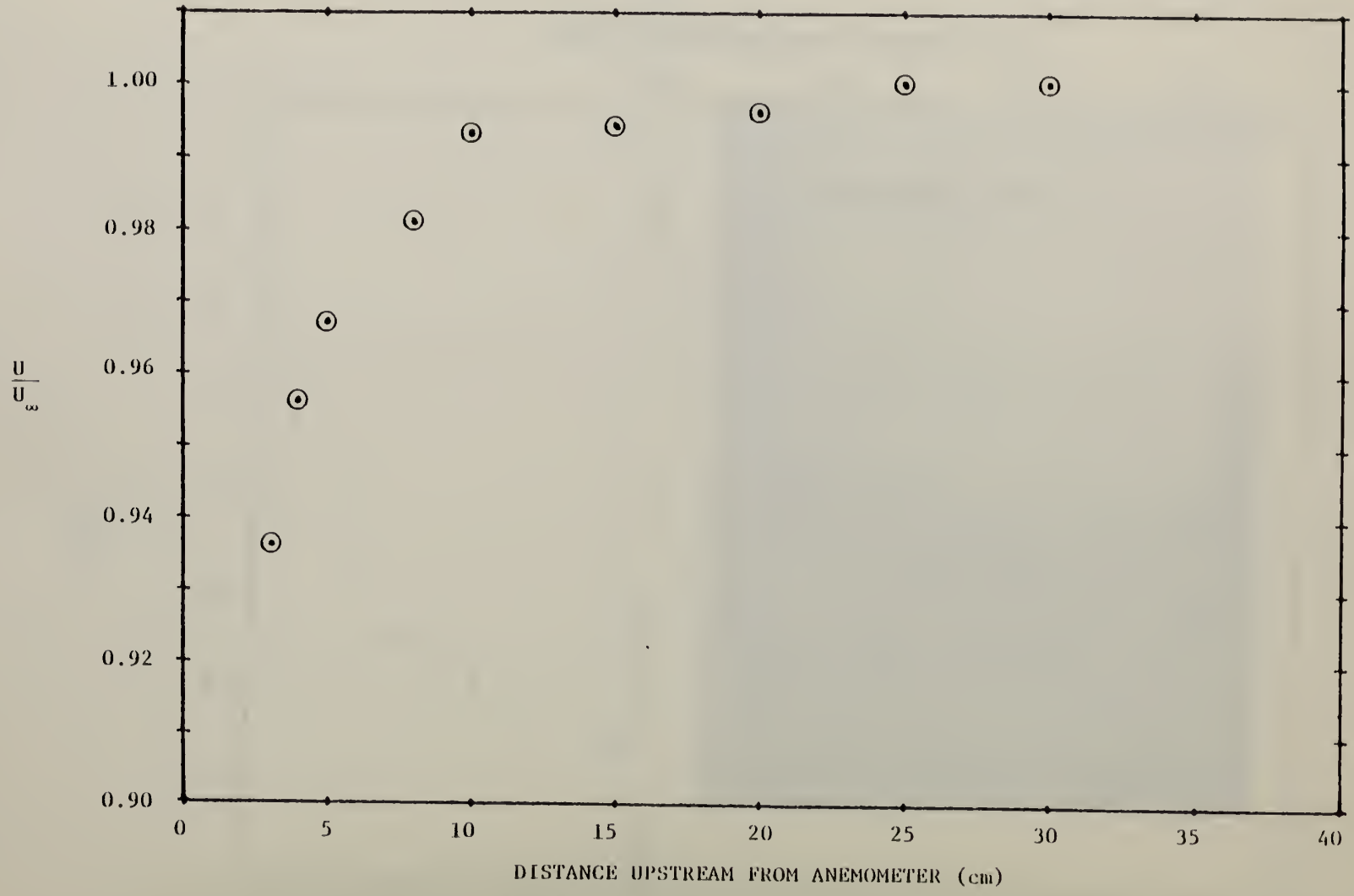

FIGURE 14. VARIATION IN VELOCITY WITH DISTANCE UPSTREAM OF INSTRUMENT F WITH LOW VELOCITY PROBE. U_∞ = 70 fpm.

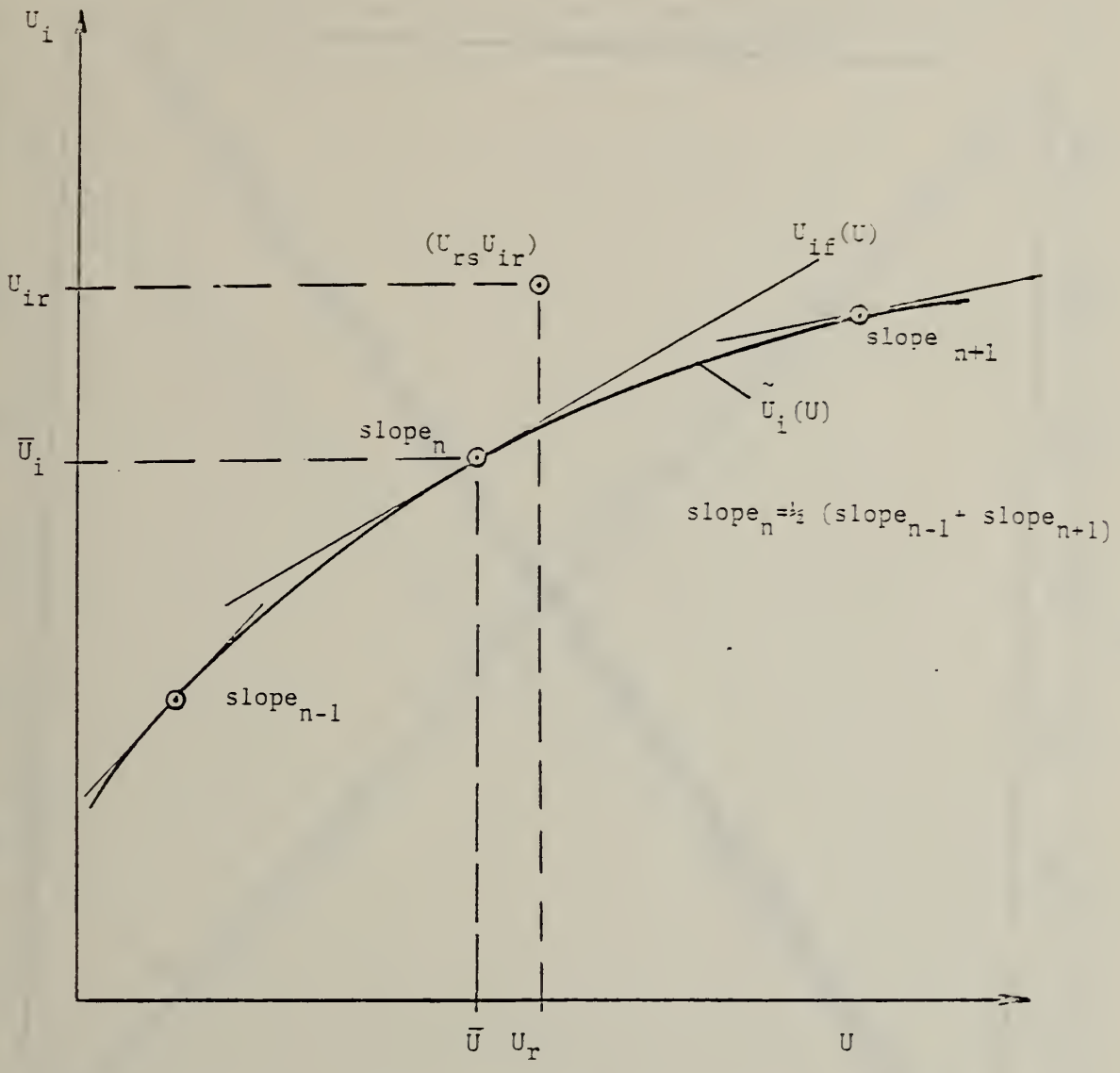

FIGURE 15. DEFINITION OF TERMS FOR CALCULATION OF σ_i.

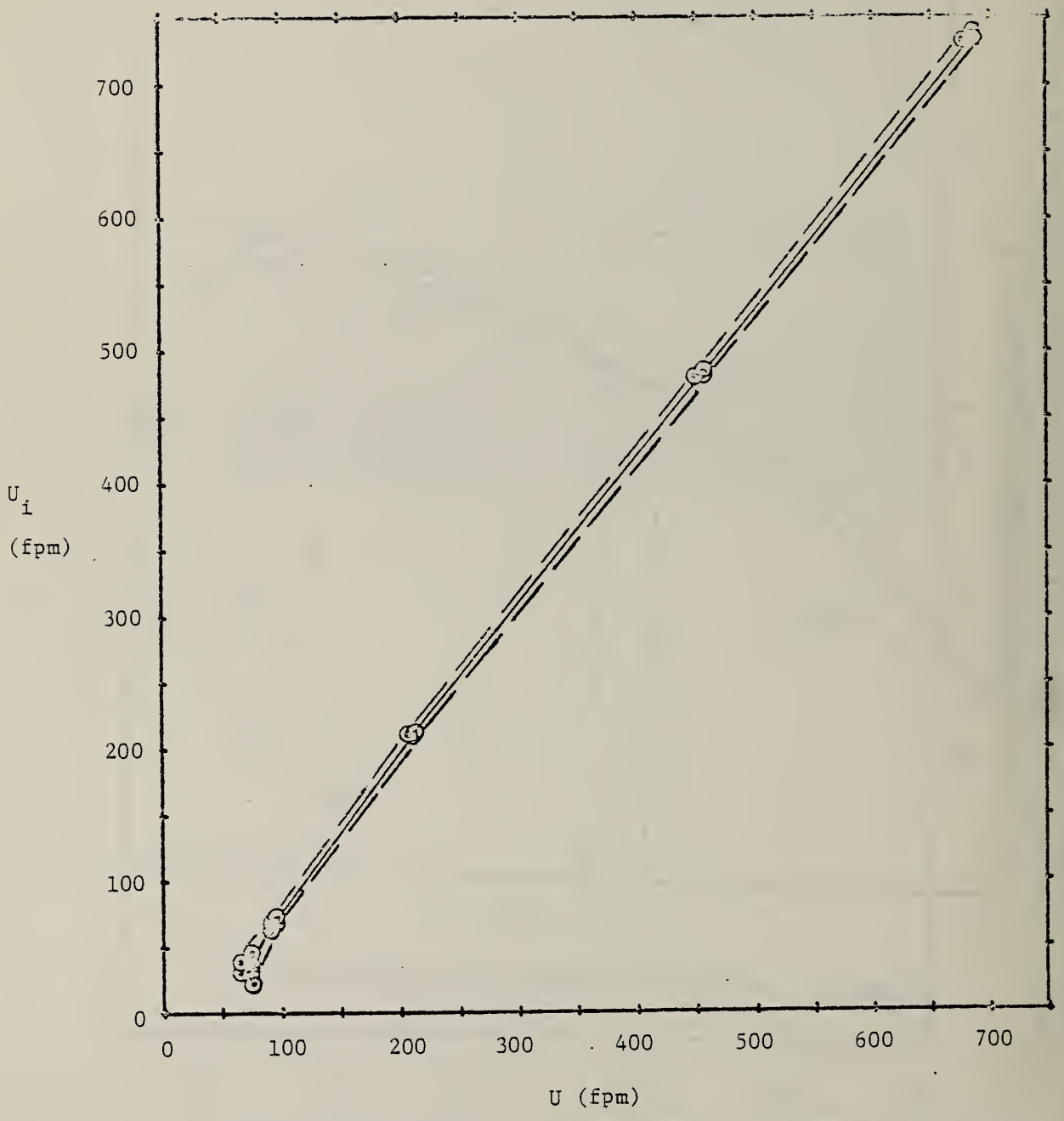

FIGURE 16. INDICATED VERSUS TRUE VELOCITY WITH ± 2σ CURVES. INSTRUMENT A.

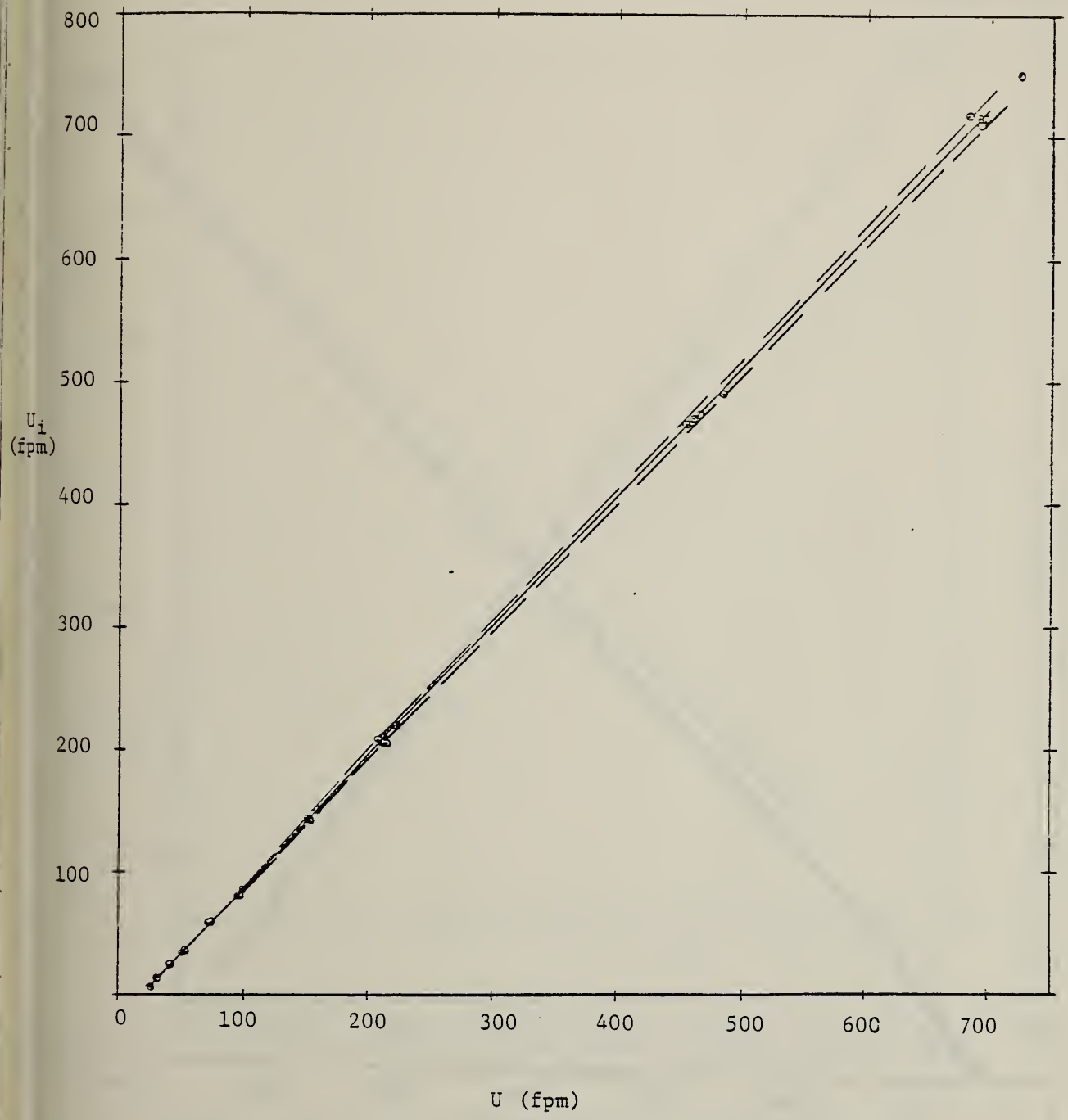

FIGURE 17. INDICATED VERSUS TRUE VELOCITY WITH ± 2σ CURVES. INSTRUMENT B.

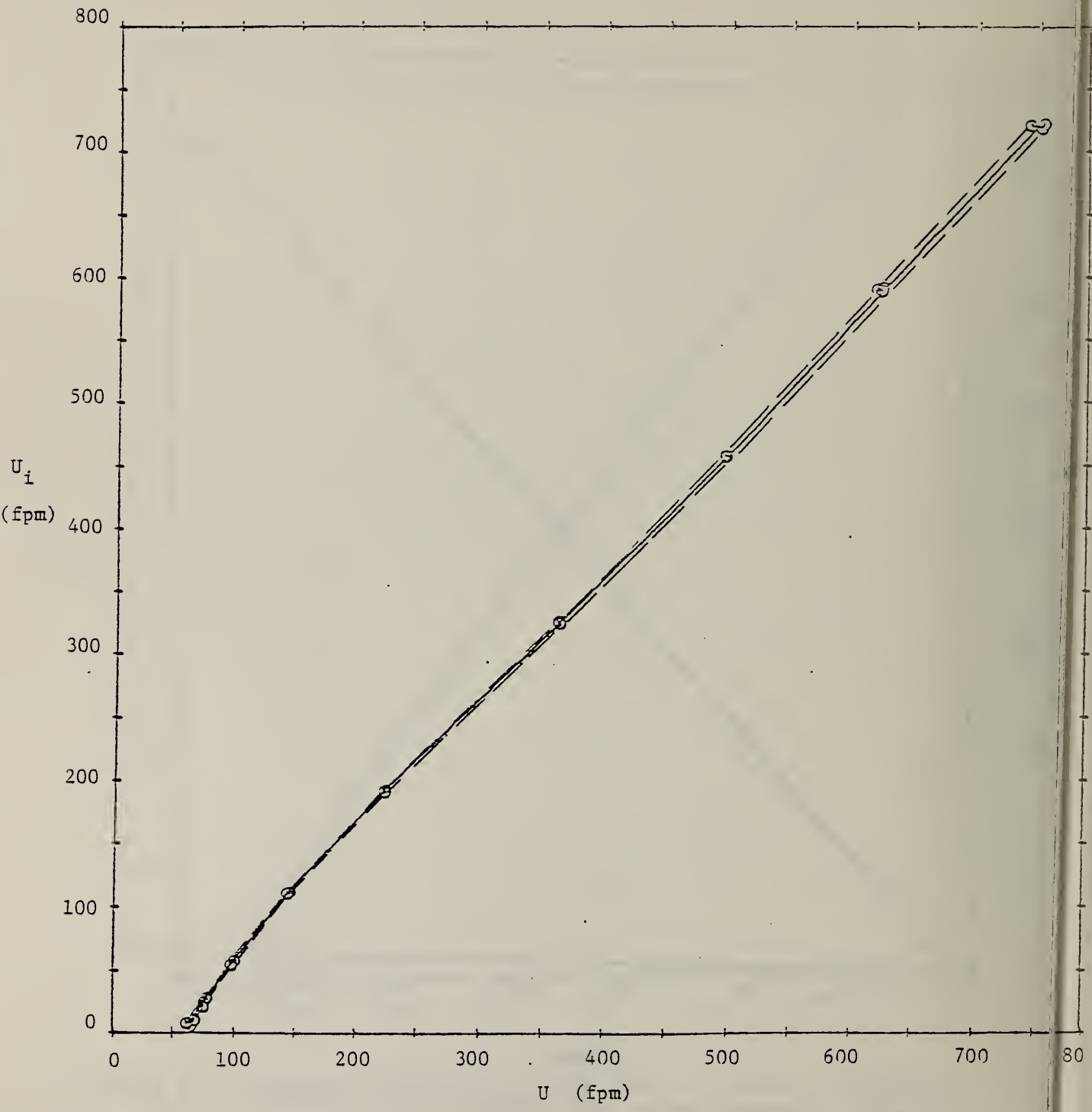

FIGURE 18. INDICATED VERSUS TRUE VELOCITY WITH ± CURVES. INSTRUMENT C.

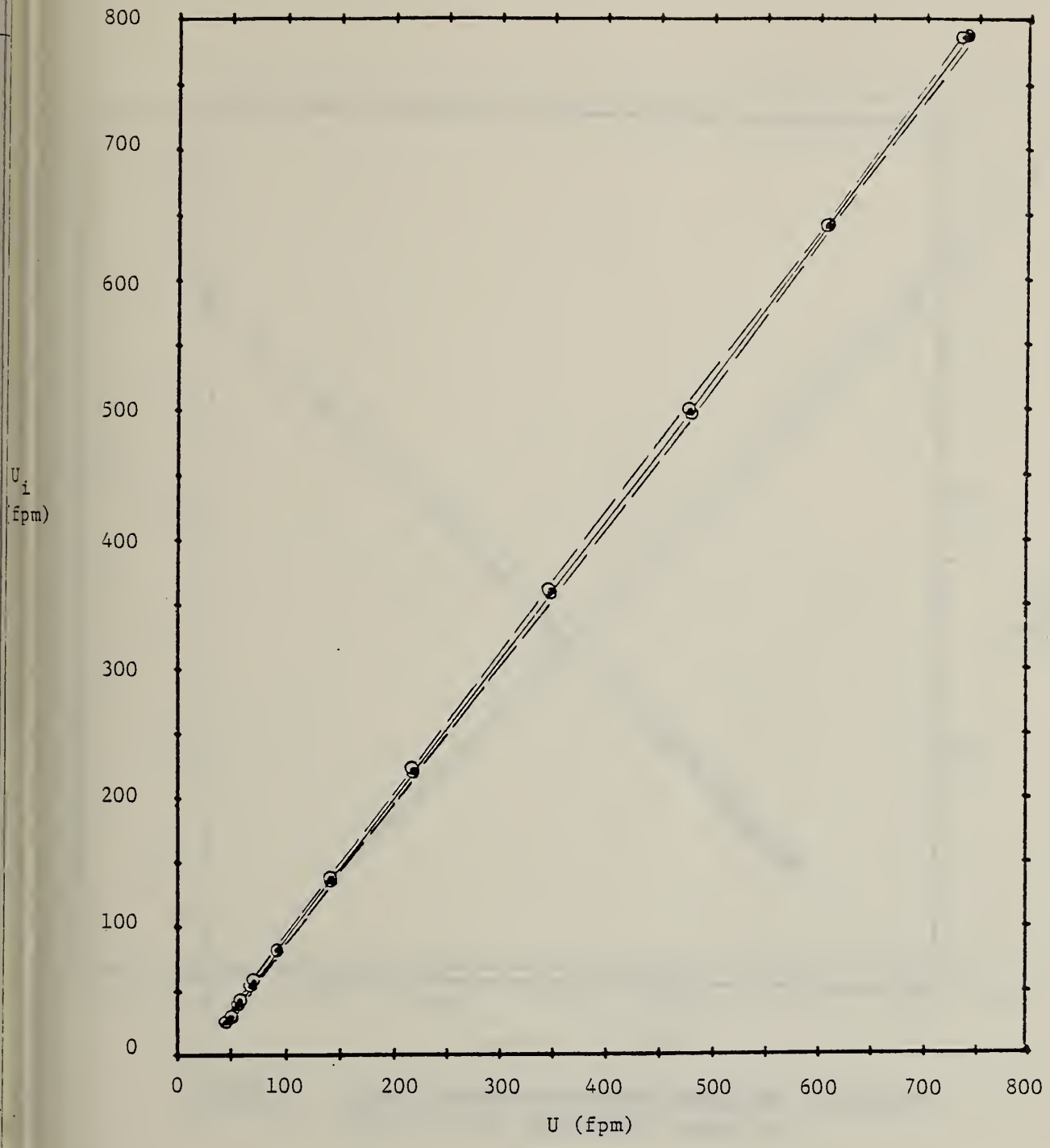

FIGURE 19. INDICATED VERSUS TRUE VELOCITY WITH ± 2σ CURVES. INSTRUMENT D.

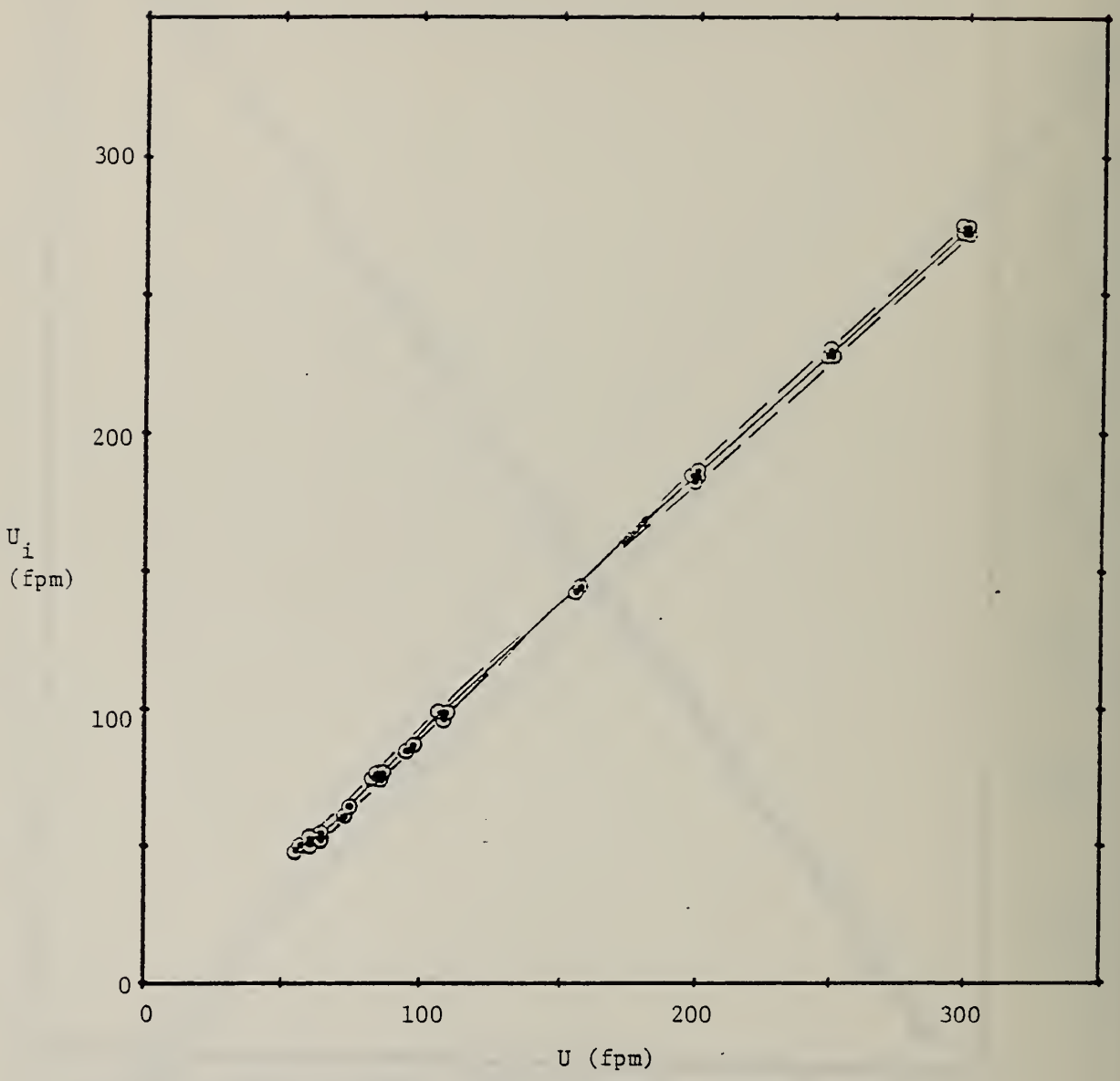

FIGURE 20. INDICATED VERSUS TRUE VELOCITY WITH ± 2σ CURVES, LOW RANGE. INSTRUMENT E.

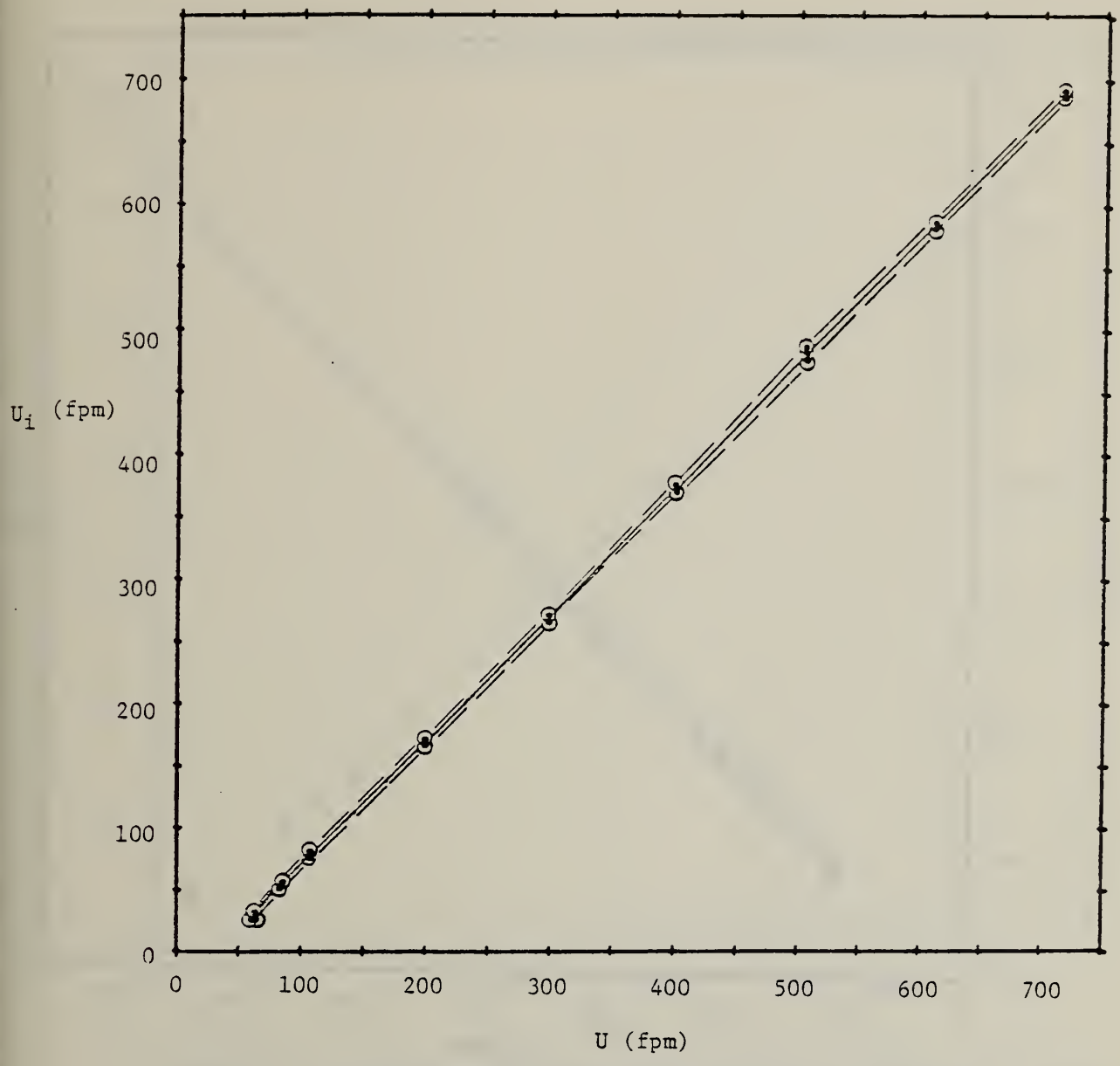

FIGURE 21. INDICATED VERSUS TRUE VELOCITY WITH ± 2σ CURVES, MEDIUM RANGE. INSTRUMENT E.

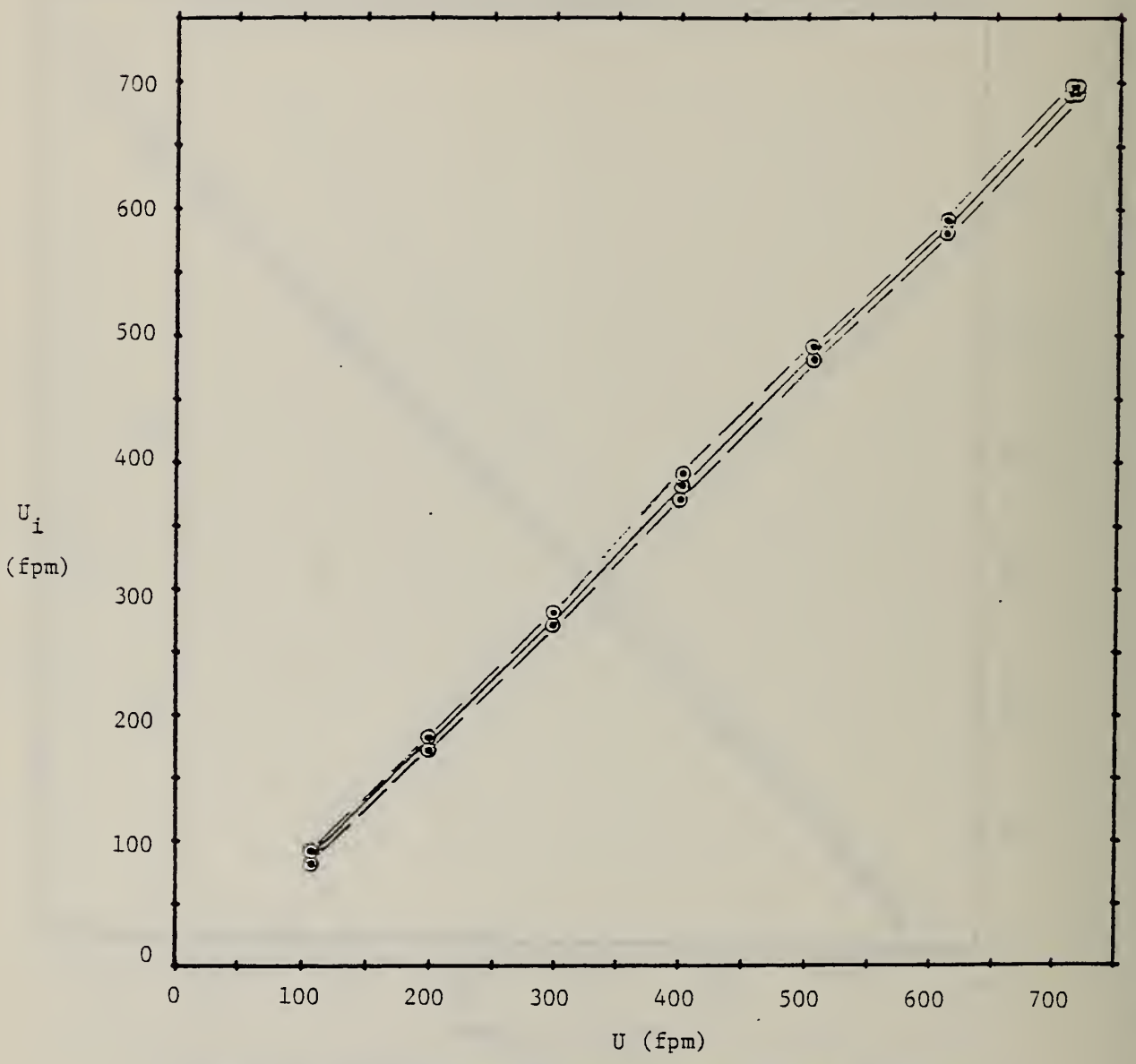

FIGURE 22. INDICATED VERSUS TRUE VELOCITY WITH ± 2σ CURVES, HIGH RANGE. INSTRUMENT E.

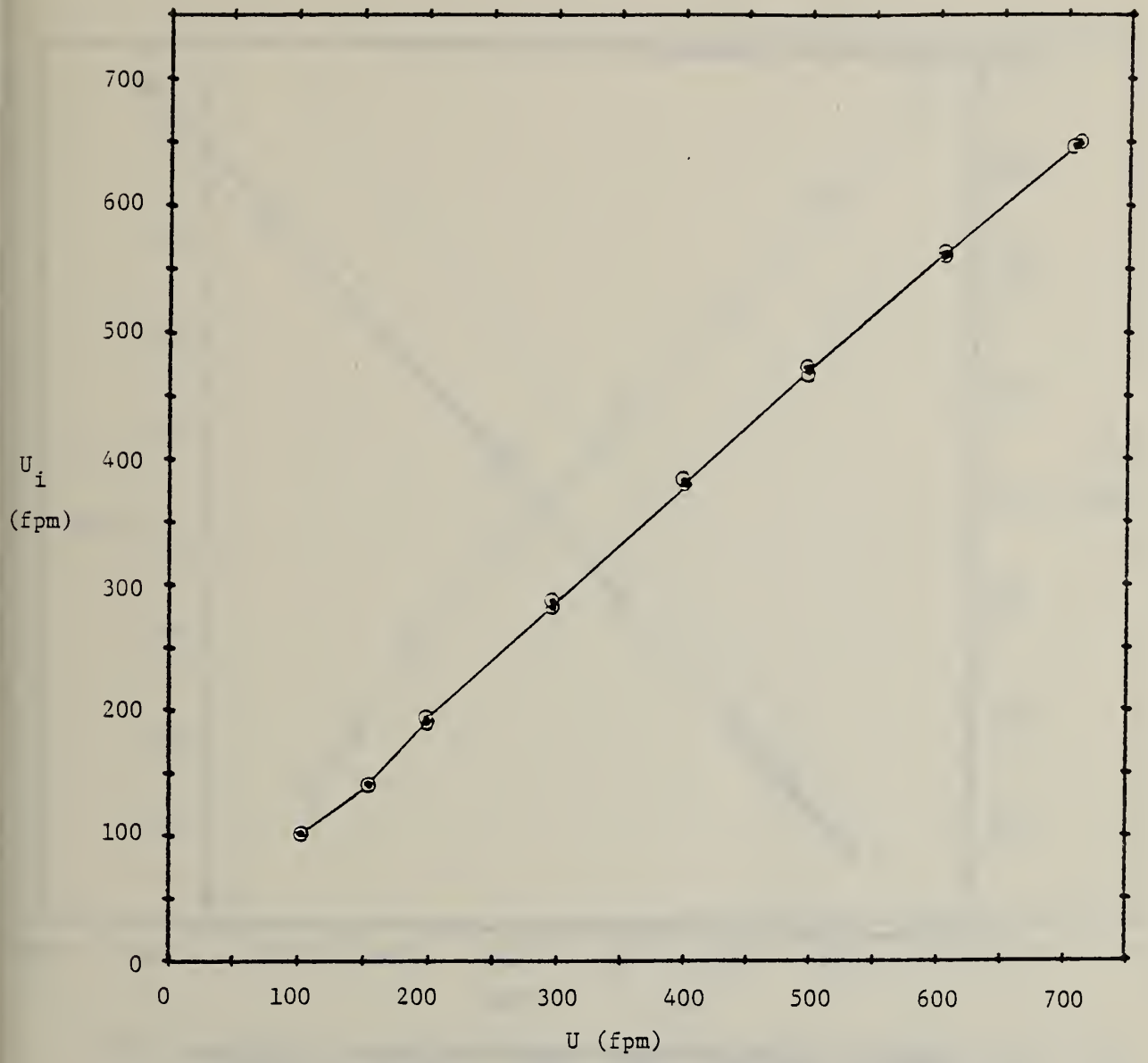

FIGURE 23. INDICATED VERSUS TRUE VELOCITY FOR PITOT PROBE, LOW RANGE. INSTRUMENT F.

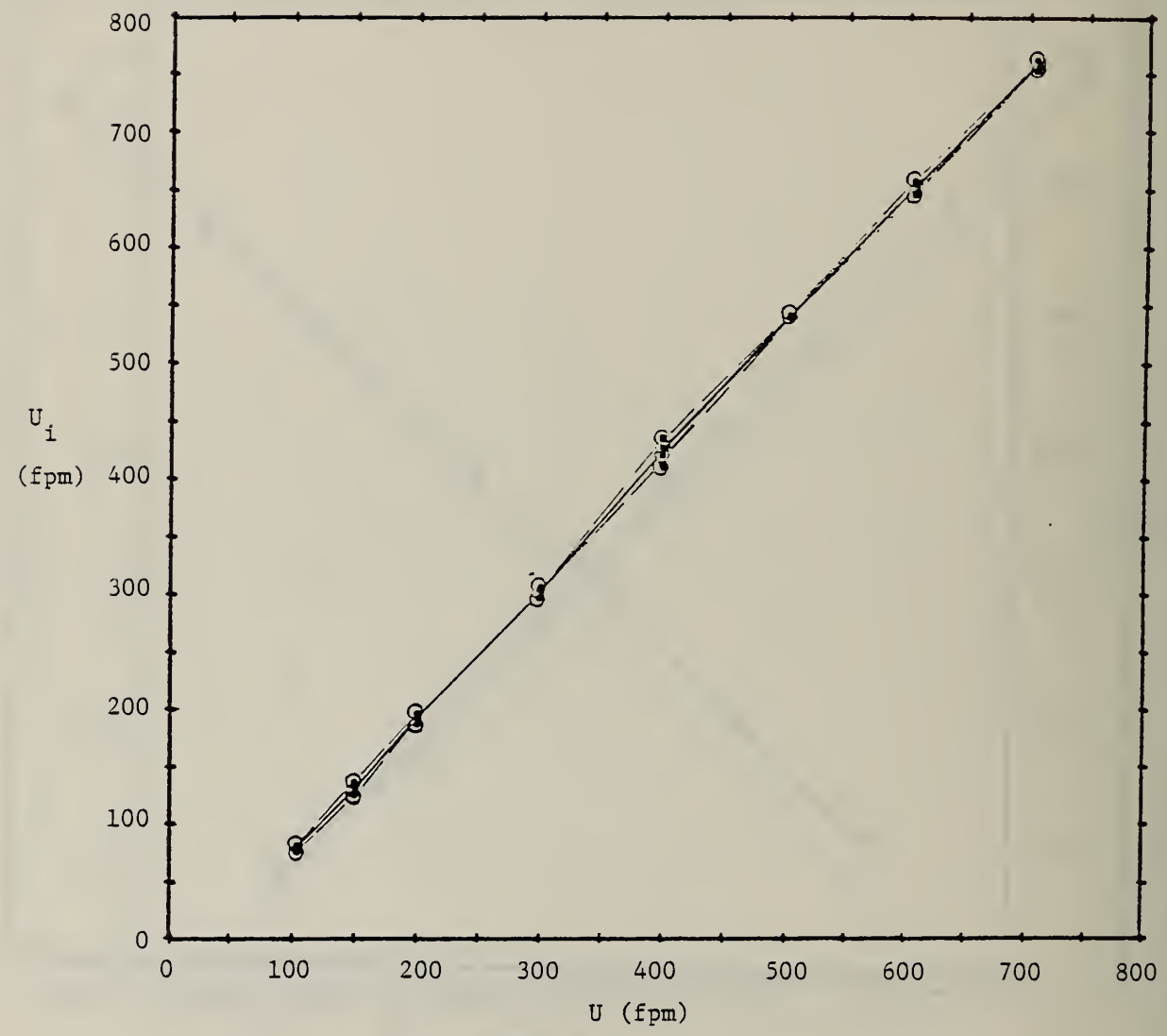

FIGURE 24. INDICATED VERSUS TRUE VELOCITY FOR PITOT PROBE, HIGH RANGE. INSTRUMENT F.

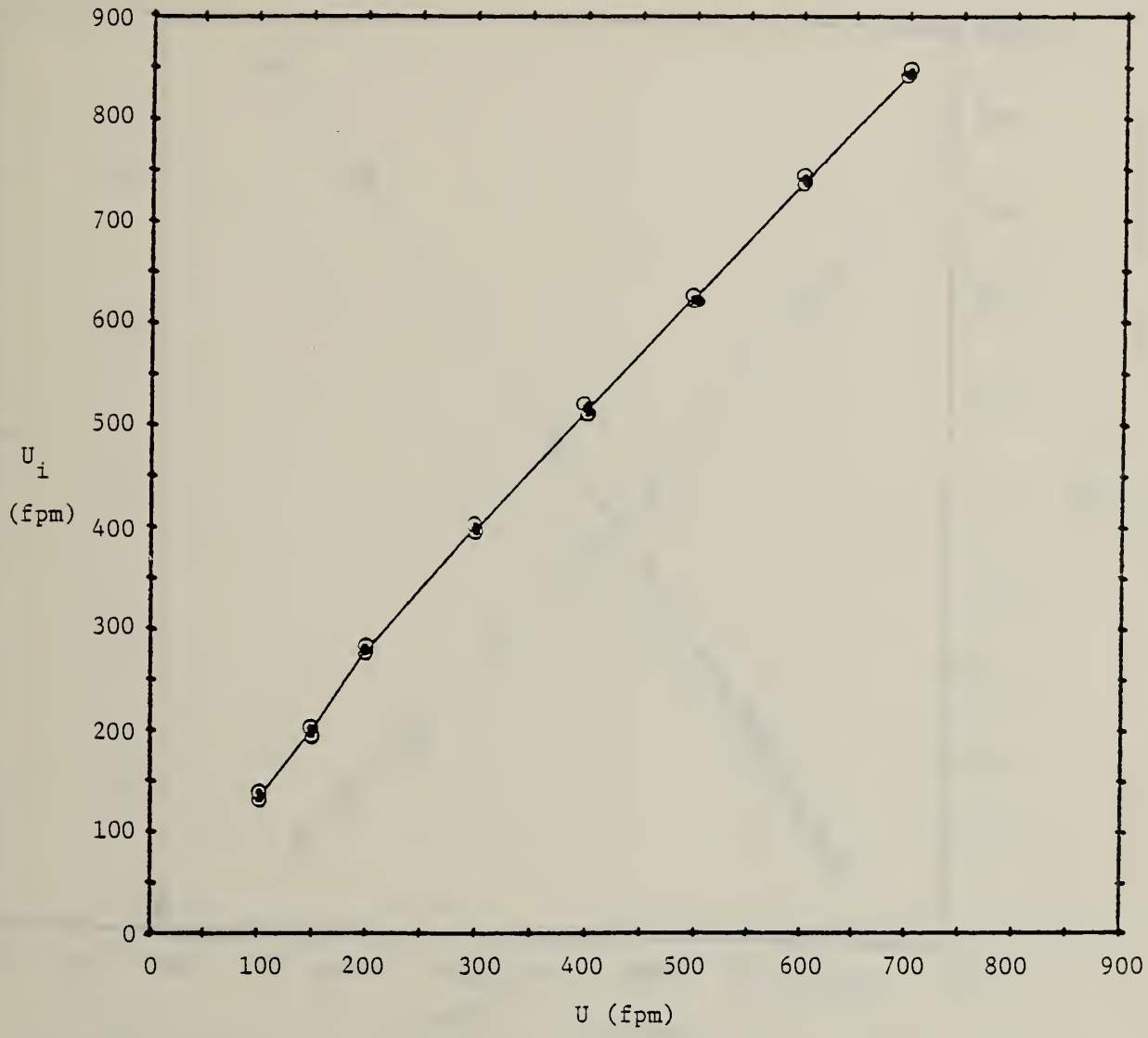

FIGURE 25. INDICATED VERSUS TRUE VELOCITY FOR DIFFUSER PROBE, LOW RANGE. INSTRUMENT F.

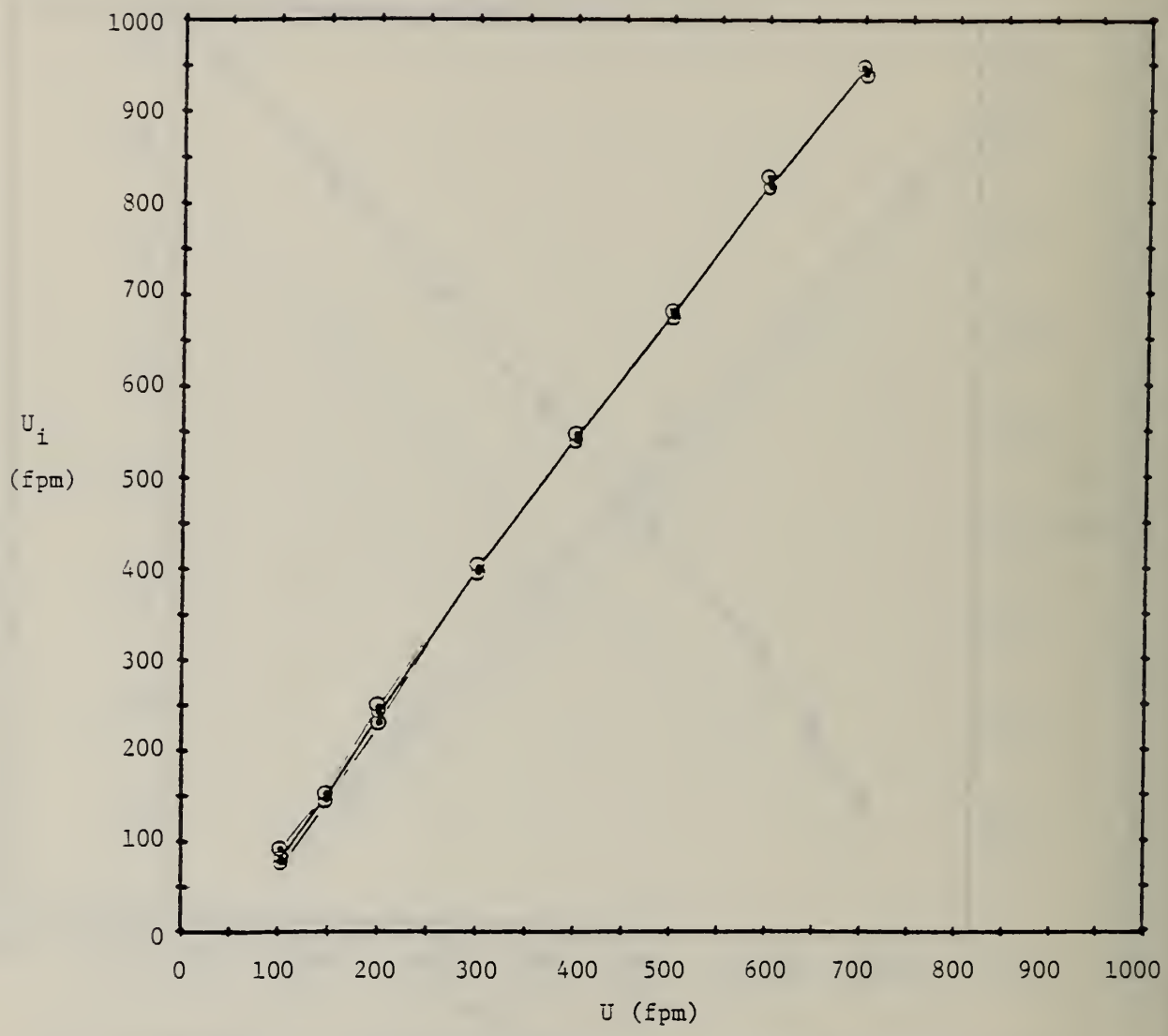

FIGURE 26. INDICATED VERSUS TRUE VELOCITY FOR DIFFUSER PROBE, HIGH RANGE. INSTRUMENT F.

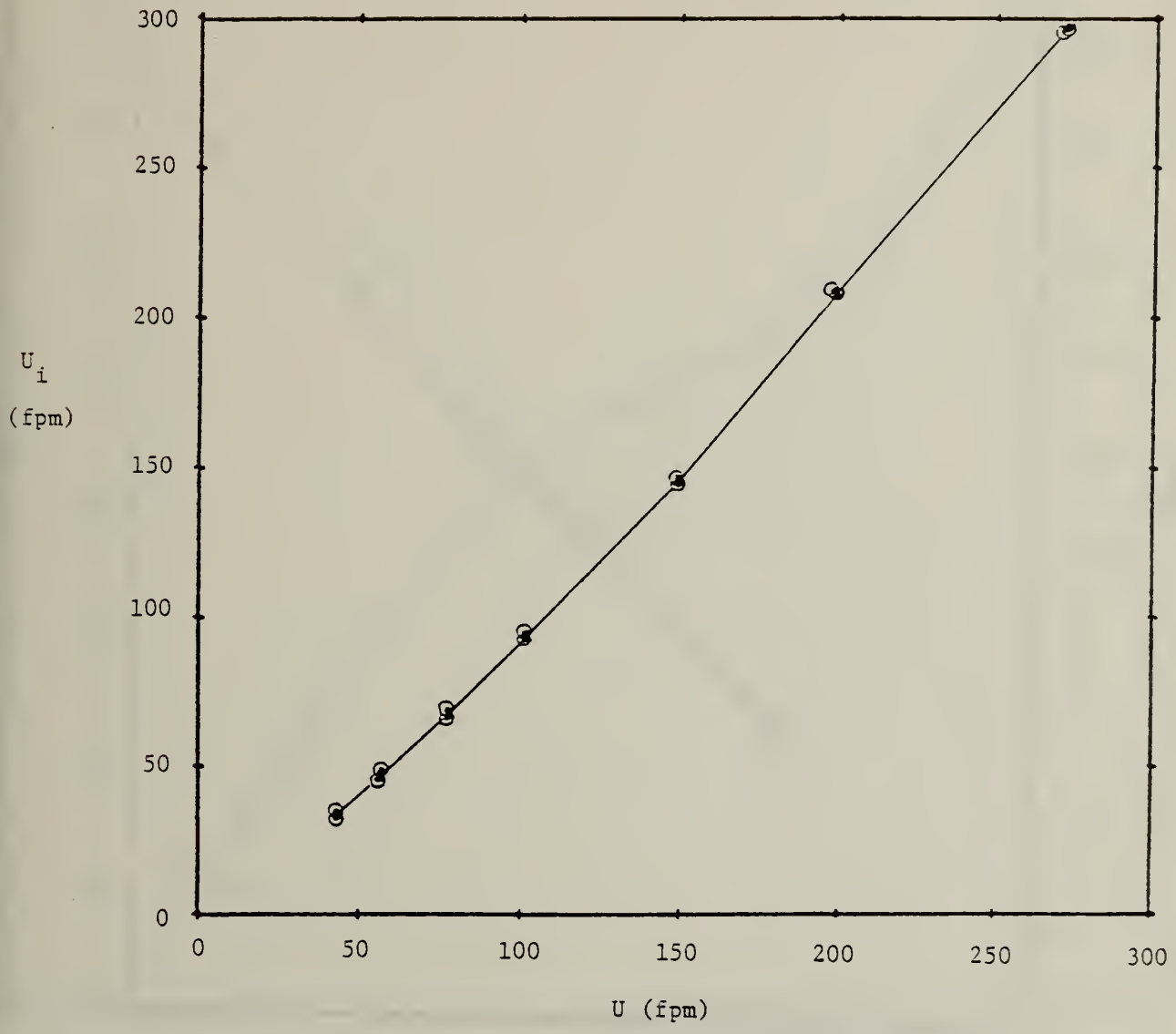

FIGURE 27. INDICATED VERSUS TRUE VELOCITY FOR LOW VELOCITY PROBE. INSTRUMENT F.

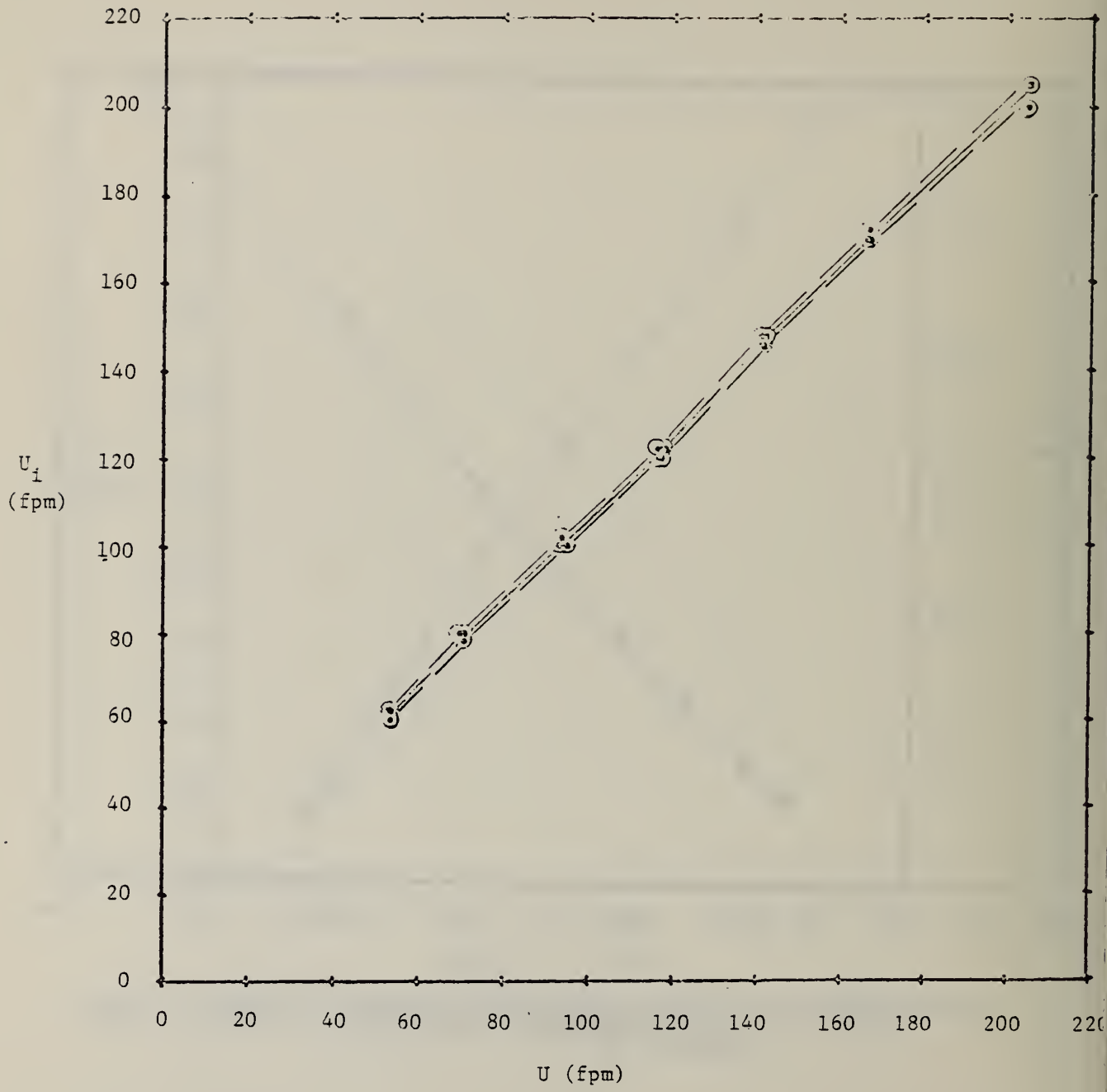

FIGURE 28. INDICATED VERSUS TRUE VELOCITY WITH ± 2 σ CURVES, LOW RANGE. INSTRUMENT G.

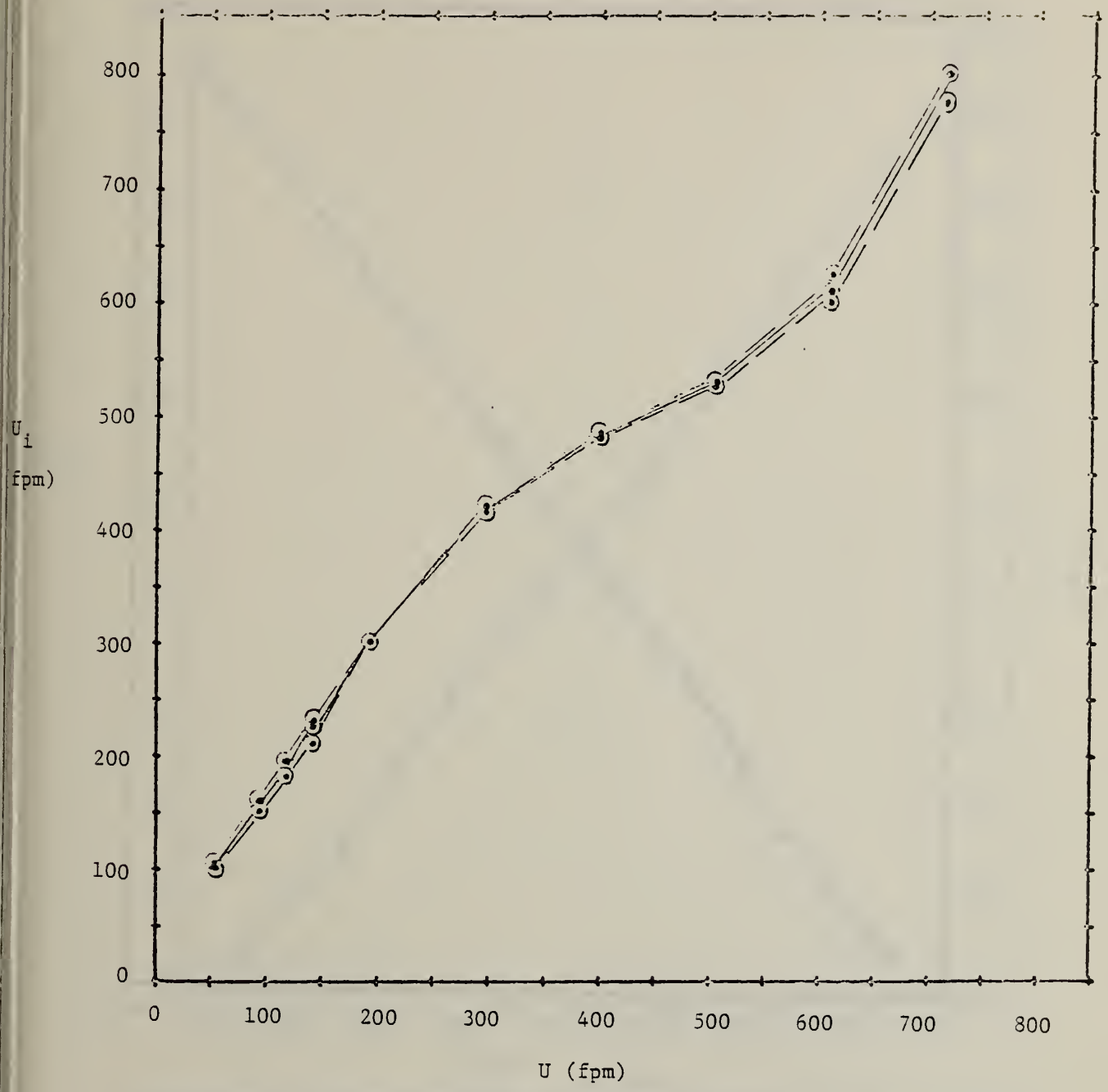

FIGURE 29. INDICATED VERSUS TRUE VELOCITY WITH ± 2 σ CURVES, HIGH RANGE. INSTRUMENT G.

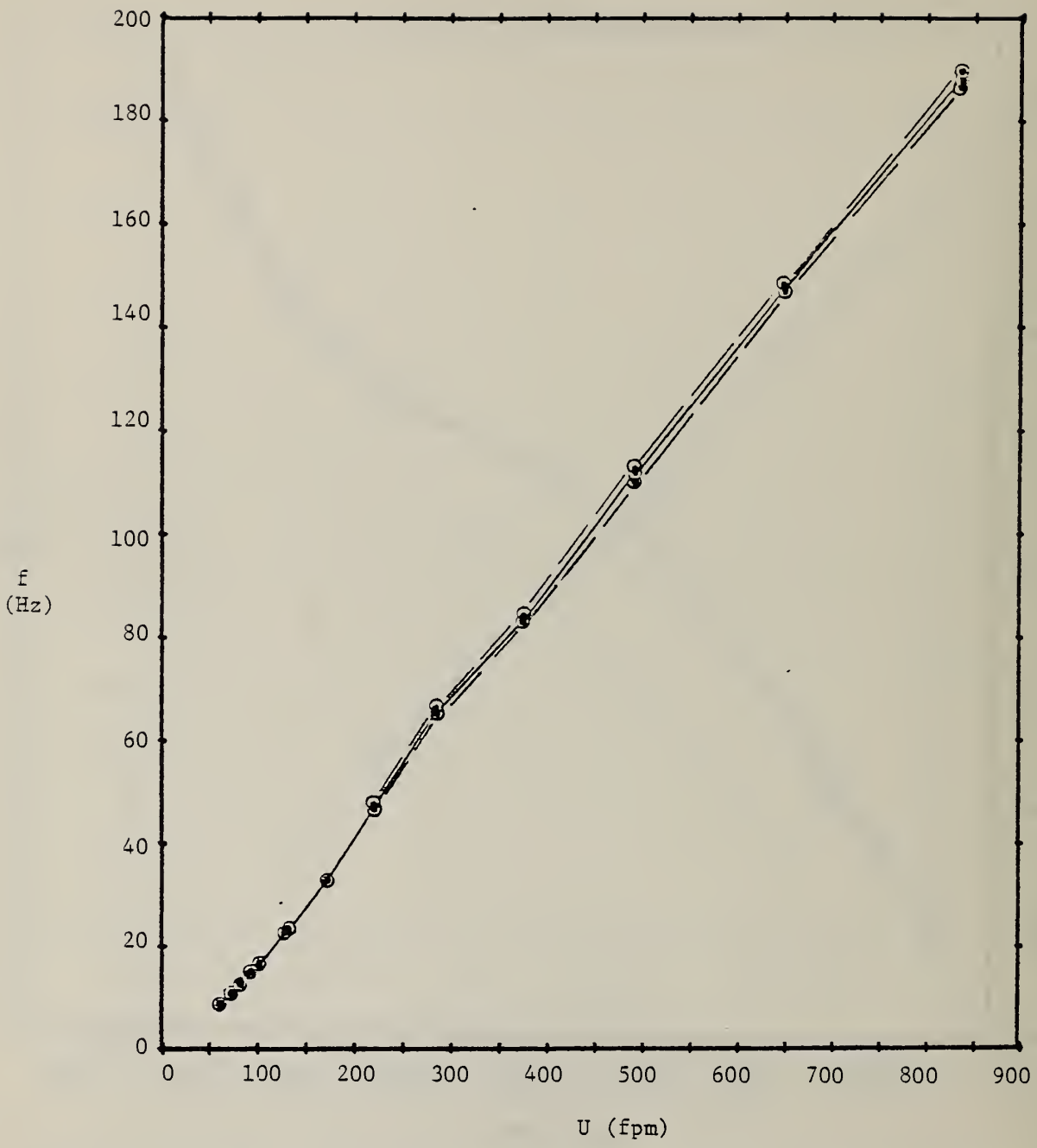

FIGURE 30. PULSE FREQUENCY VERSUS TRUE VELOCITY WITH ± $2\sigma_f$ CURVES. INSTRUMENT H.

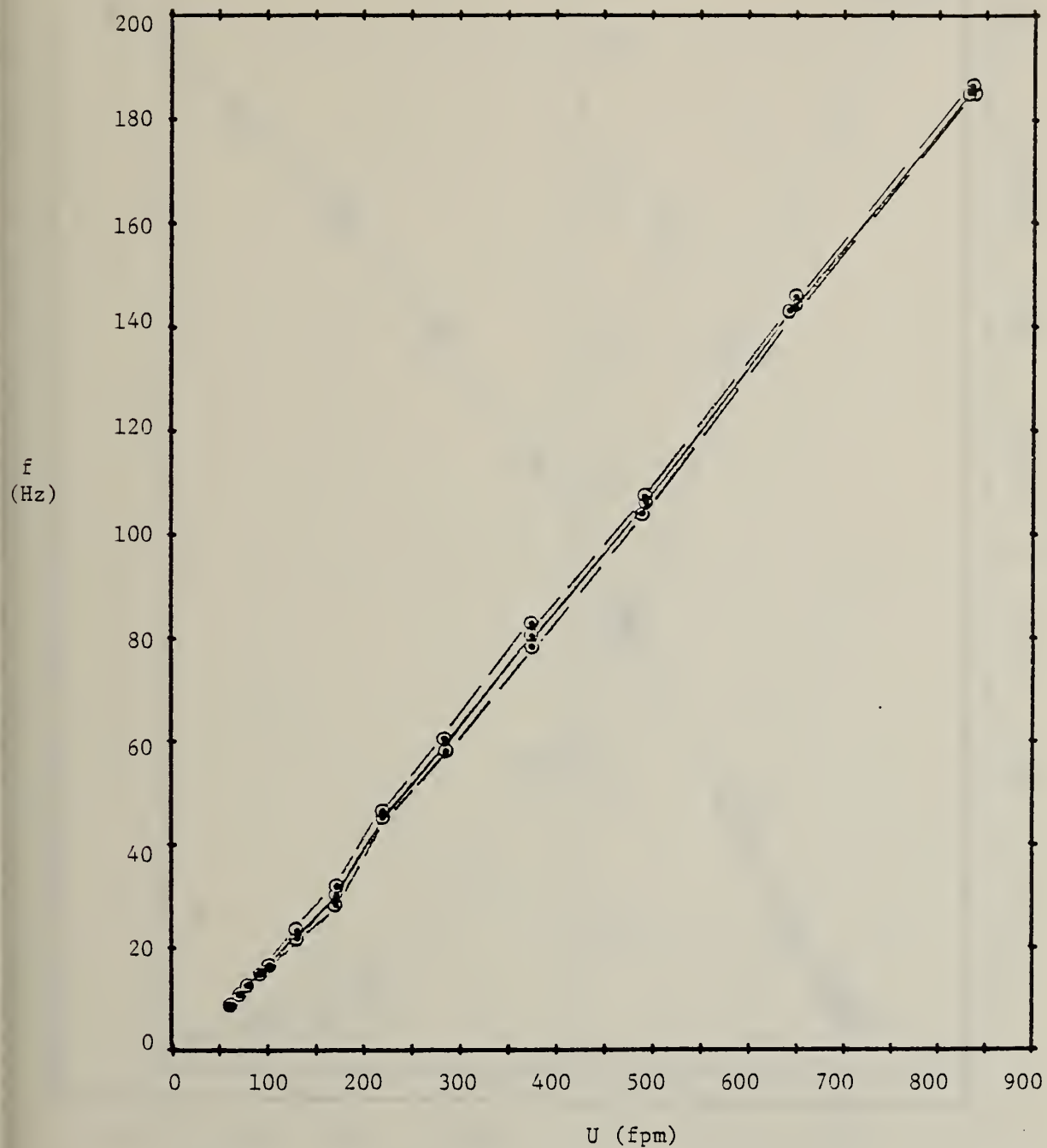

FIGURE 31. PULSE FREQUENCY VERSUS TRUE VELOCITY WITH $\pm 2\sigma_f$ CURVES. INSTRUMENT I.

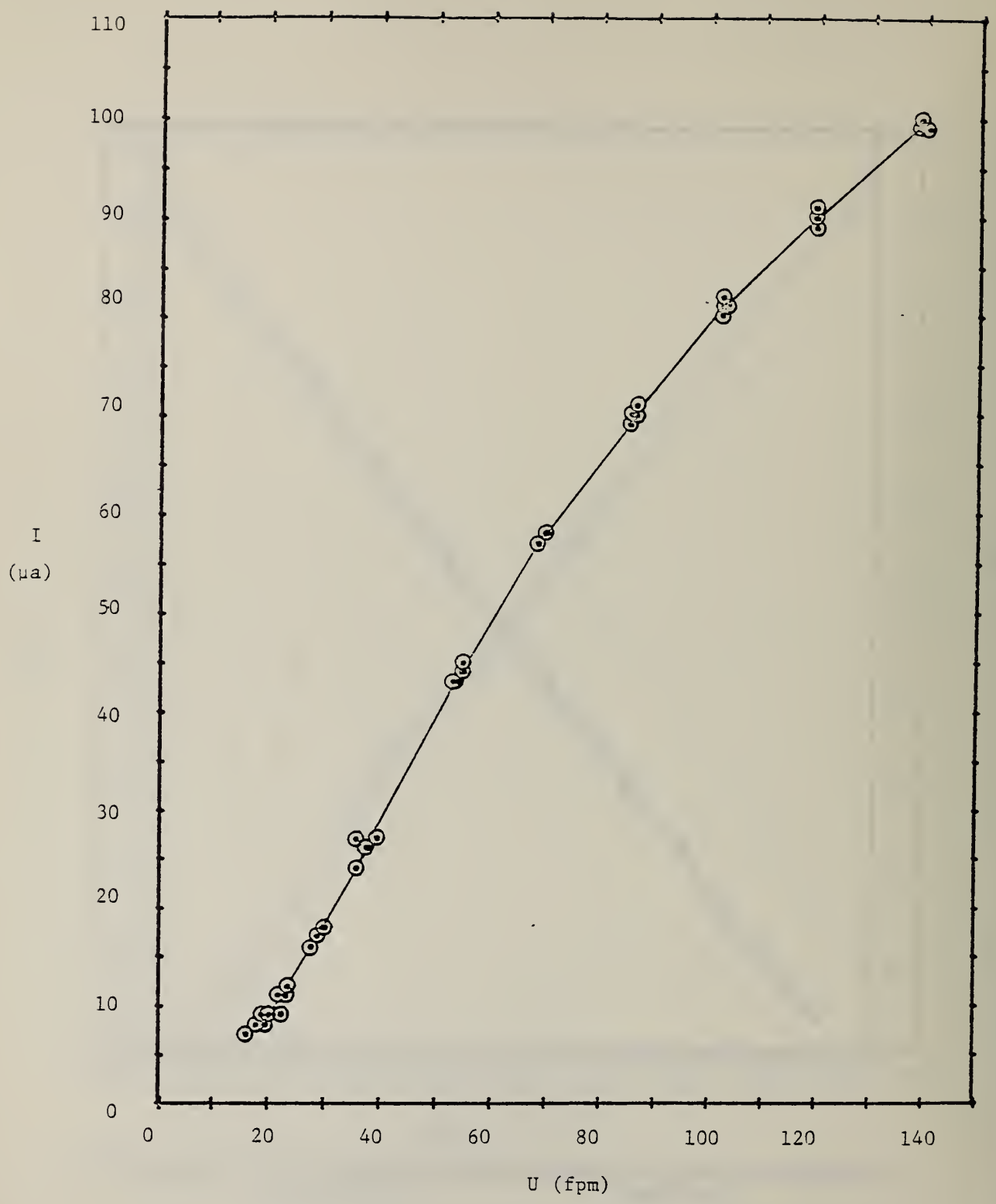

FIGURE 32. OUTPUT OF INSTRUMENT J AGAINST VELOCITY.

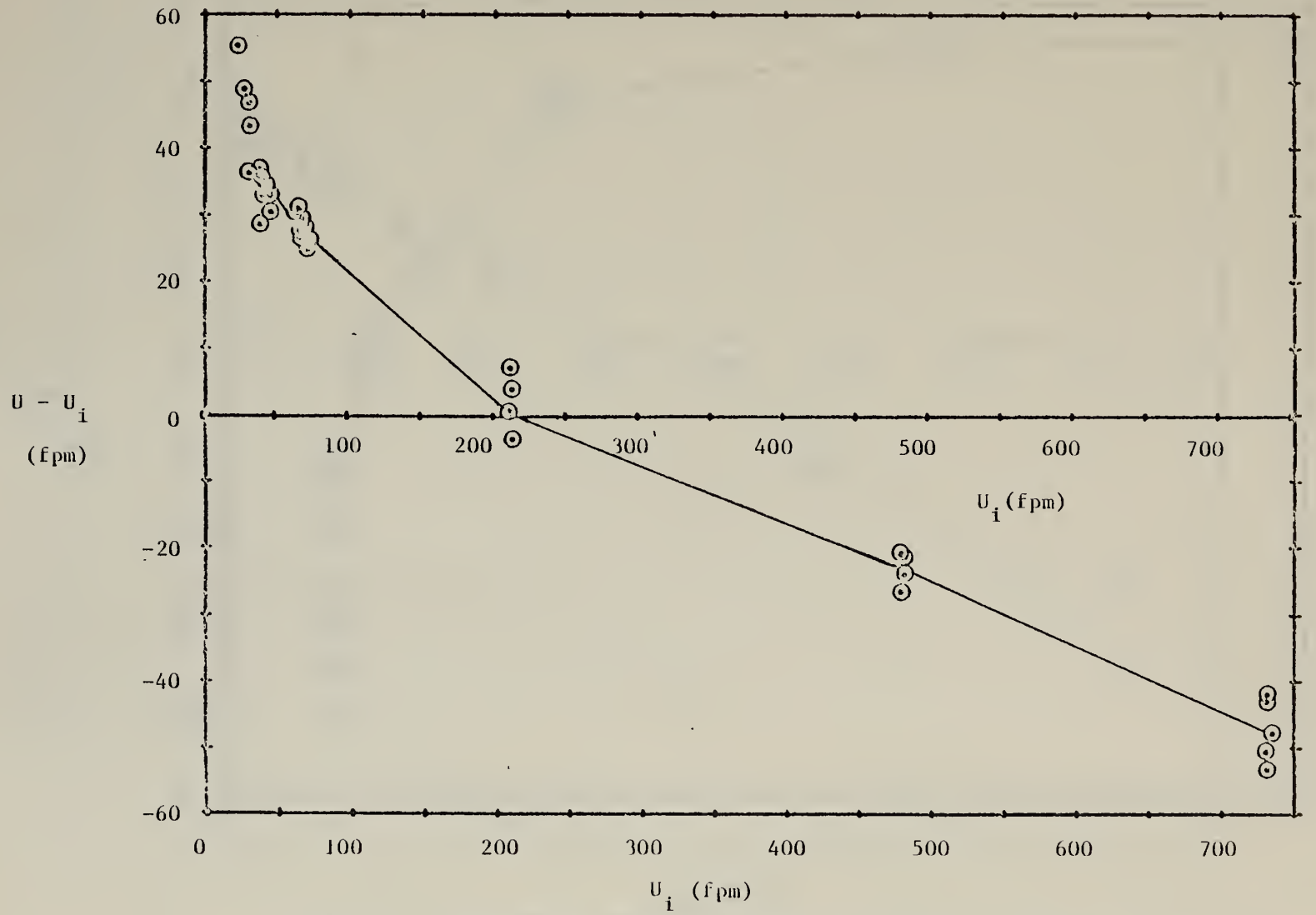

FIGURE 33. DEVIATION OF INDICATED FROM TRUE VELOCITY. INSTRUMENT A.

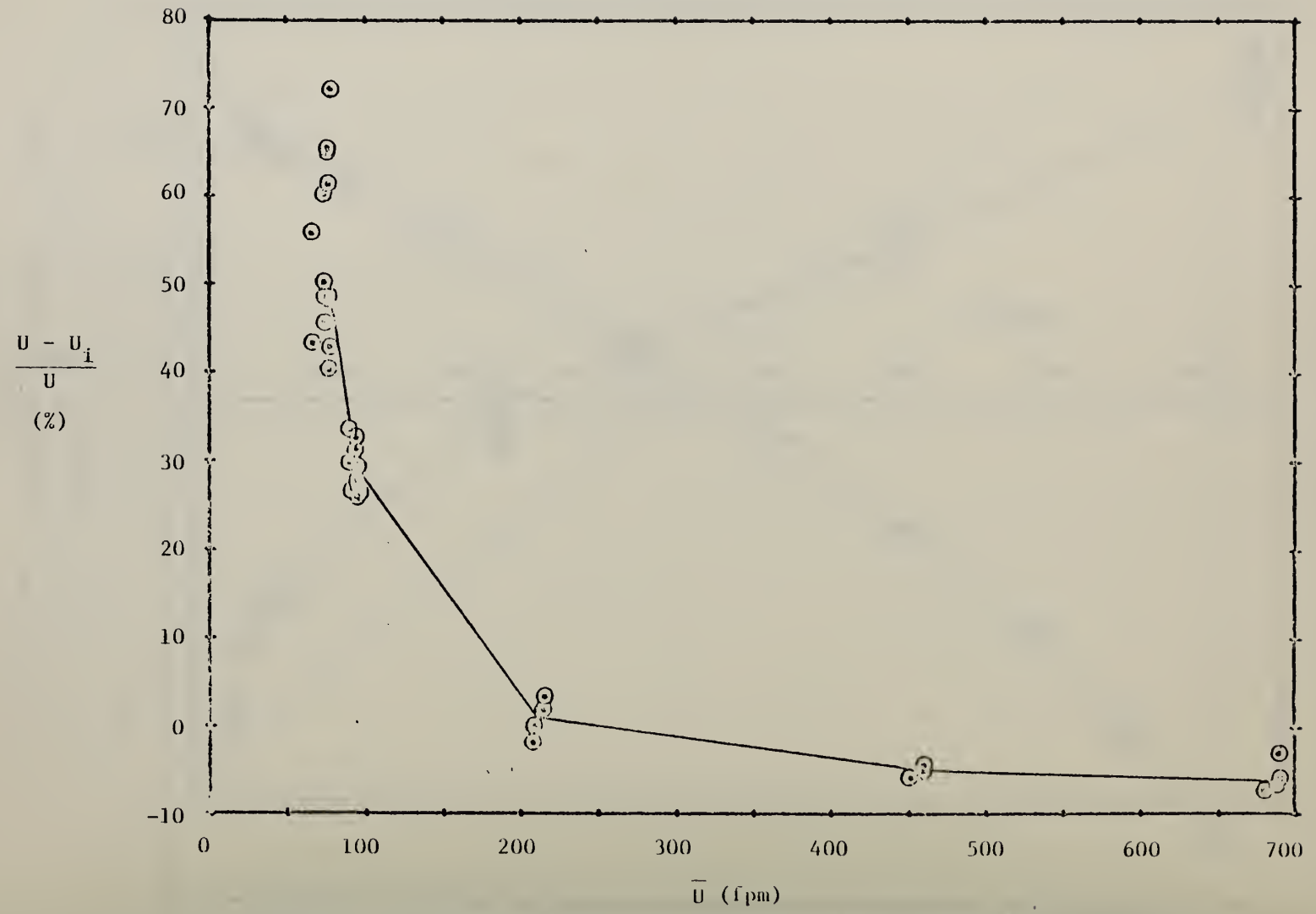

FIGURE 34. PERCENT DEVIATION OF INDICATED FROM TRUE VELOCITY. INSTRUMENT A.

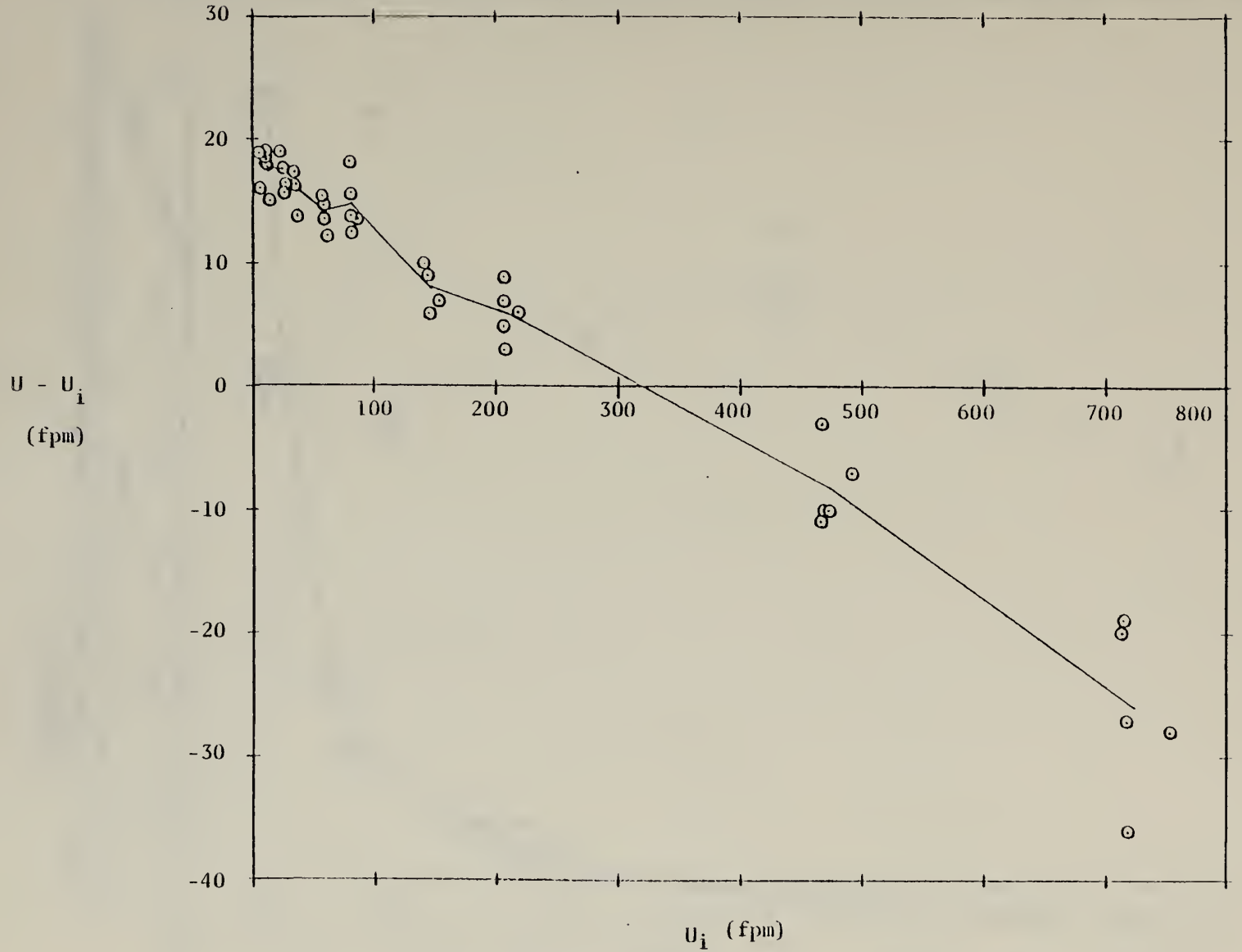

FIGURE 35. DEVIATION OF INDICATED VELOCITY FROM TRUE VELOCITY. INSTRUMENT B.

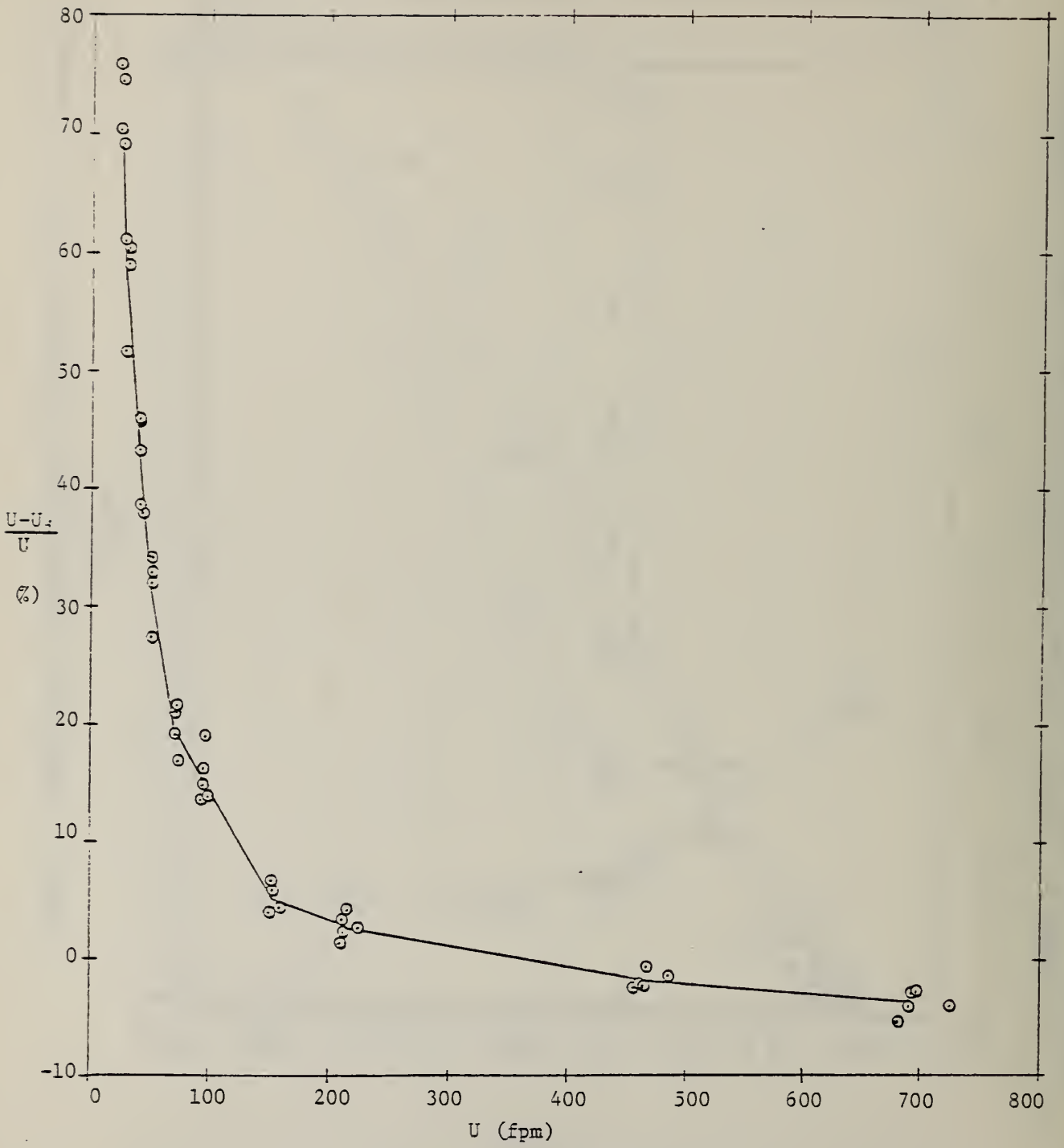

FIGURE 36. PERCENT DEVIATION OF INDICATED VELOCITY FROM TRUE VELOCITY. INSTRUMENT B.

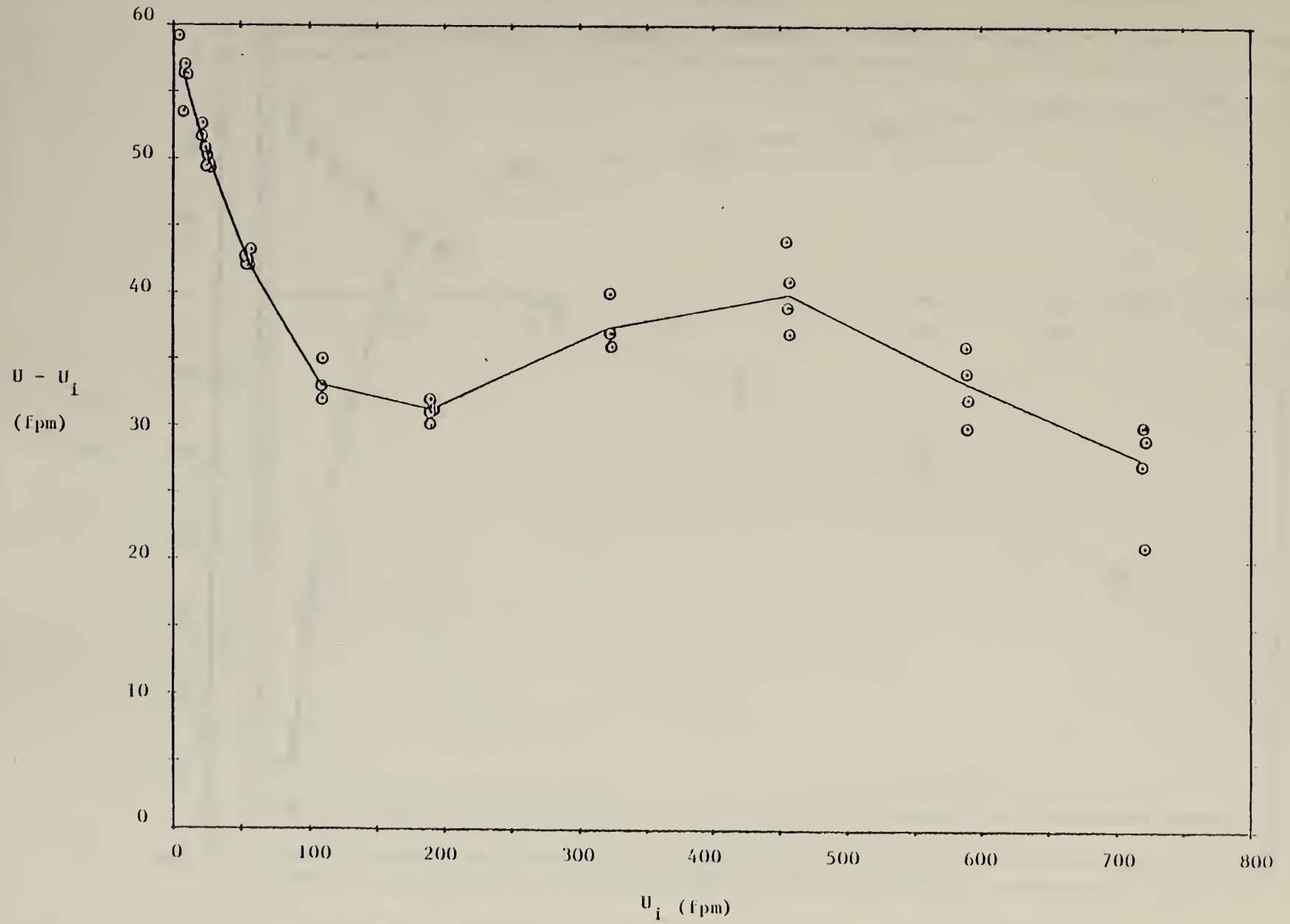

FIGURE 37. DEVIATION OF INDICATED VELOCITY FROM TRUE VELOCITY. INSTRUMENT C.

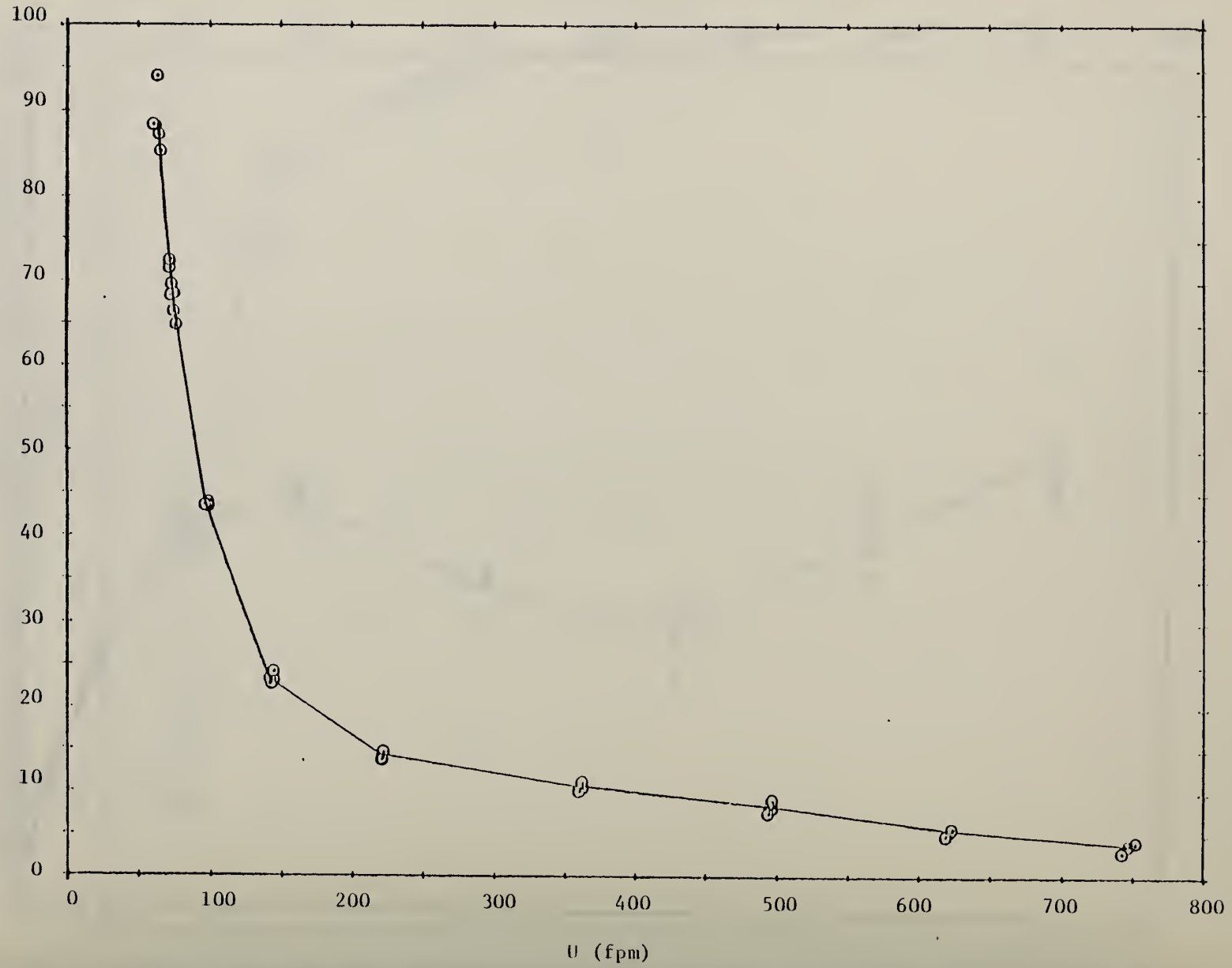

FIGURE 38. PERCENT DEVIATION OF INDICATED VELOCITY FROM TRUE VELOCITY. INSTRUMENT C.

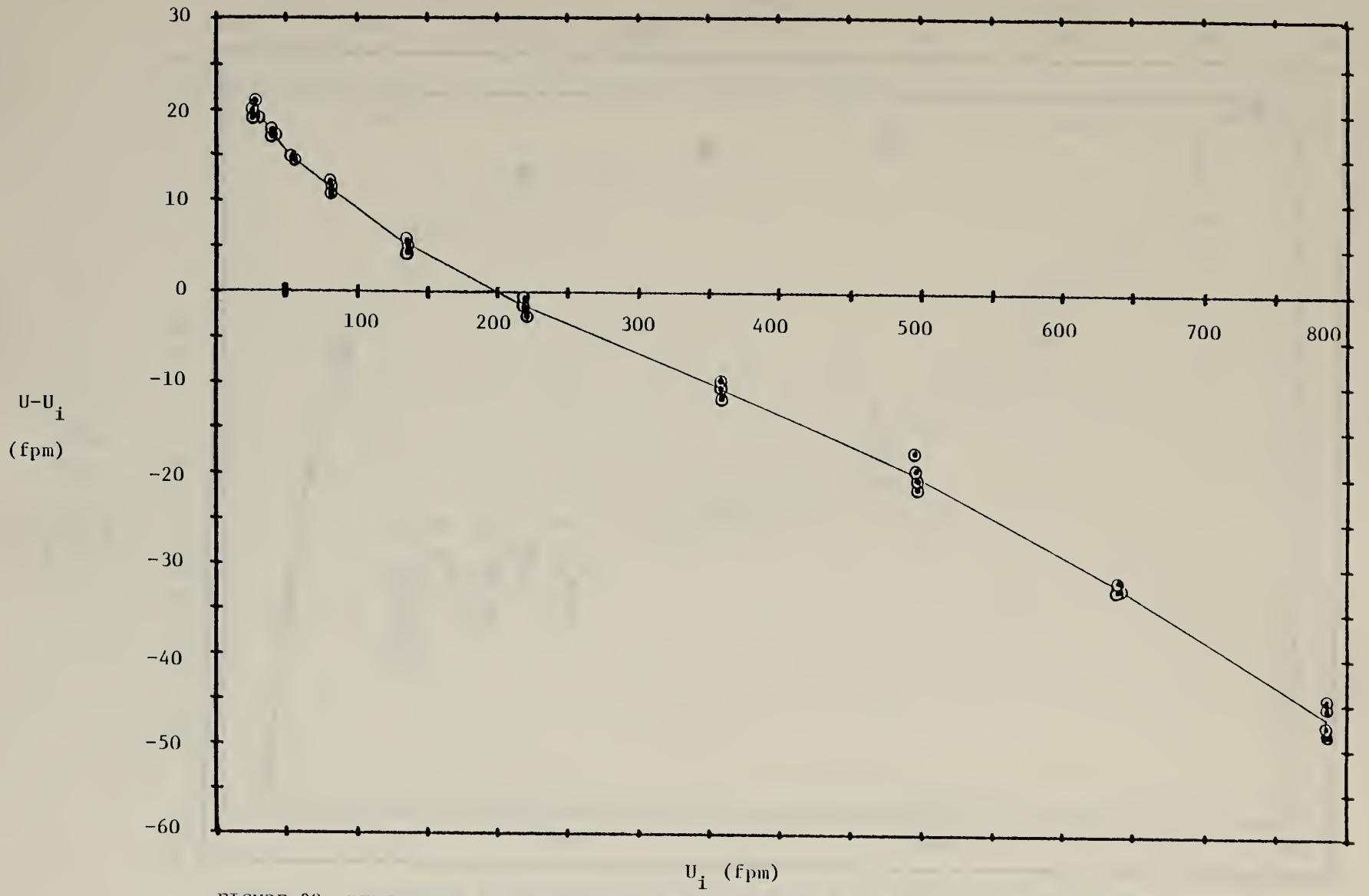

FIGURE 39. DEVIATION OF INDICATED VELOCITY FROM TRUE VELOCITY. INSTRUMENT D.

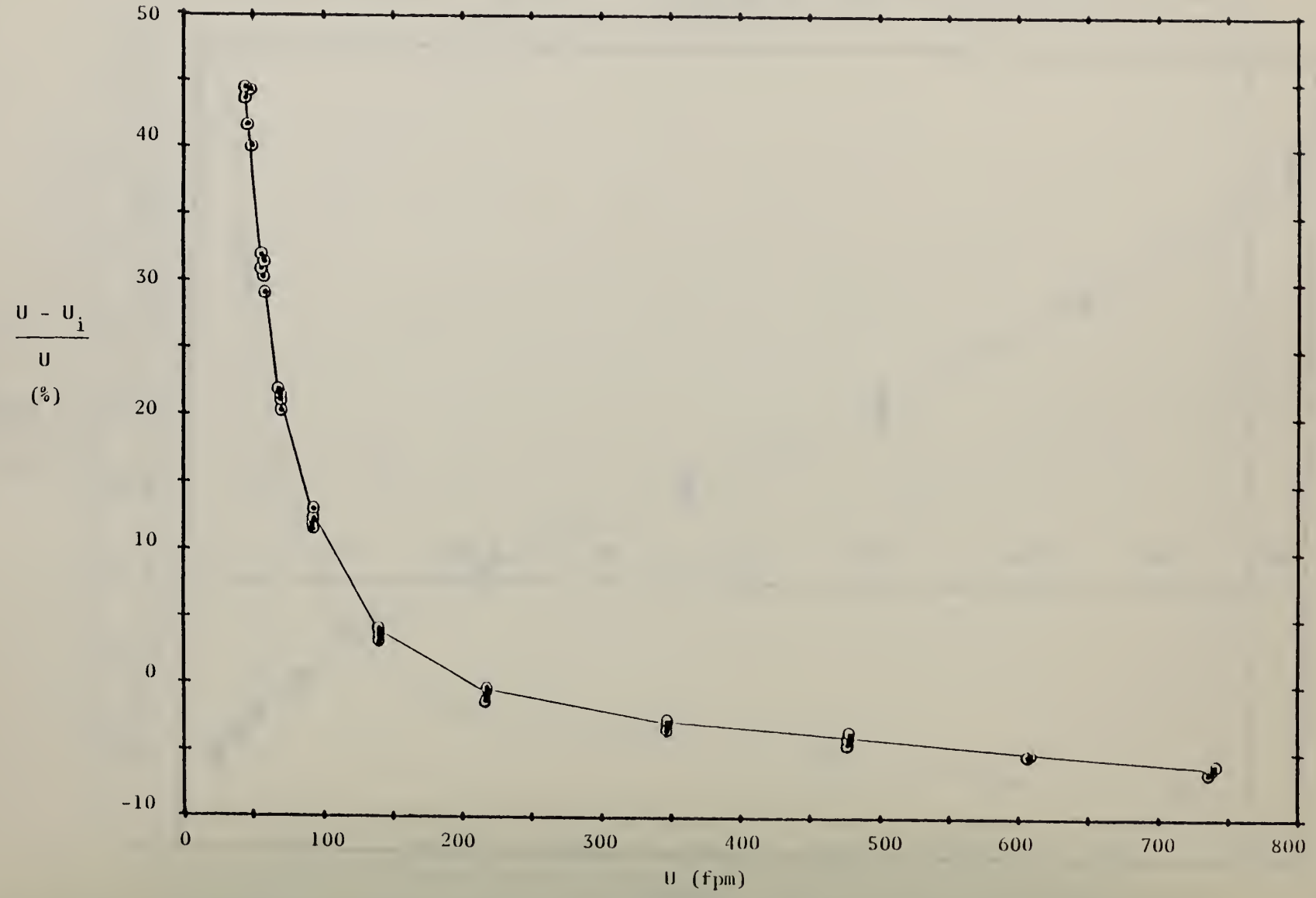

FIGURE 40. PERCENT DEVIATION OF INDICATED VELOCITY FROM TRUE VELOCITY. INSTRUMENT D.

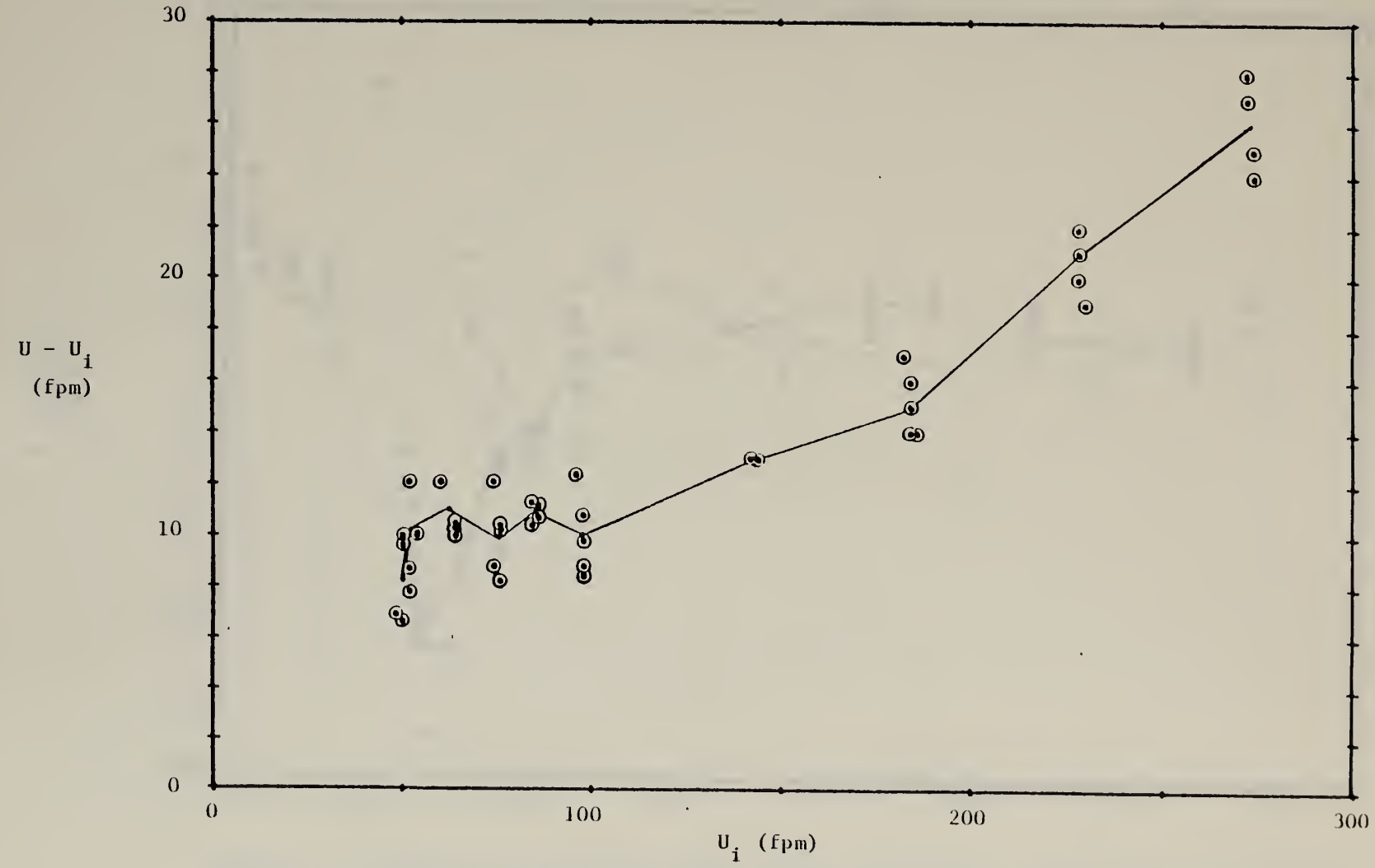

FIGURE 41. DEVIATION OF INDICATED VELOCITY FROM TRUE VELOCITY, LOW RANGE. INSTRUMENT E.

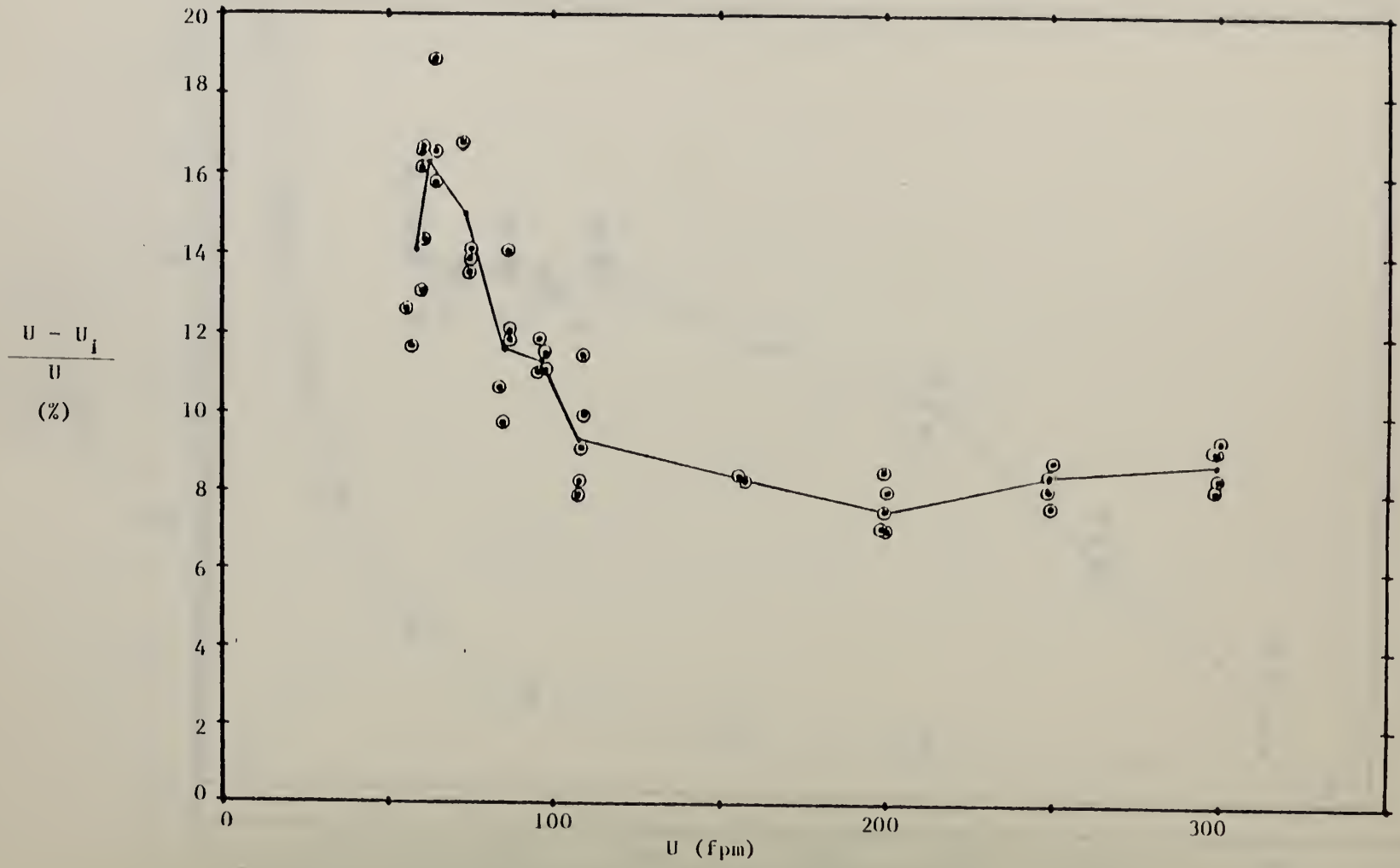

FIGURE 42. PERCENT DEVIATION OF INDICATED FROM TRUE VELOCITY, LOW RANGE. INSTRUMENT E.

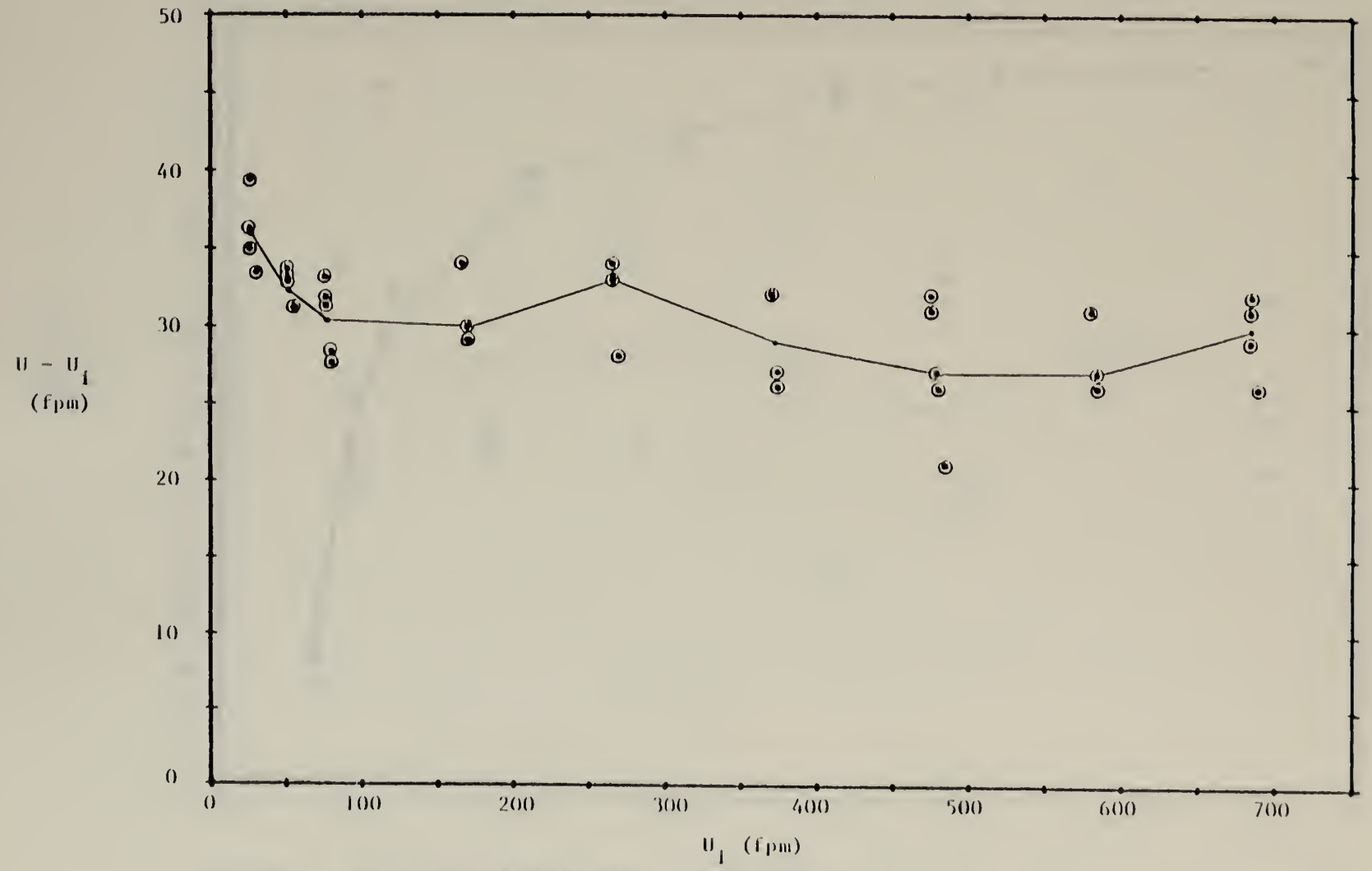

FIGURE 43 DEVIATION OF INDICATED VELOCITY FROM TRUE VELOCITY, MEDIUM RANGE. INSTRUMENT E.

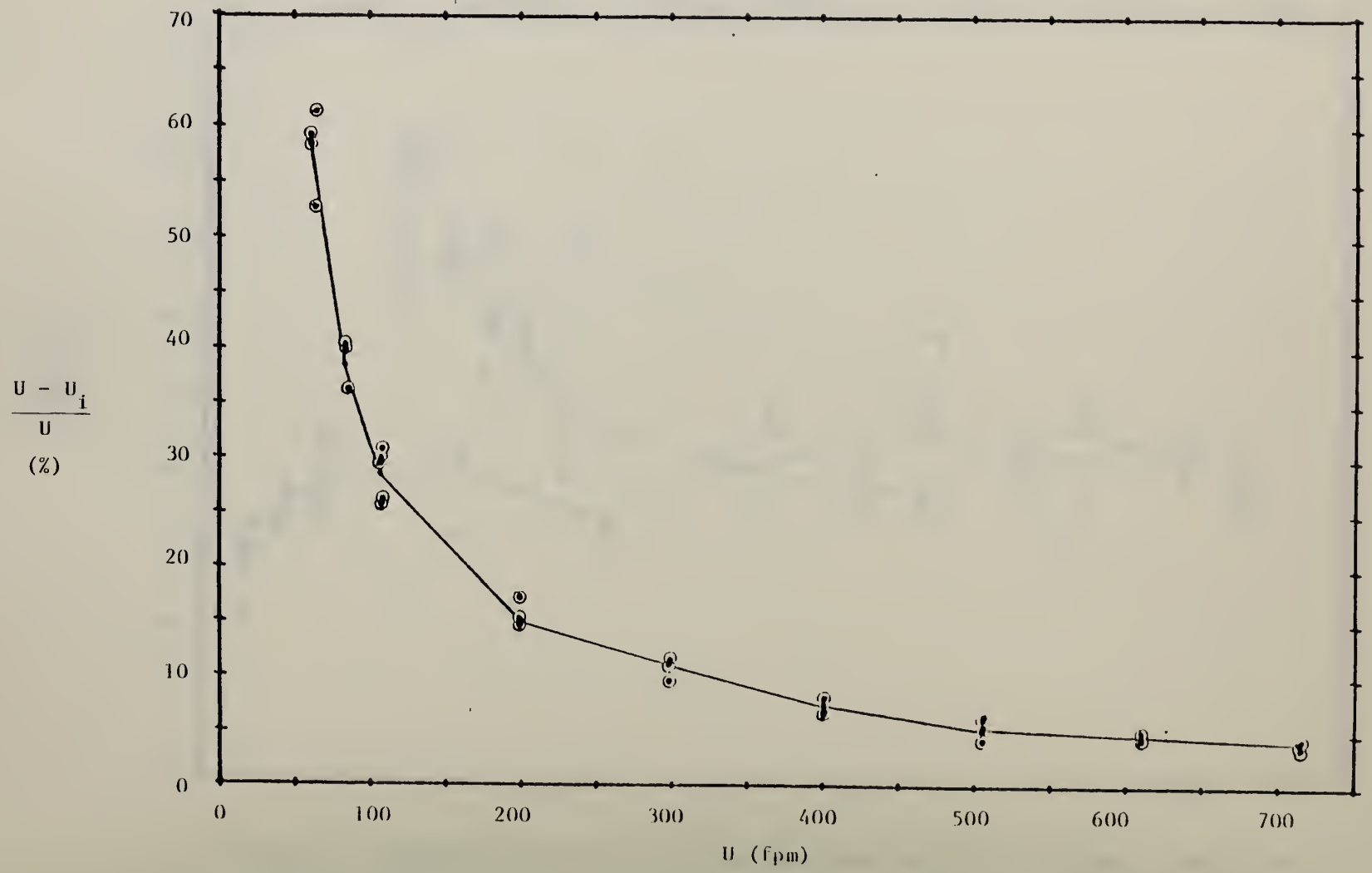

FIGURE 44. PERCENT DEVIATION OF INDICATED FROM TRUE VELOCITY, MEDIUM RANGE. INSTRUMENT E.

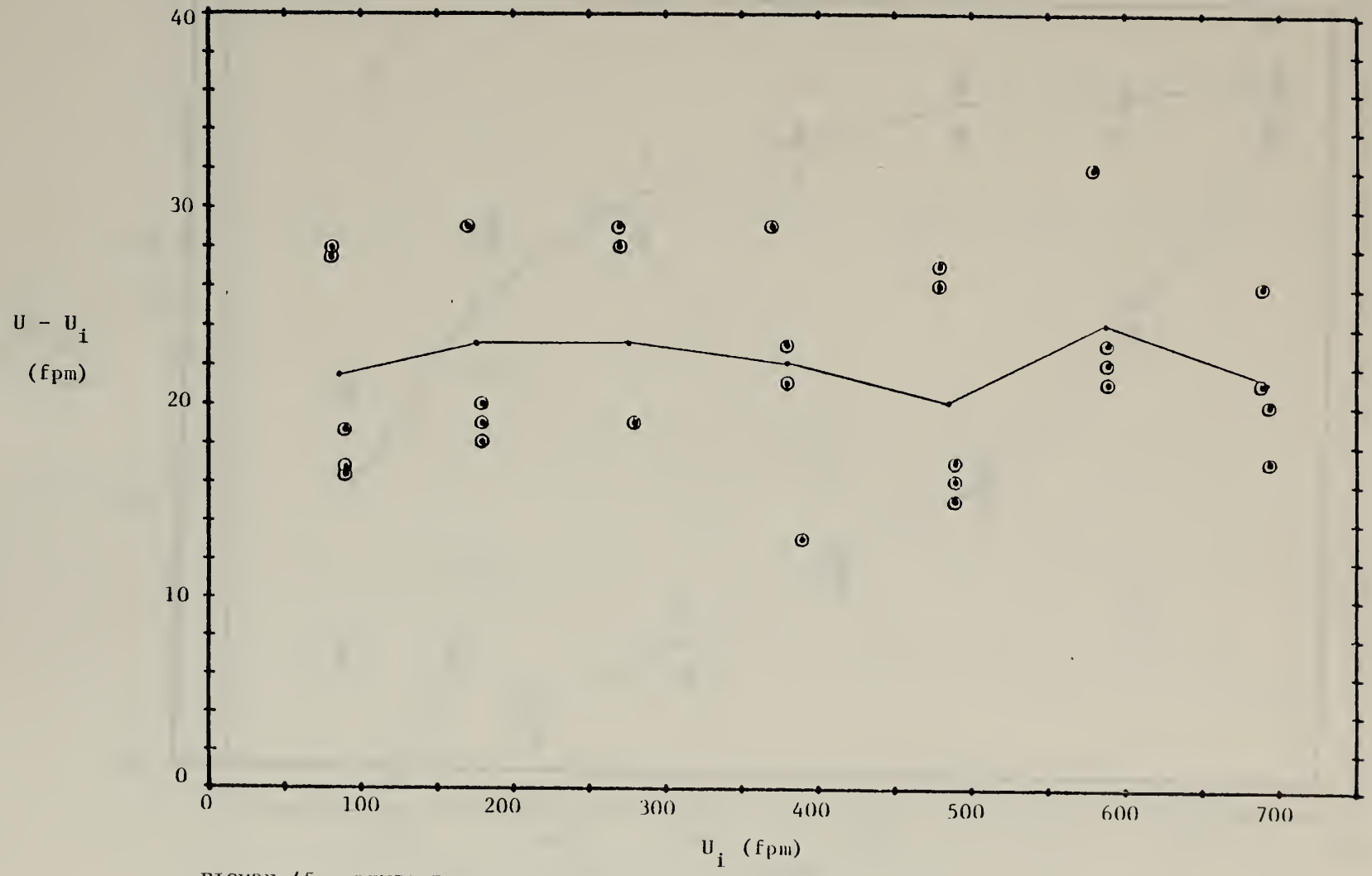

FIGURE 45. DEVIATION OF INDICATED VELOCITY FROM TRUE VELOCITY, HIGH RANGE. INSTRUMENT E.

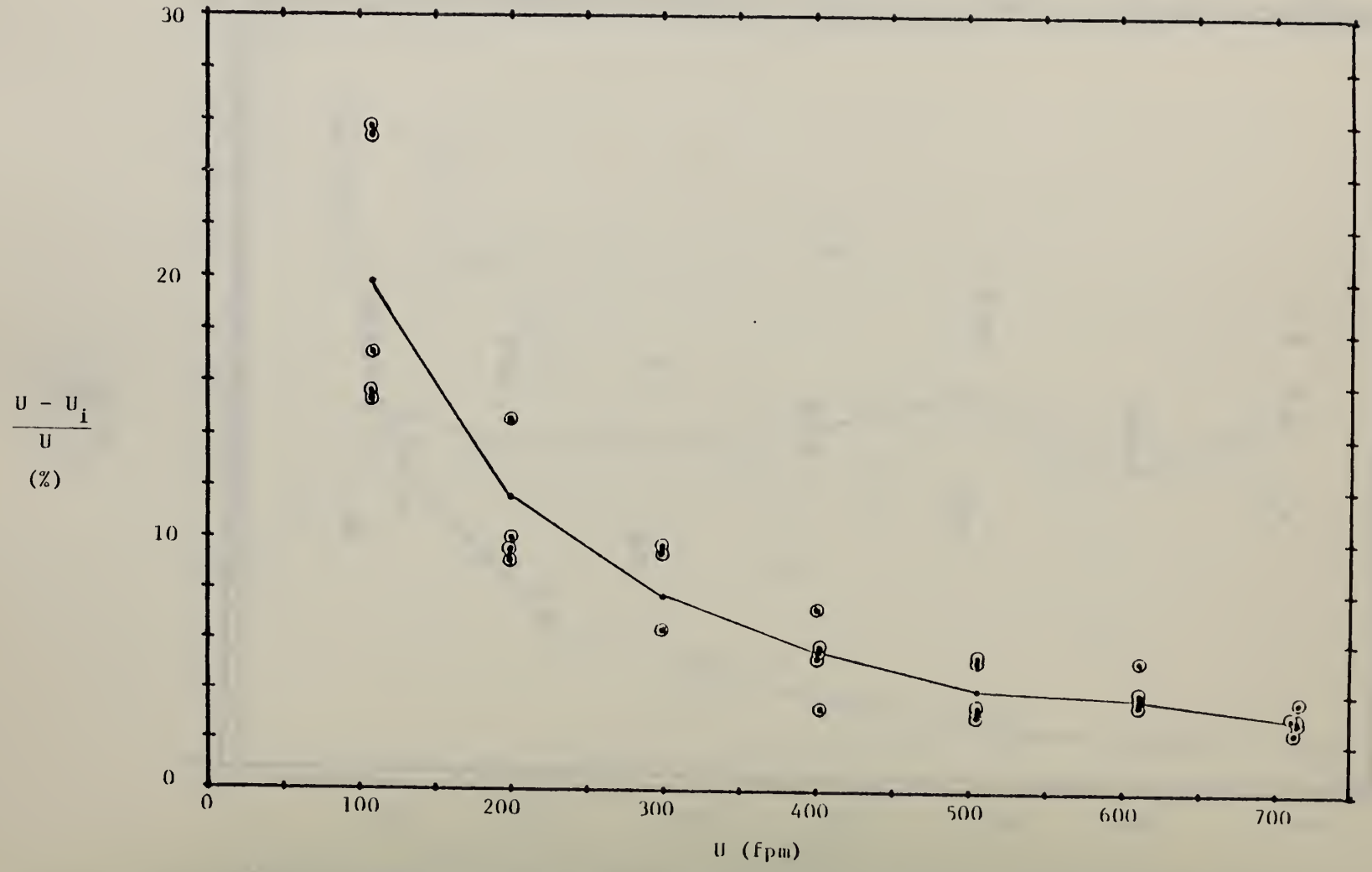

FIGURE 46. PERCENT DEVIATION OF INDICATED FROM TRUE VELOCITY, HIGH RANGE. INSTRUMENT E.

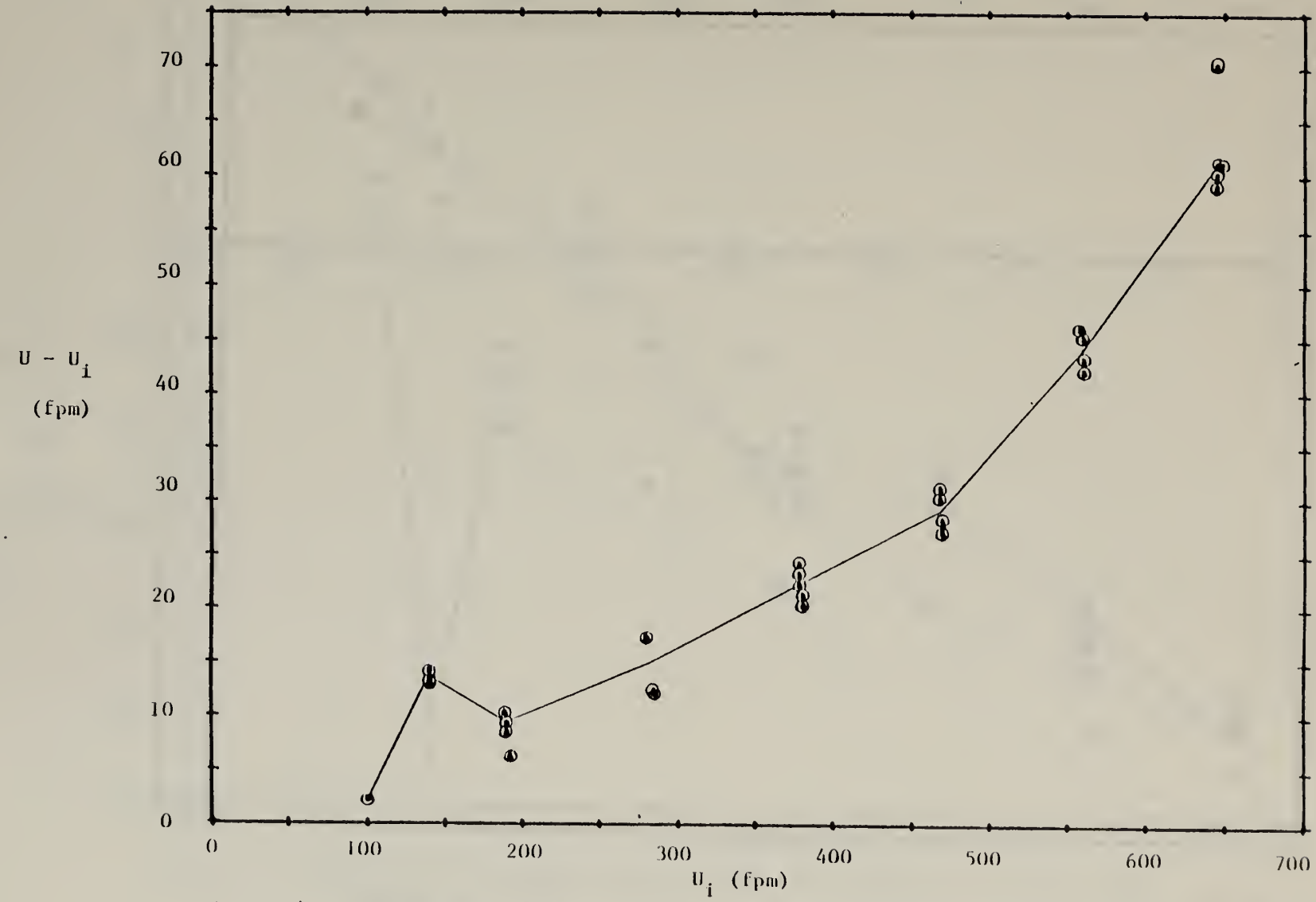

FIGURE 47. DEVIATION OF INDICATED VELOCITY FROM TRUE VELOCITY FOR PITOT PROBE, LOW RANGE. INSTRUMENT F.

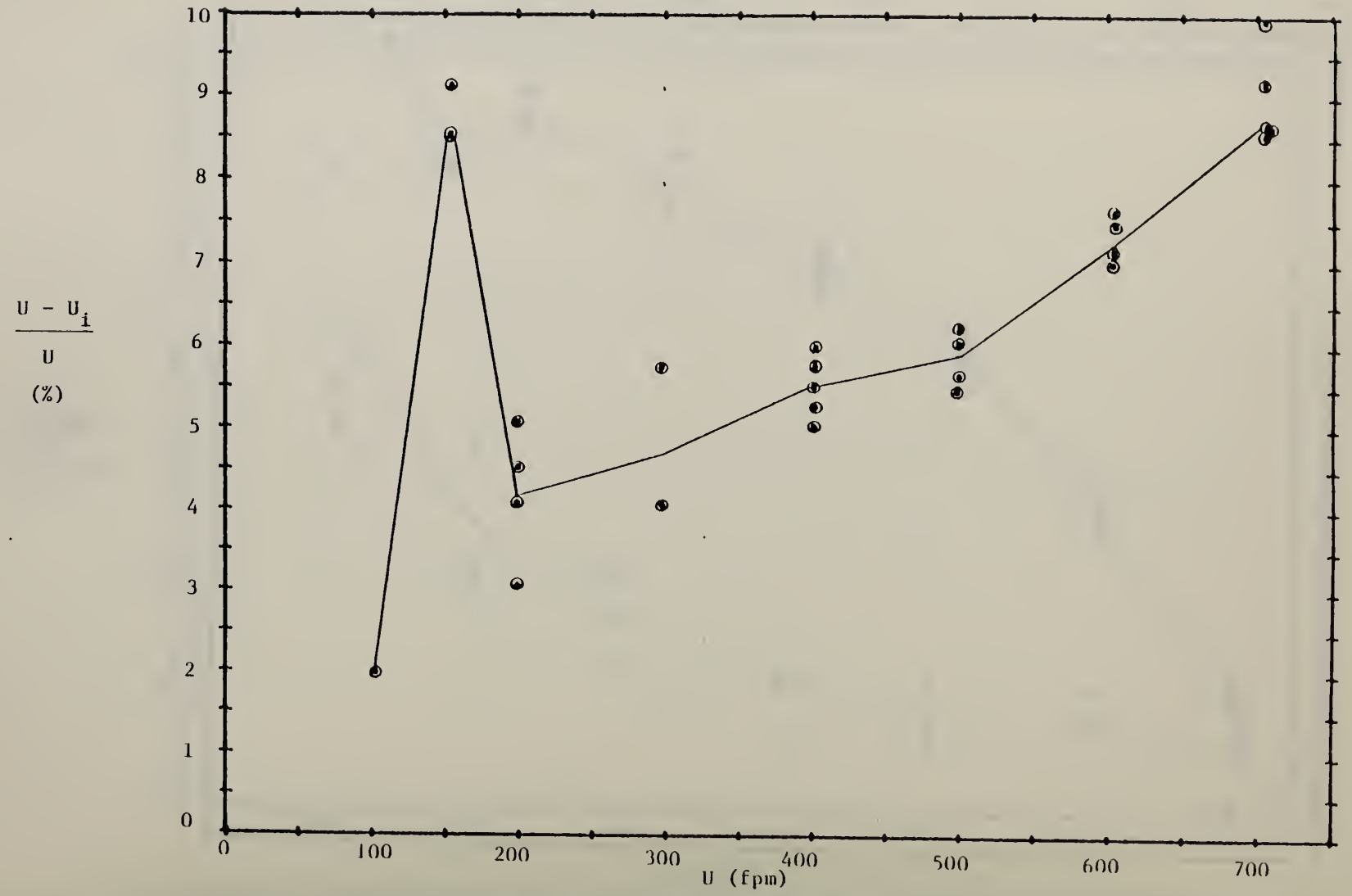

FIGURE 48. PERCENT DEVIATION OF INDICATED FROM TRUE VELOCITY FOR PITOT PROBE, LOW RANGE. INSTRUMENT F.

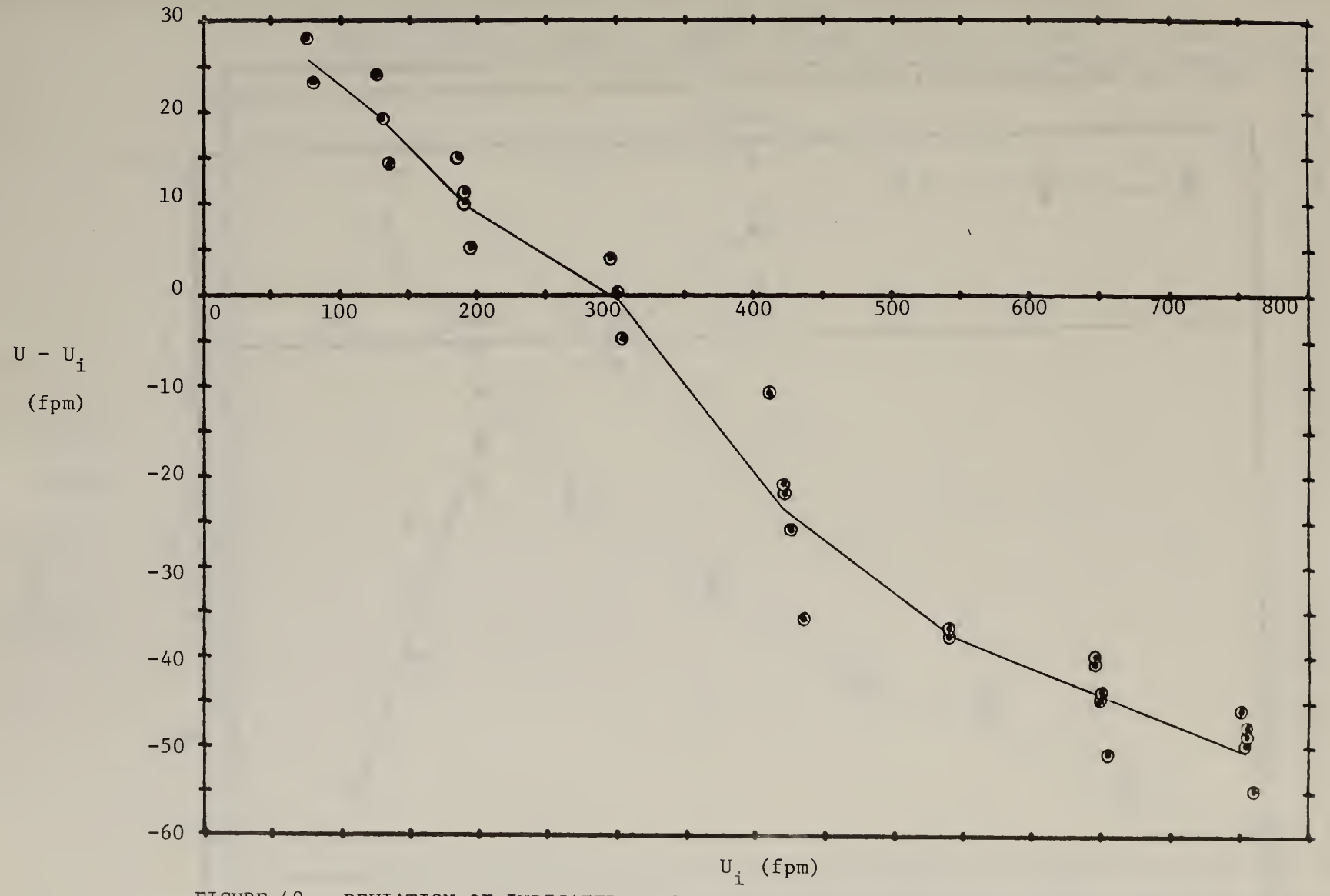

FIGURE 49. DEVIATION OF INDICATED VELOCITY FROM TRUE VELOCITY FOR PITOT PROBE, HIGH RANGE. INSTRUMENT F.

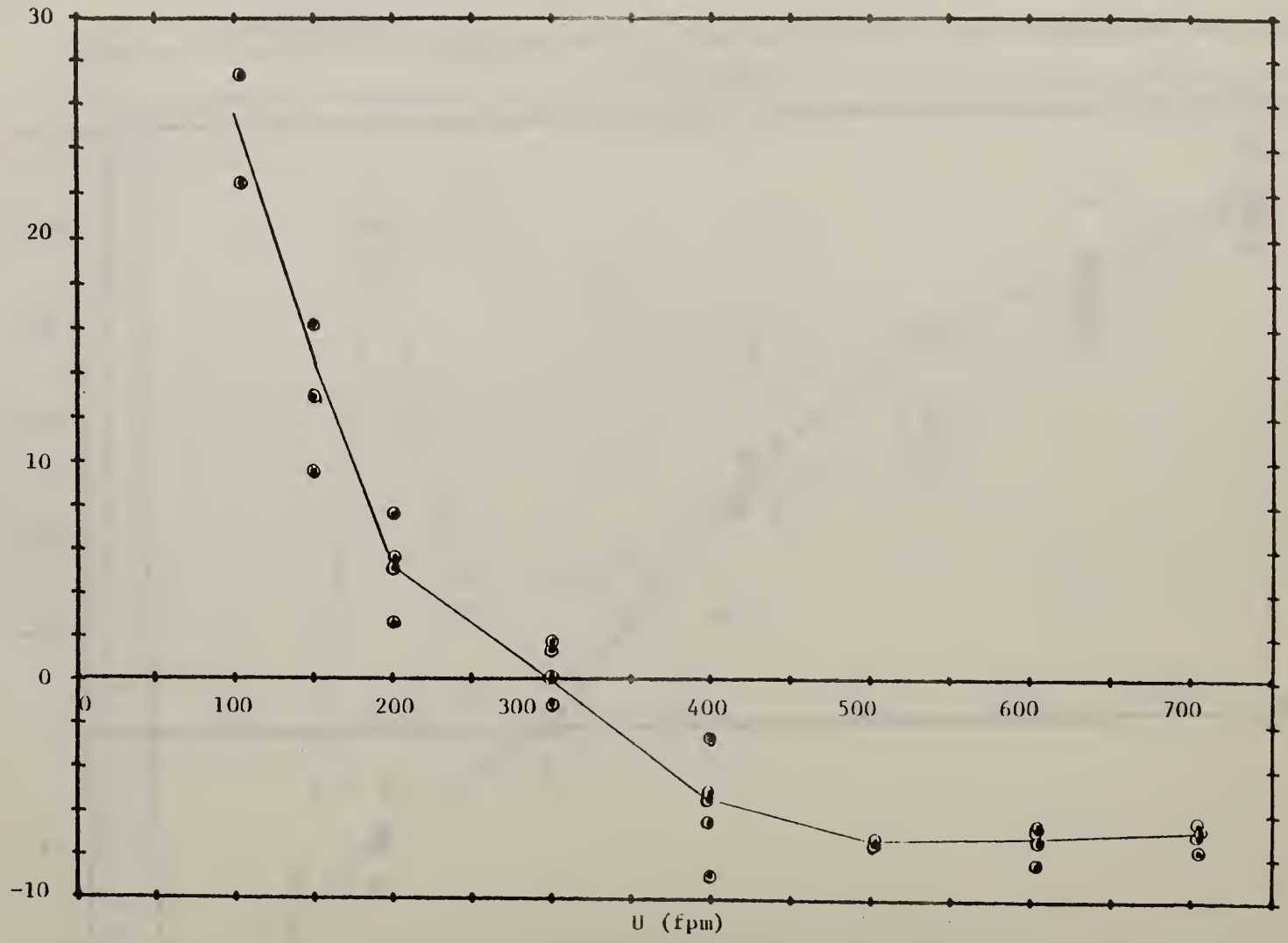

FIGURE 50. PERCENT DEVIATION OF INDICATED FROM TRUE VELOCITY FOR PITOT PROBE, HIGH RANGE. INSTRUMENT F.

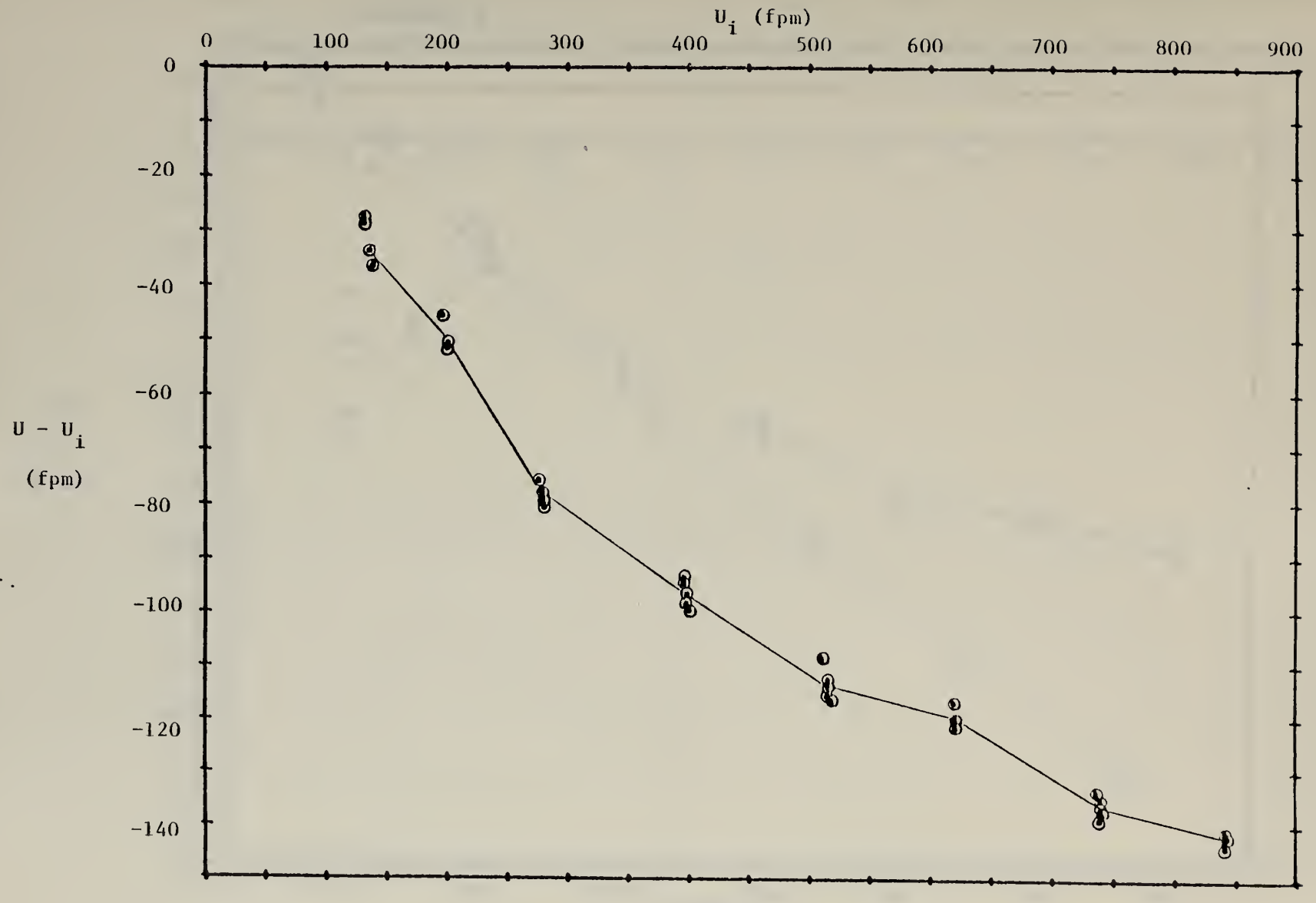

FIGURE 51. DEVIATION OF INDICATED VELOCITY FROM TRUE VELOCITY FOR DIFFUSER PROBE, LOW RANGE. INSTRUMENT F.

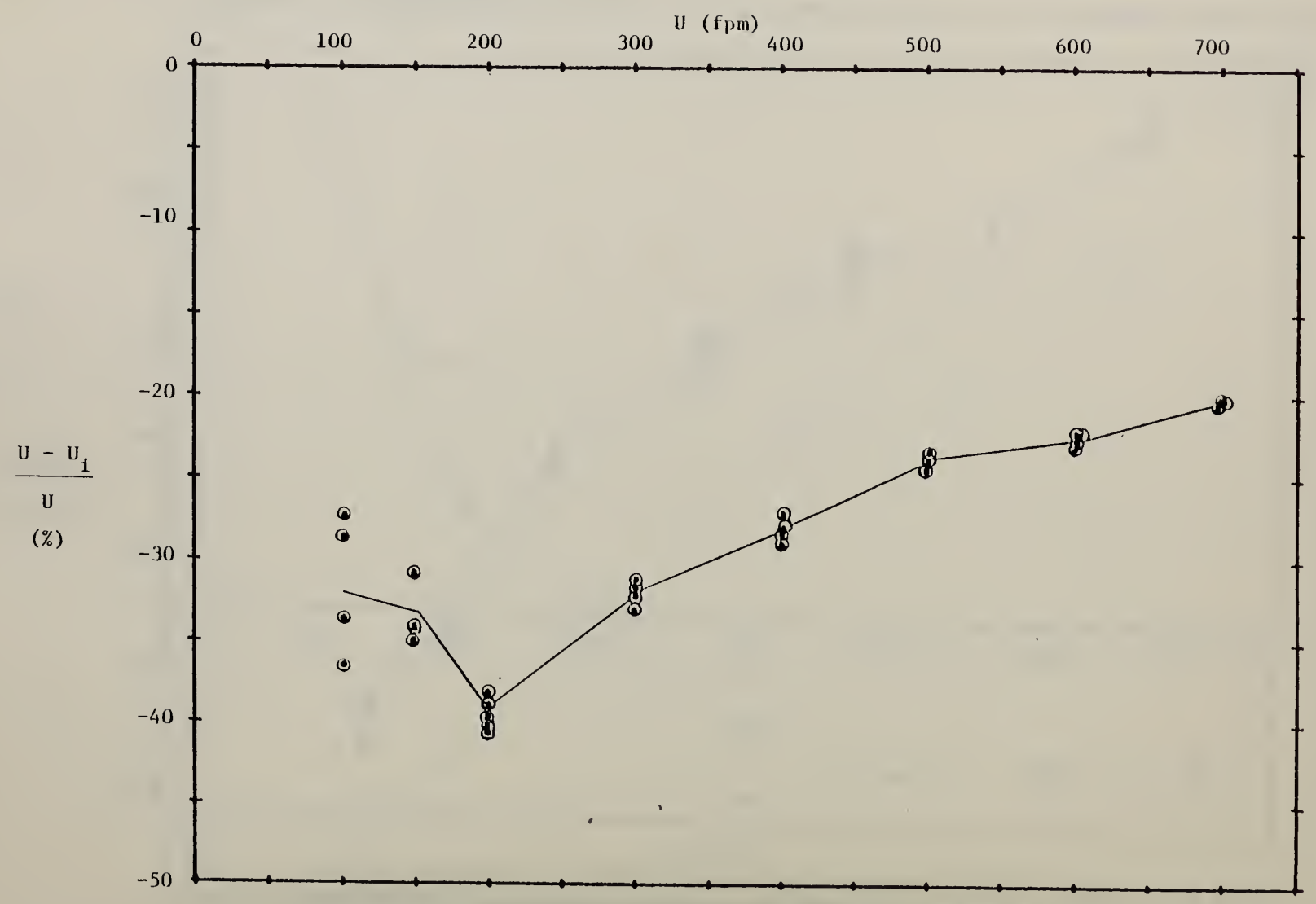

FIGURE 52. PERCENT DEVIATION OF INDICATED FROM TRUE VELOCITY FOR DIFFUSER PROBE, LOW RANGE. INSTRUMENT F.

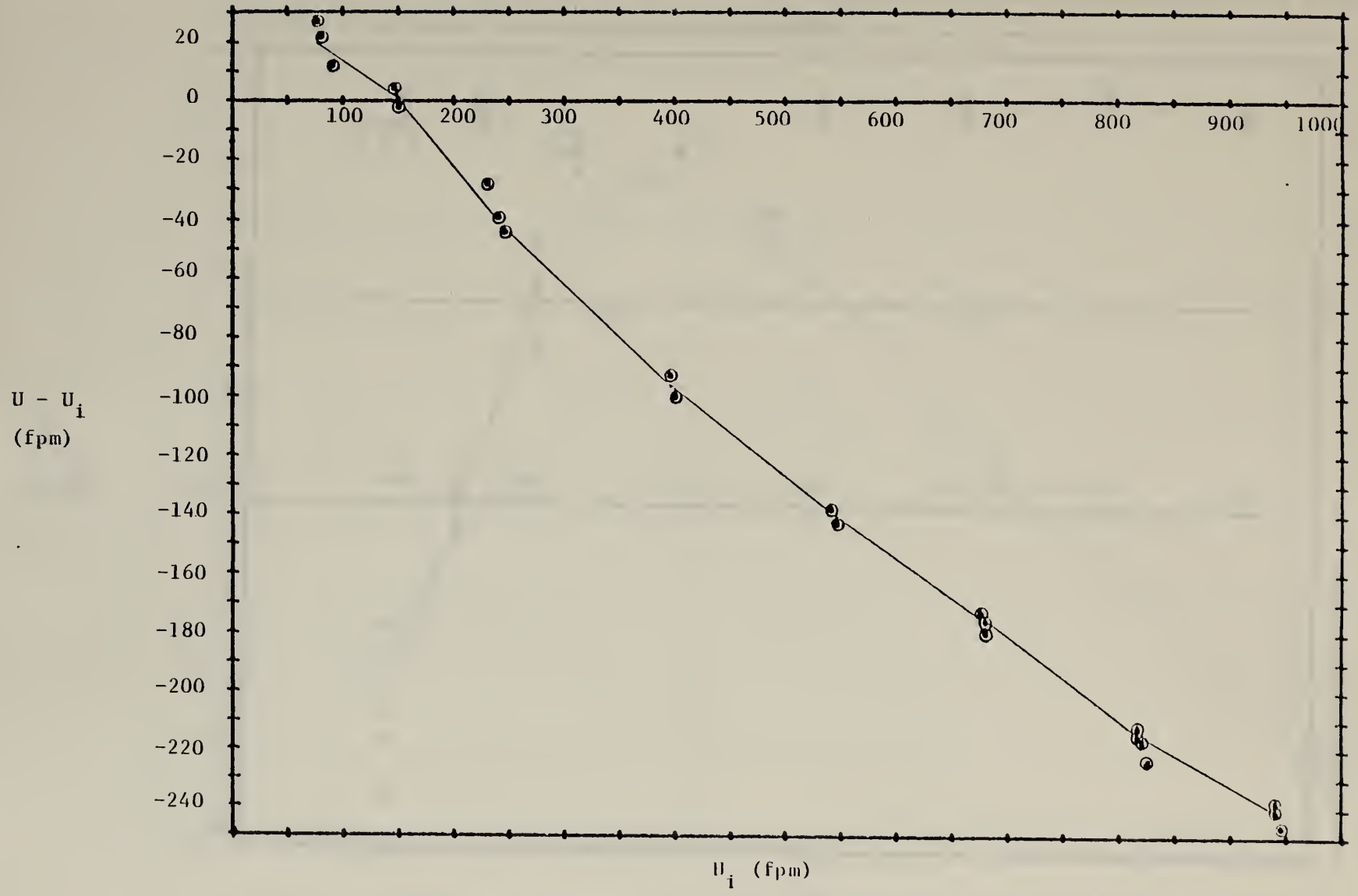

FIGURE 53. DEVIATION OF INDICATED VELOCITY FROM TRUE VELOCITY FOR DIFFUSER PROBE, HIGH RANGE. INSTRUMENT F.

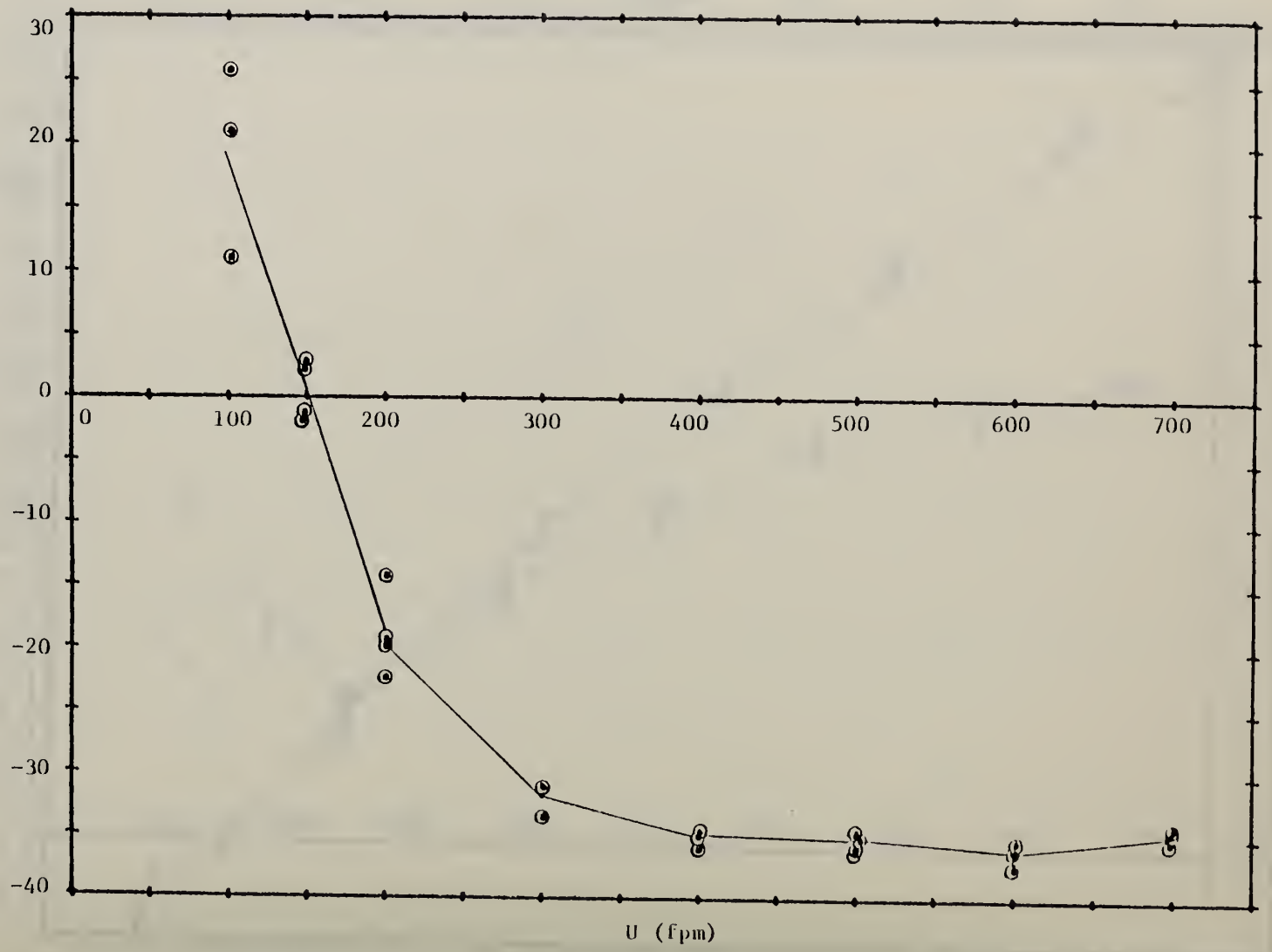

FIGURE 54. PERCENT DEVIATION OF INDICATED FROM TRUE VELOCITY FOR DIFFUSER PROBE, HIGH RANGE. INSTRUMENT F.

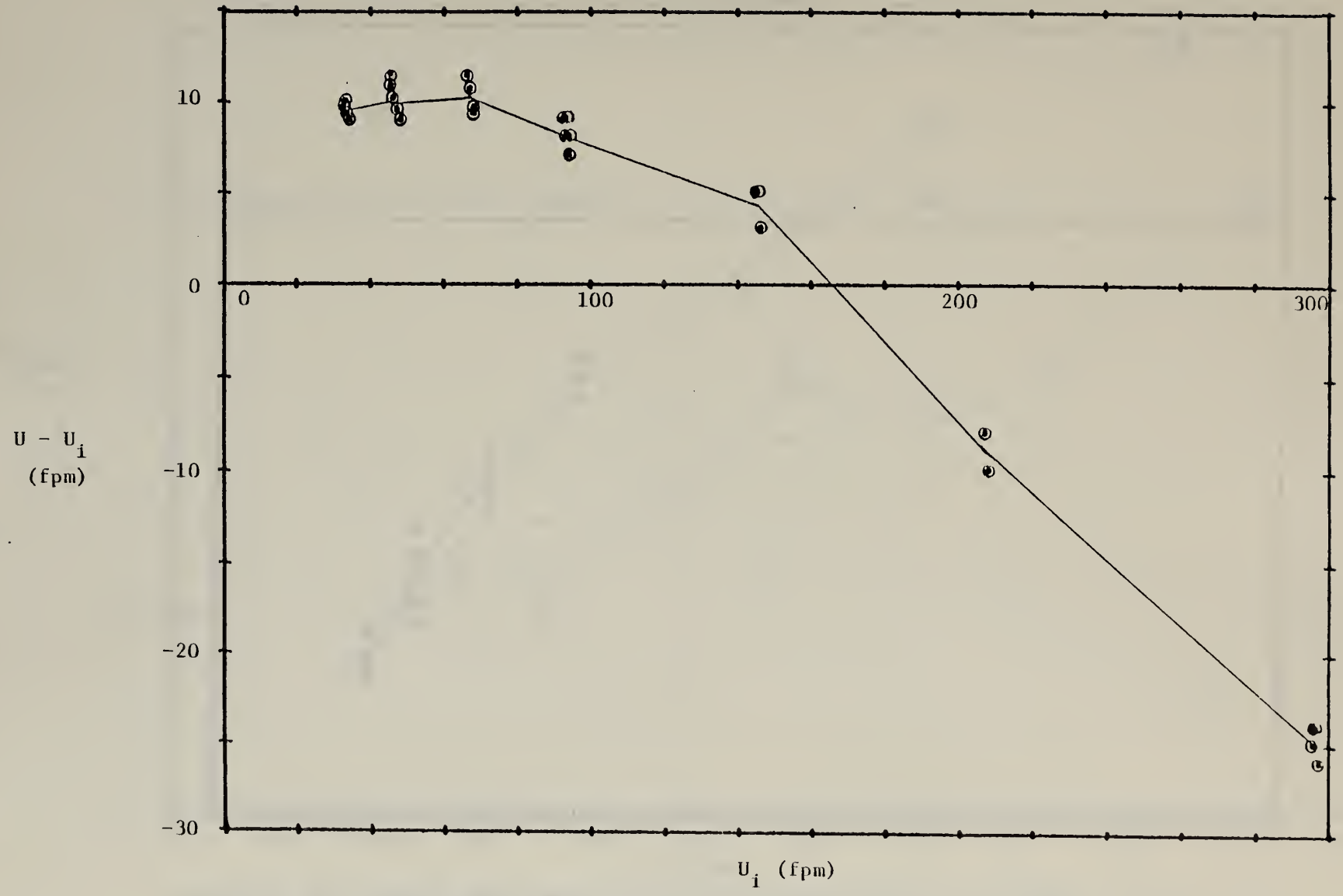

FIGURE 55. DEVIATION OF INDICATED VELOCITY FROM TRUE VELOCITY FOR LOW VELOCITY PROBE. INSTRUMENT F.

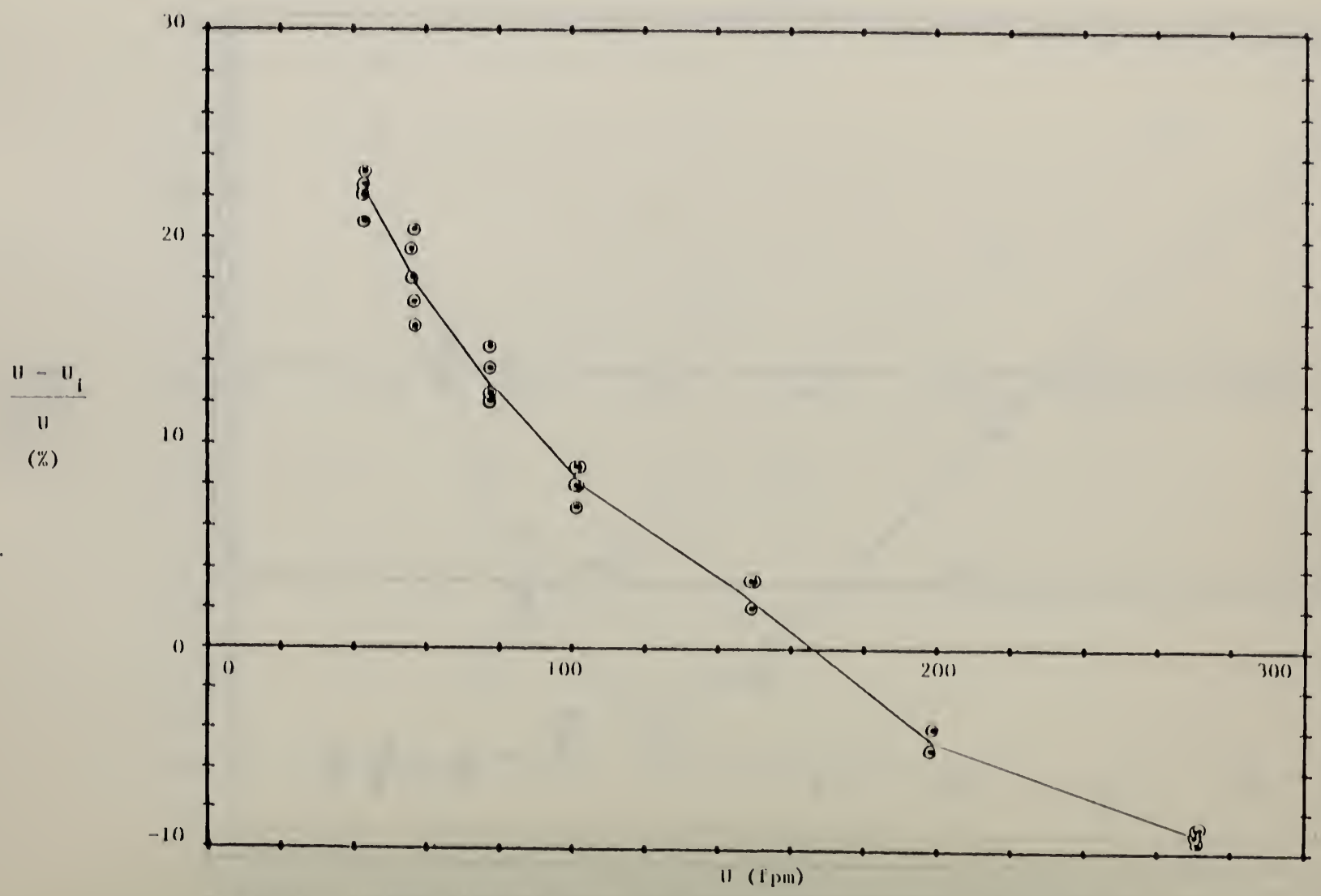

FIGURE 56. PERCENT DEVIATION OF INDICATED FROM TRUE VELOCITY FOR LOW VELOCITY PROBE. INSTRUMENT F.

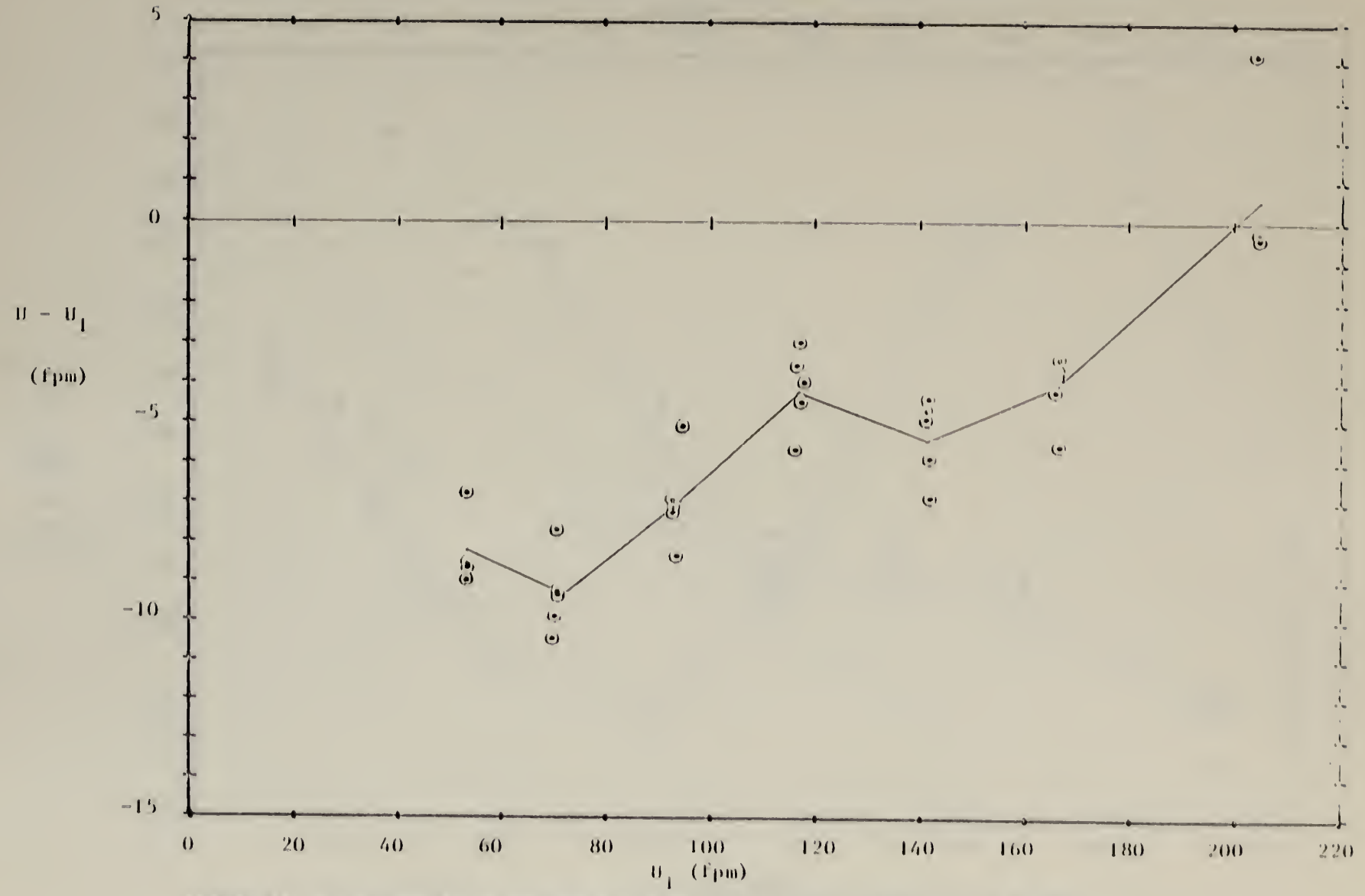

FIGURE 57. DEVIATION OF INDICATED VELOCITY FROM TRUE VELOCITY, LOW RANGE. INSTRUMENT G.

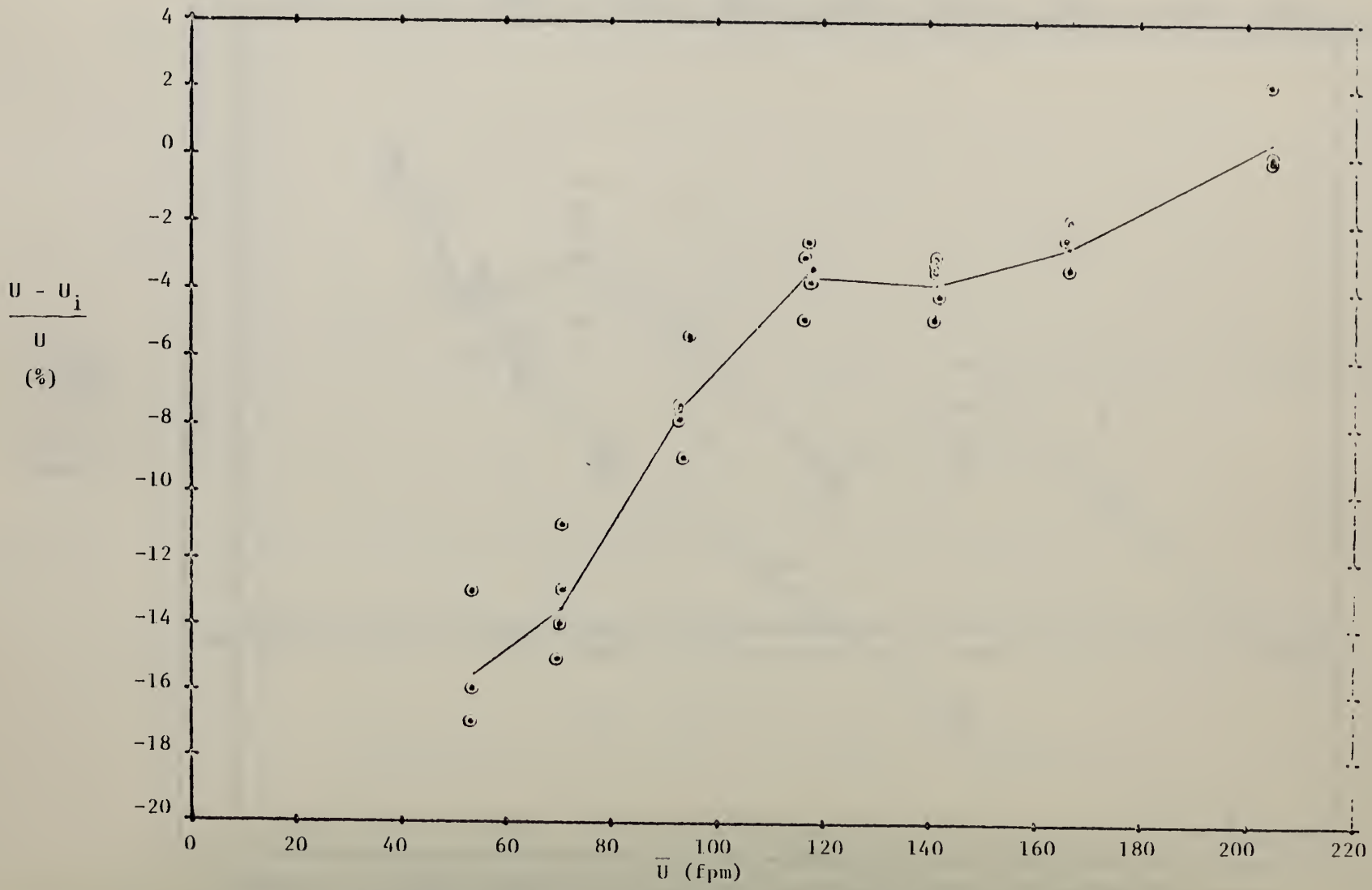

FIGURE 58. PERCENT DEVIATION OF INDICATED VELOCITY FROM TRUE VELOCITY, LOW RANGE. INSTRUMENT G.

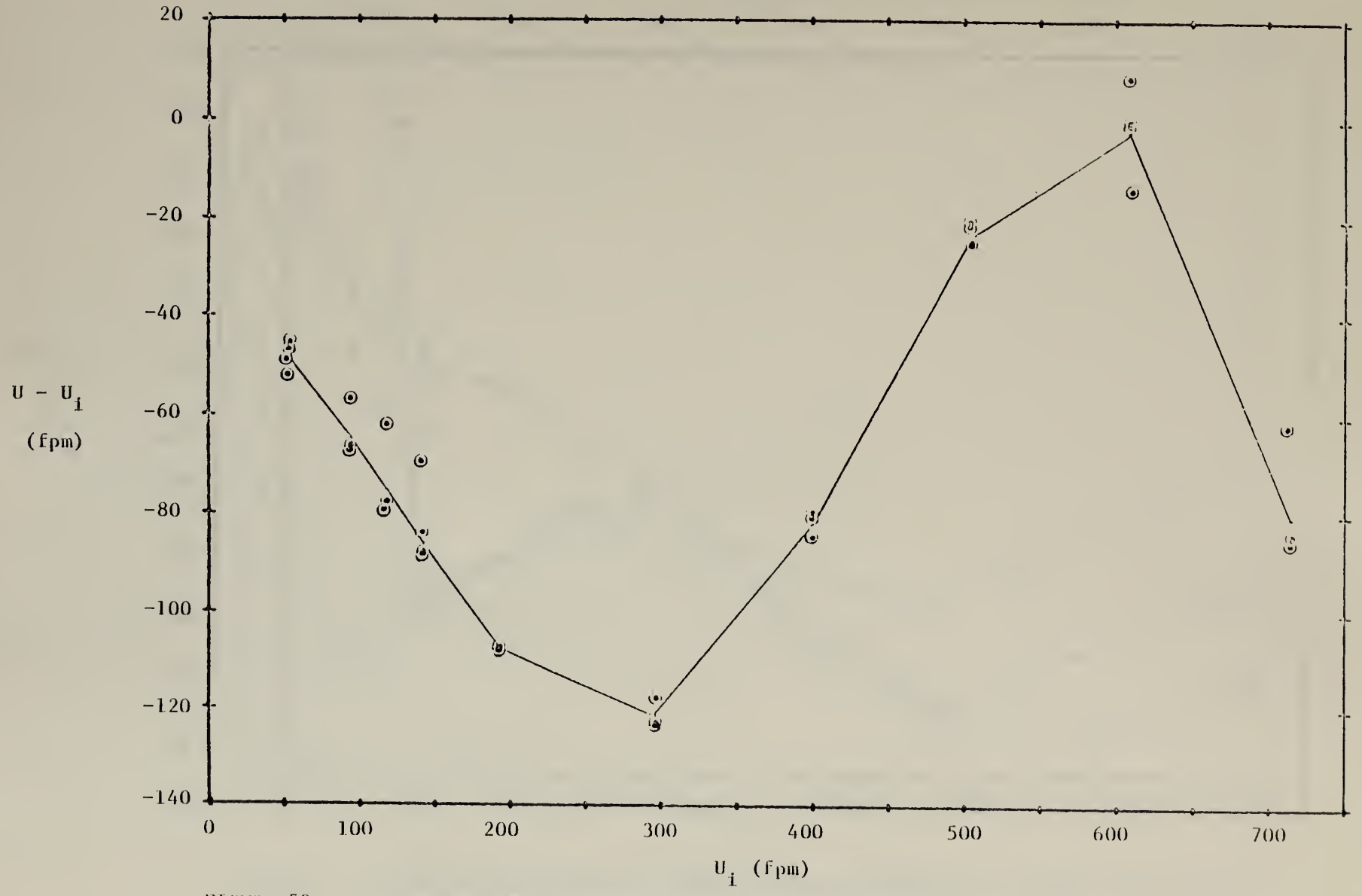

FIGURE 59. DEVIATION OF INDICATED VELOCITY FROM TRUE VELOCITY, HIGH RANGE. INSTRUMENT C.

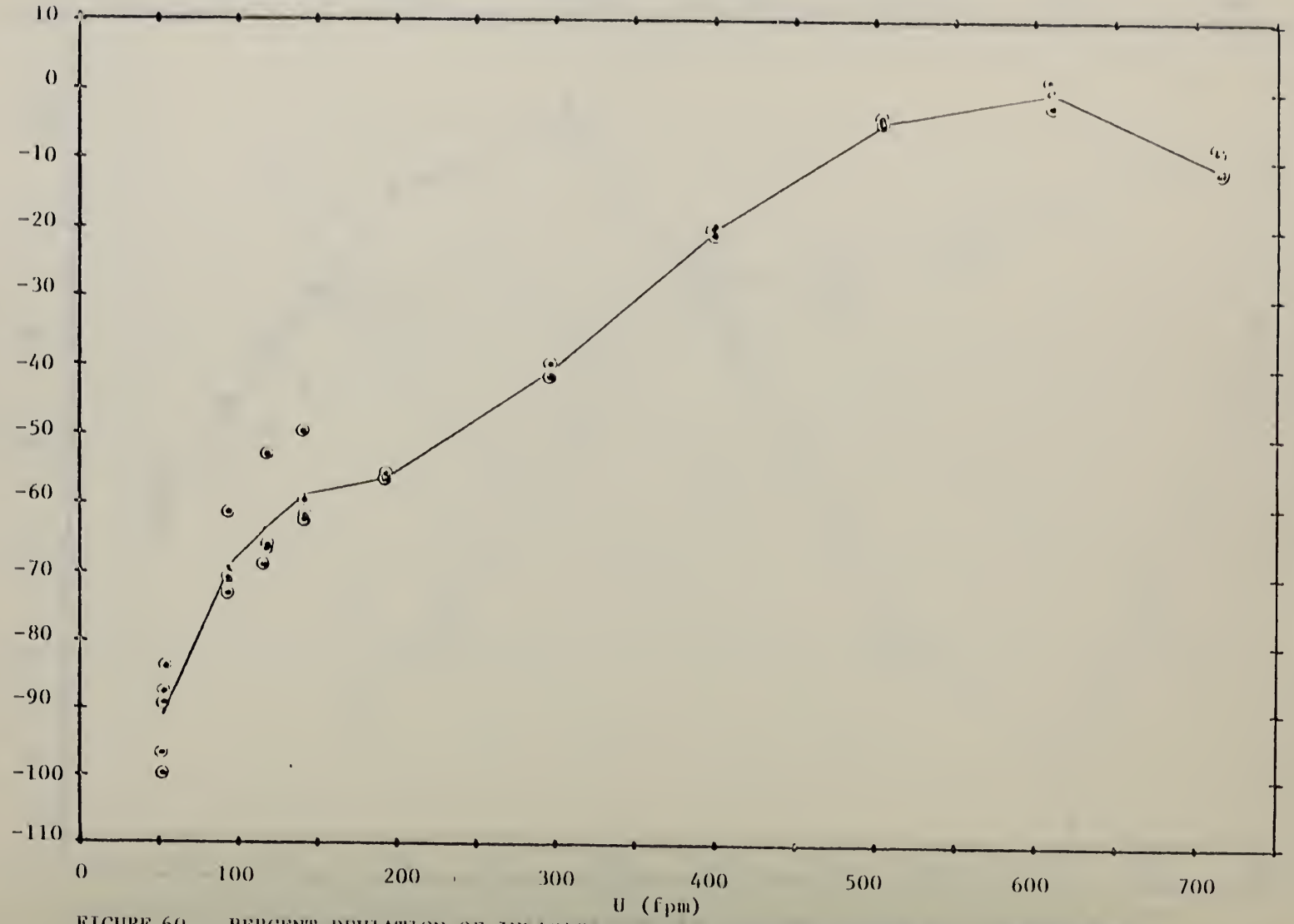

FIGURE 60. PERCENT DEVIATION OF INDICATED VELOCITY FROM TRUE VELOCITY, HIGH RANGE. INSTRUMENT G.

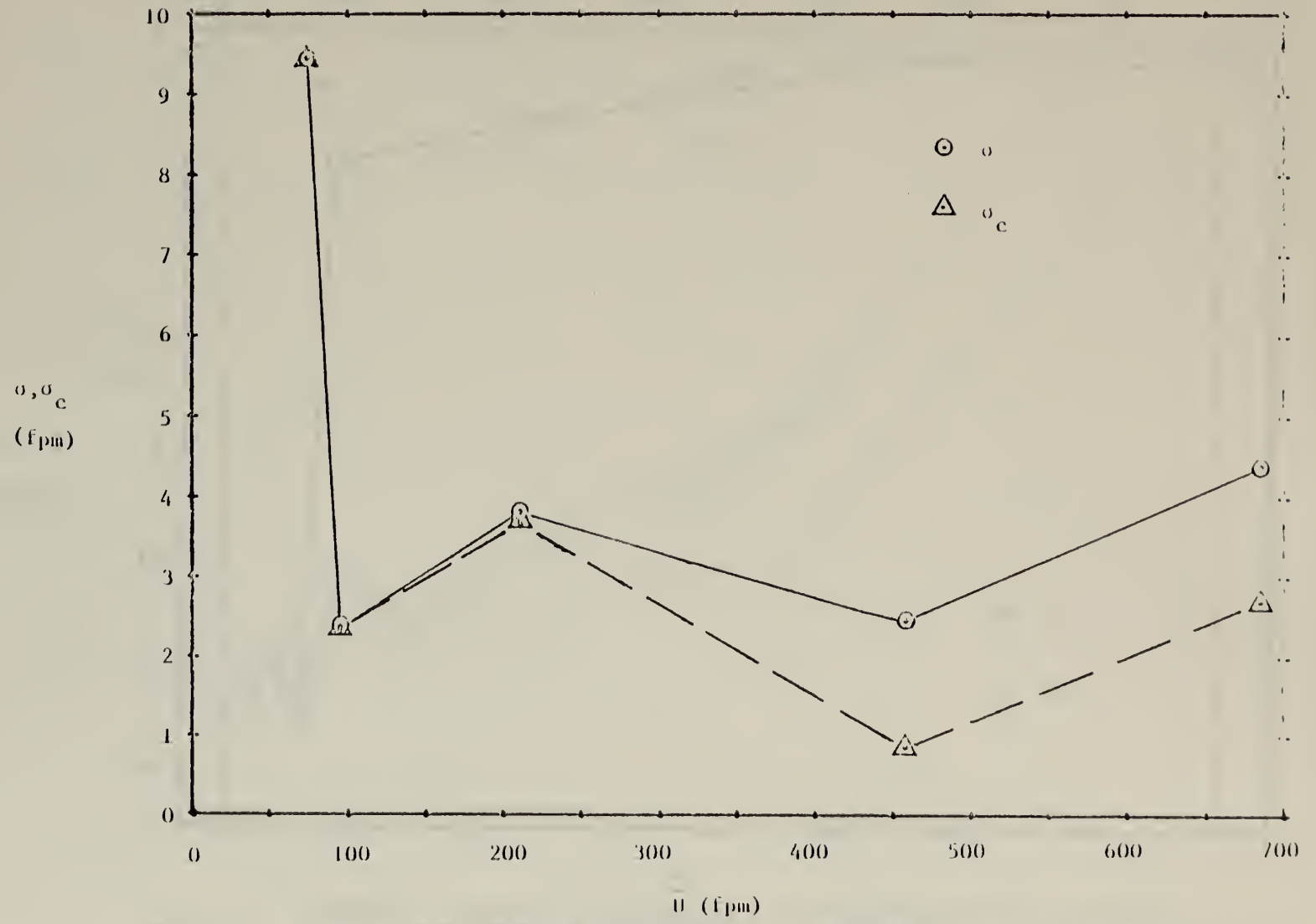

FIGURE 61. STANDARD DEVIATION AND CORRECTED STANDARD DEVIATION IN TERMS OF TRUE VELOCITY. INSTRUMENT A.

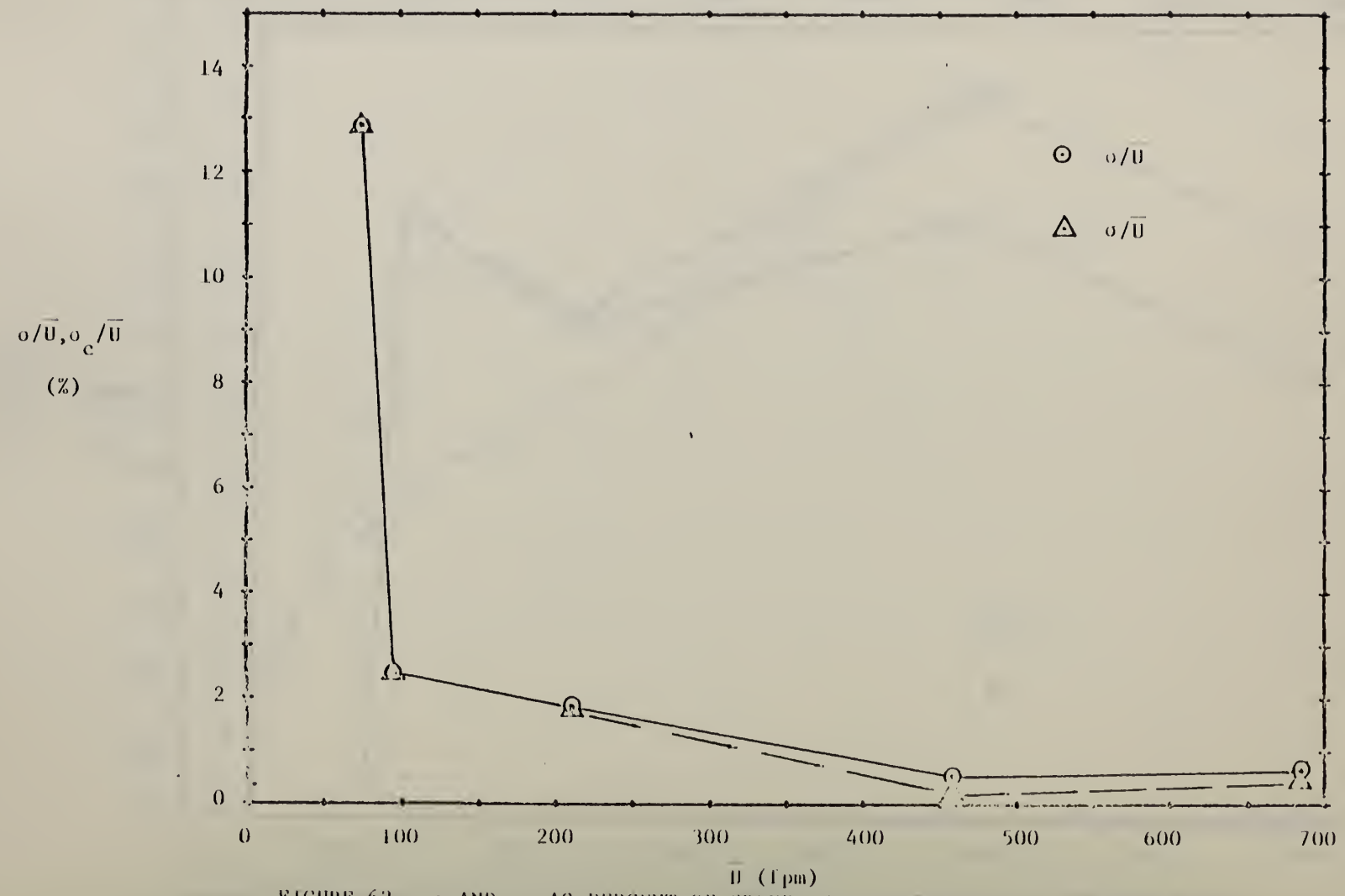

FIGURE 62. σ AND σ_c AS PERCENT OF GROUP MEAN TRUE VELOCITY. INSTRUMENT A.

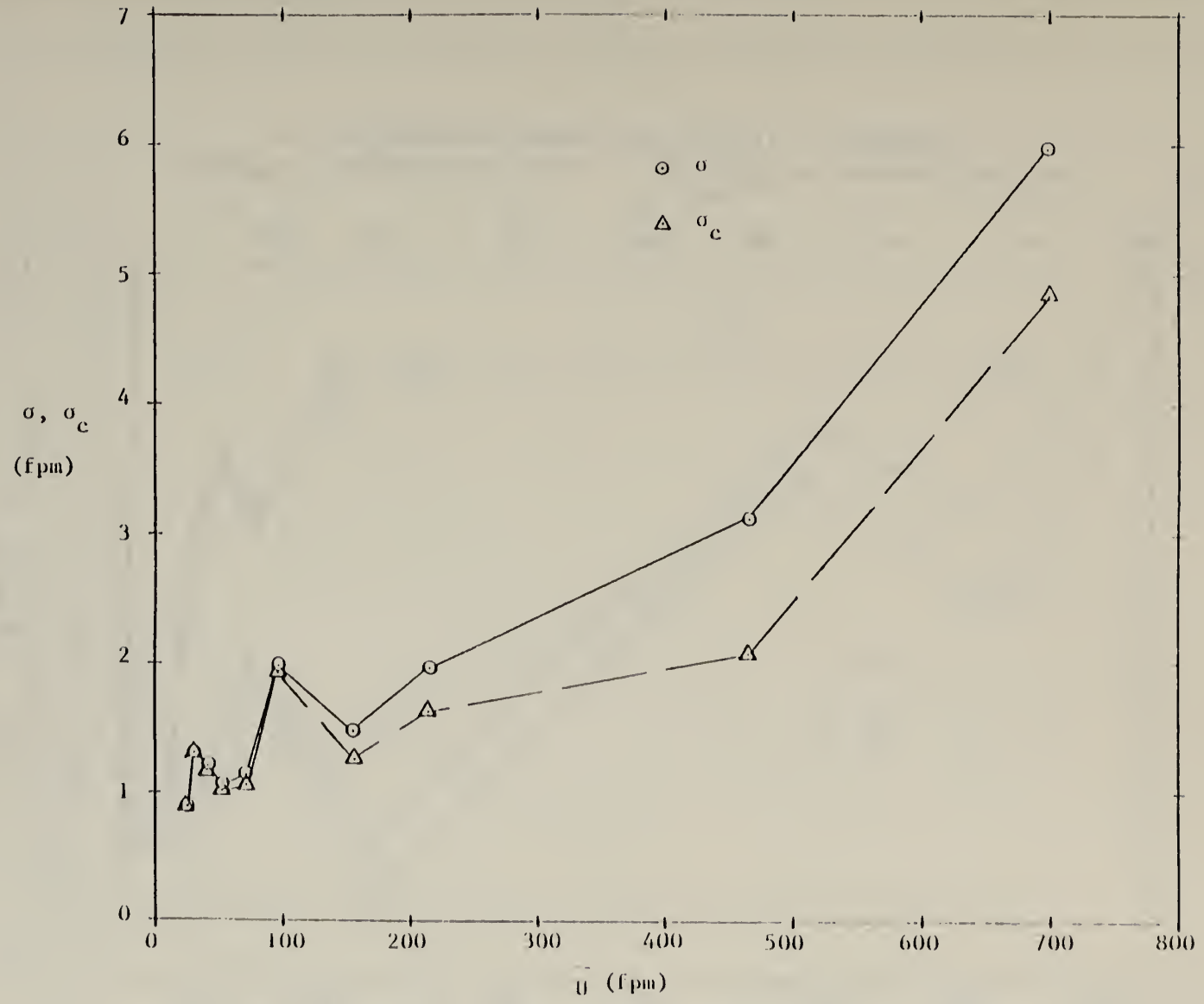

FIGURE 63. STANDARD DEVIATION, σ, AND CORRECTED STANDARD DEVIATION σ_c, IN TERMS OF TRUE VELOCITY. INSTRUMENT B.

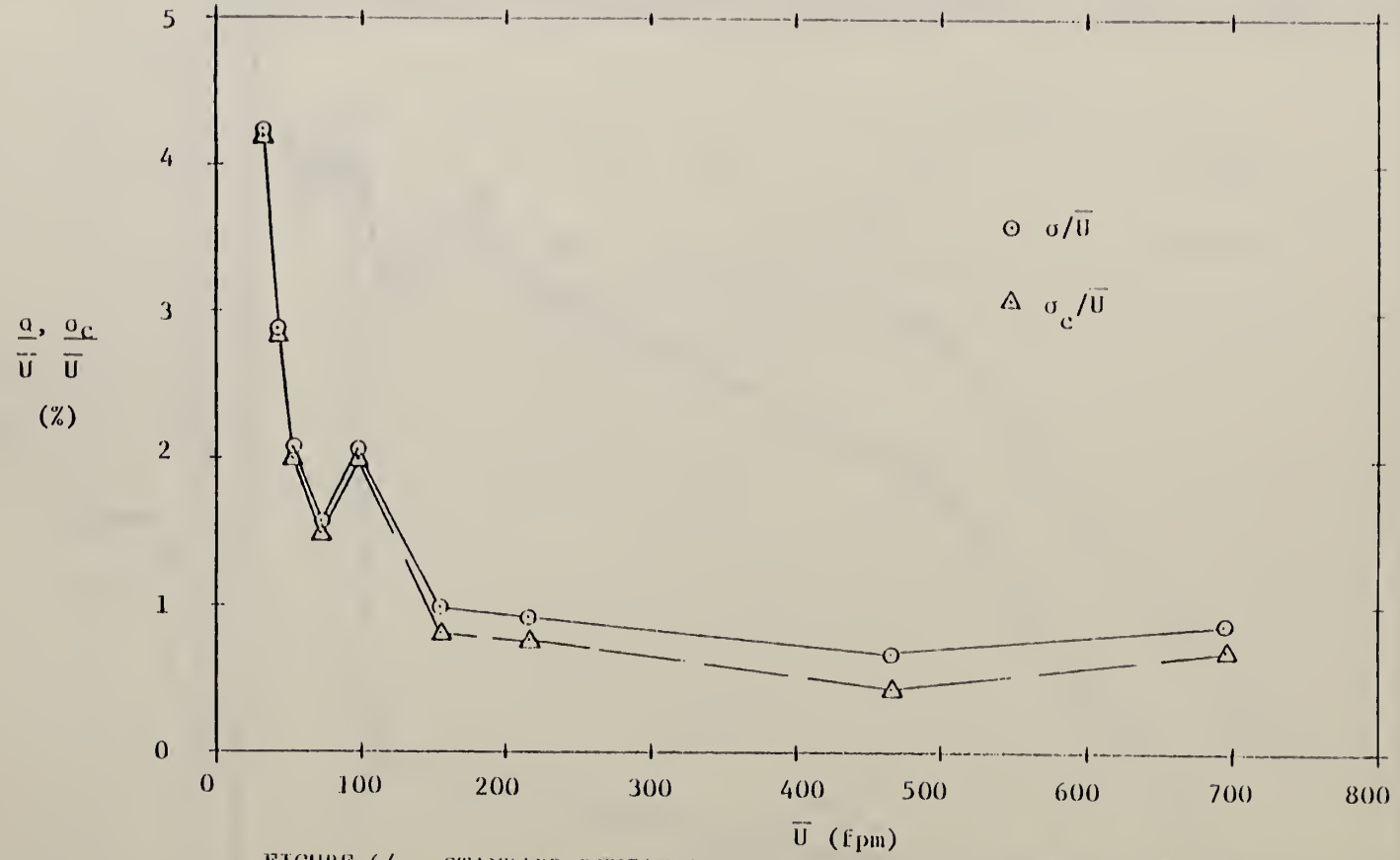

FIGURE 64. STANDARD DEVIATION, σ, AND CORRECTED STANDARD DEVIATION, σ_c, AS PERCENT OF GROUP MEAN VELOCITY. INSTRUMENT B.

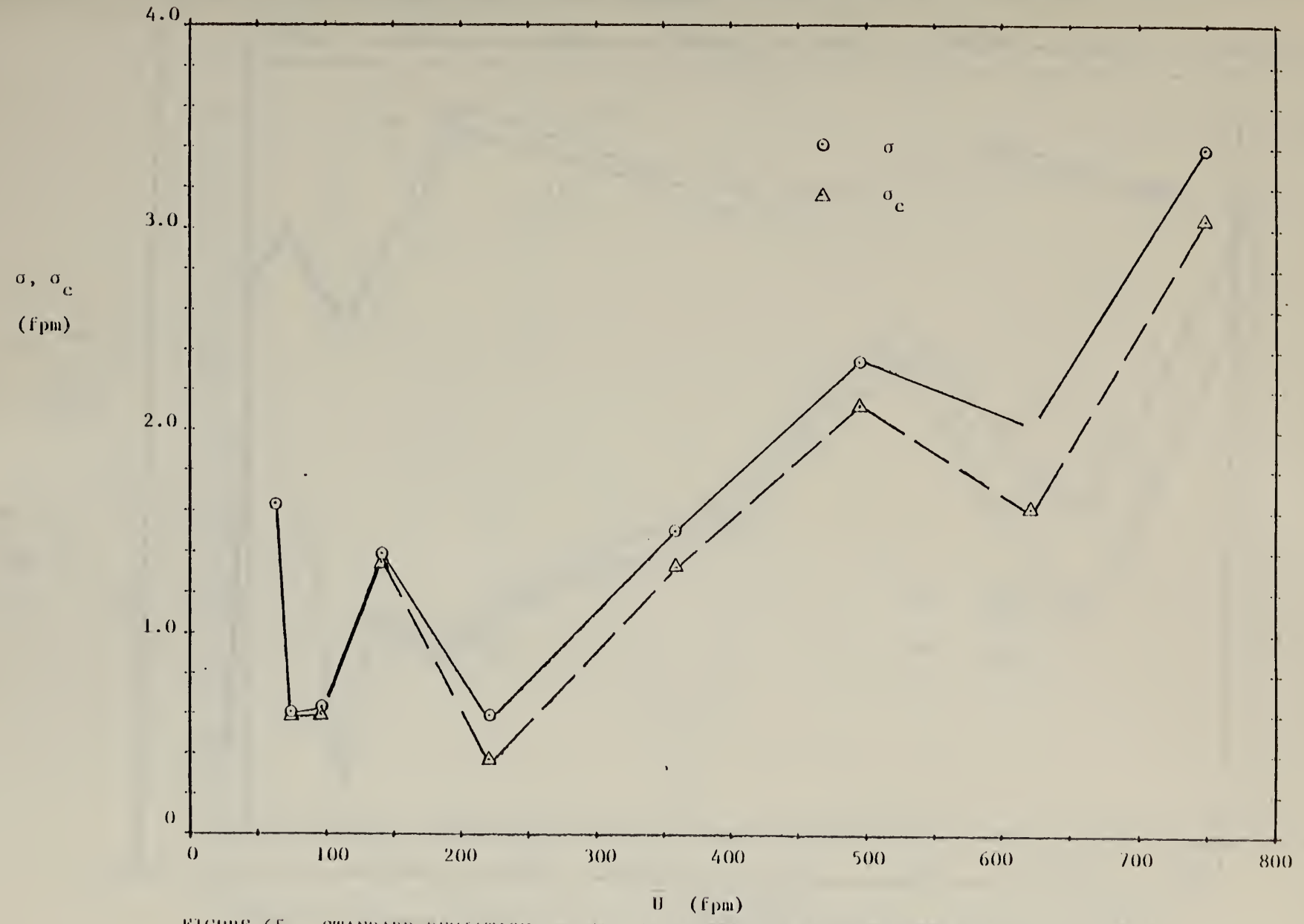

FIGURE 65. STANDARD DEVIATION, σ, AND CORRECTED STANDARD DEVIATION, σ_c. INSTRUMENT C.

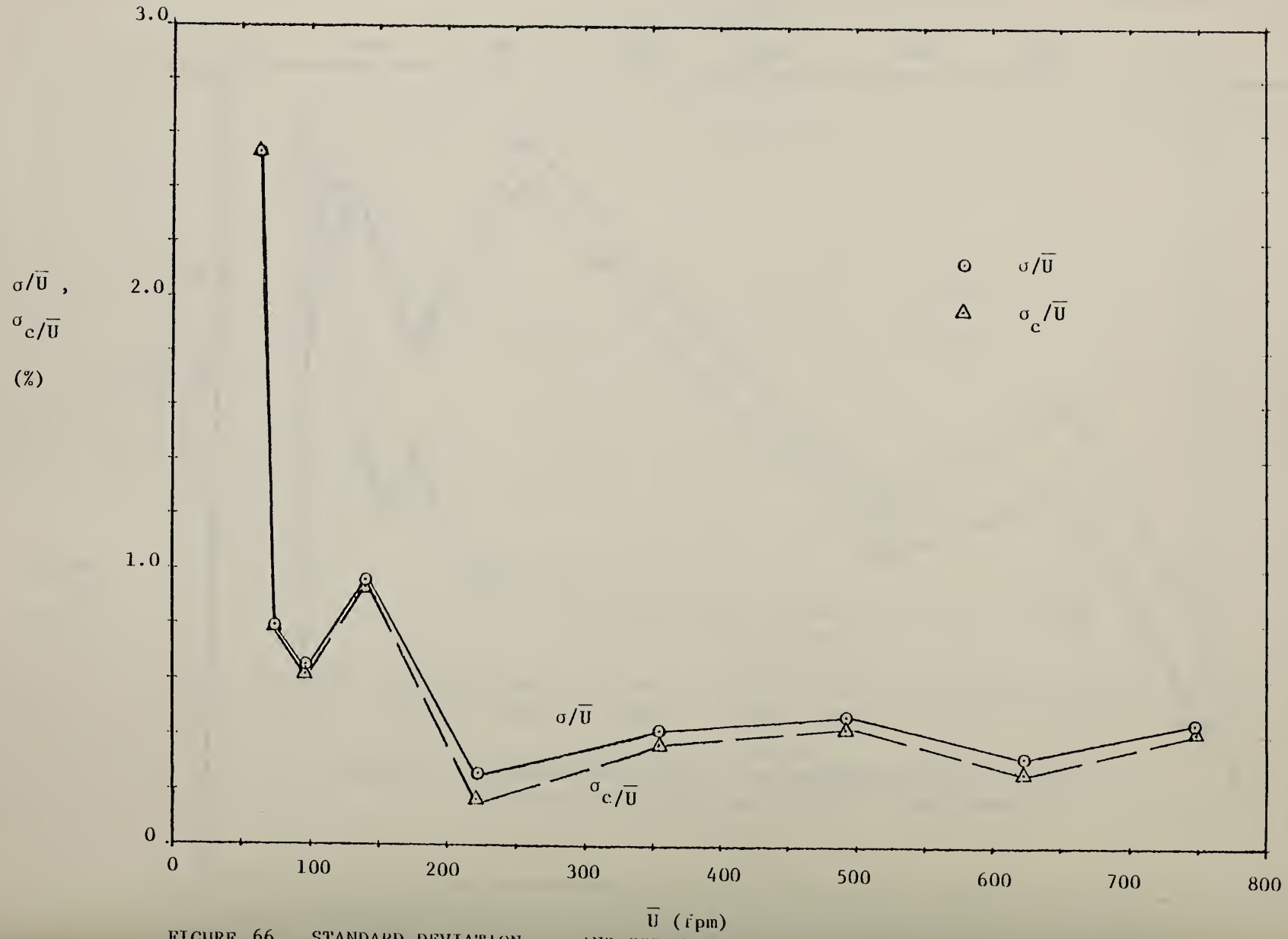

FIGURE 66. STANDARD DEVIATION, σ, AND CORRECTED STANDARD DEVIATION, σ_c, AS PERCENT OF GROUP MEAN VELOCITY. INSTRUMENT C.

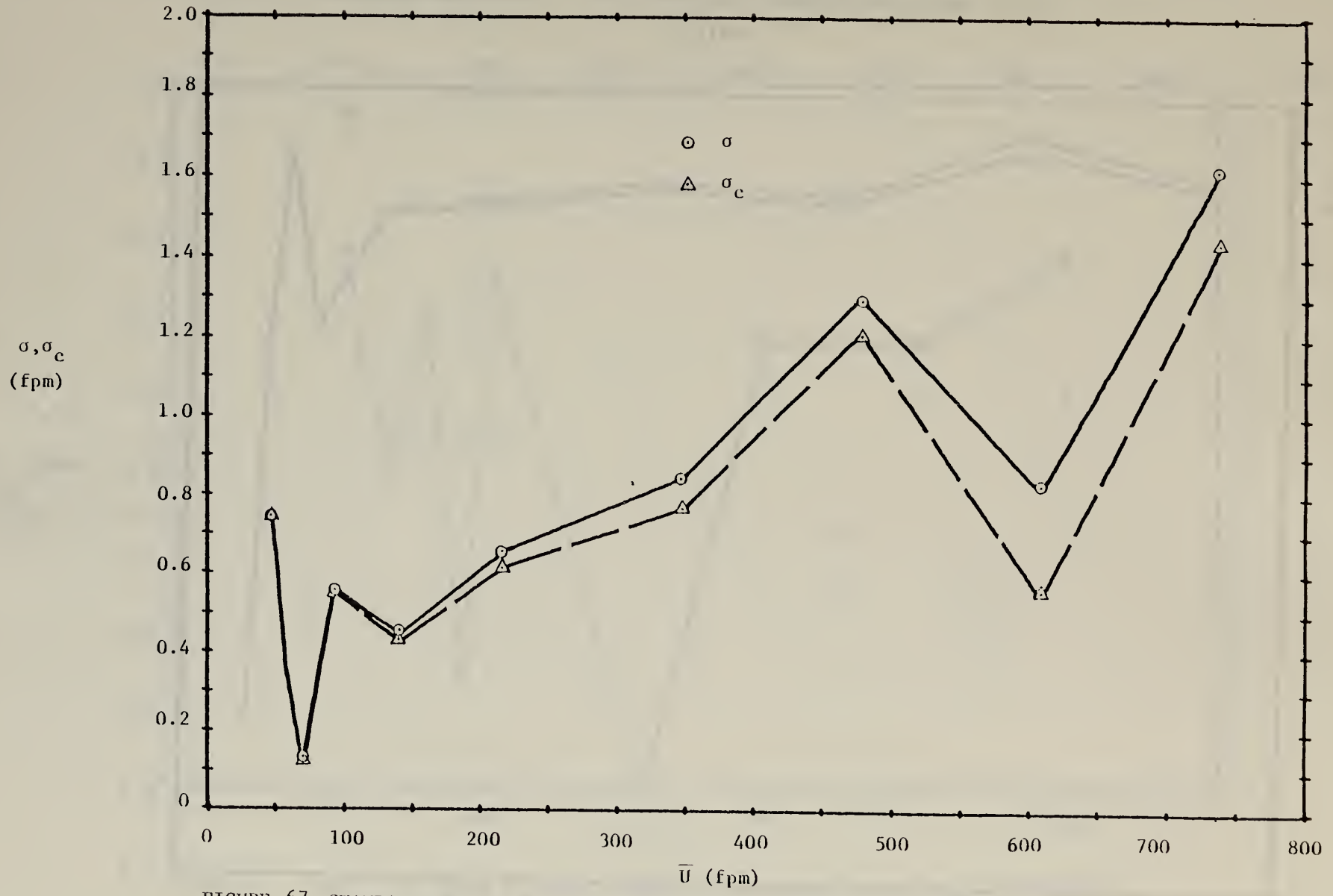

FIGURE 67. STANDARD DEVIATION, σ, AND CORRECTED STANDARD DEVIATION, σ_c, OF INDICATED VELOCITY IN TERMS OF TRUE VELOCITY. INSTRUMENT D.

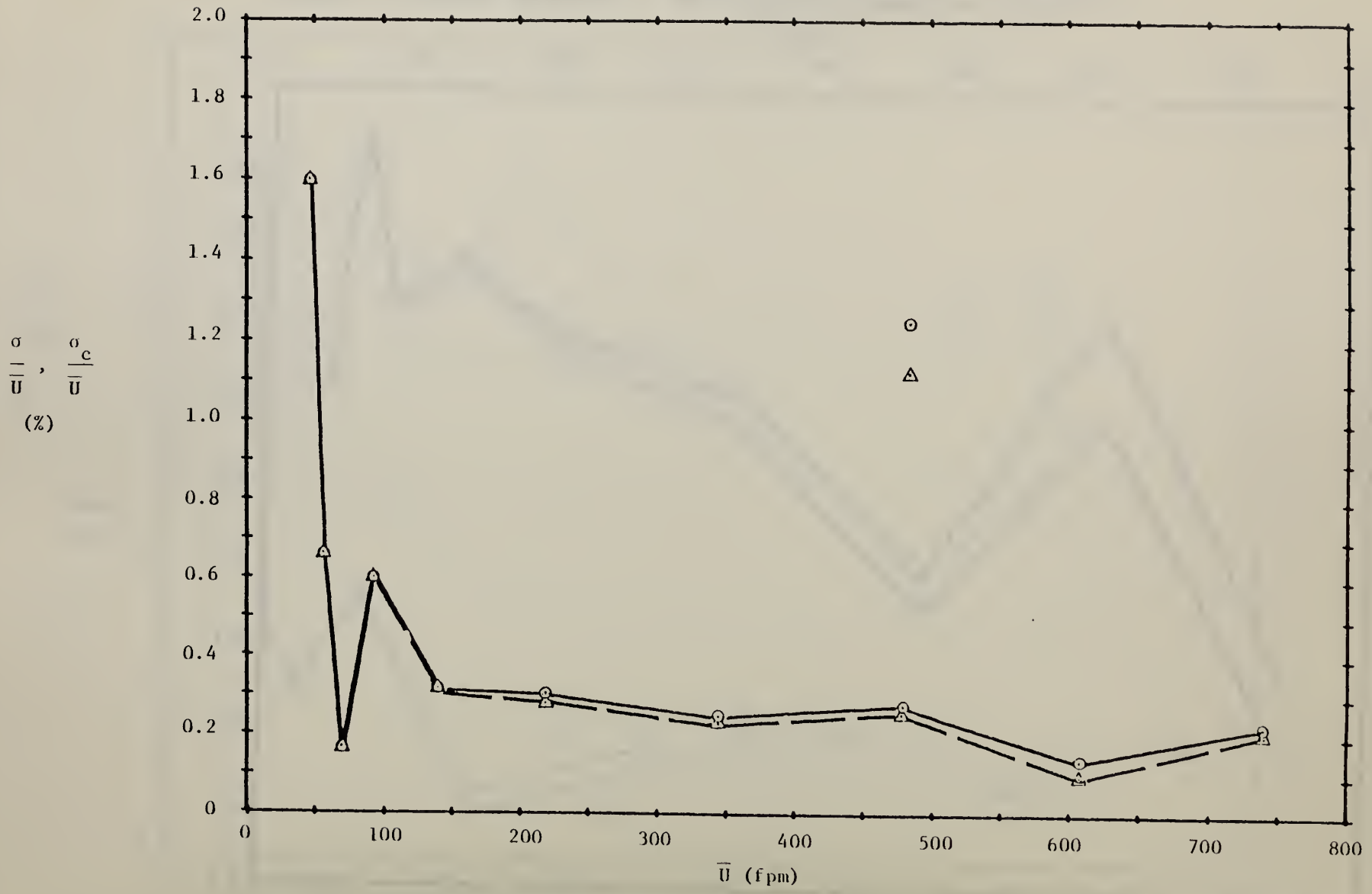

FIGURE 68. STANDARD DEVIATION, σ, AND CORRECTED STANDARD DEVIATION, σ_c, AS PERCENT OF GROUP MEAN VELOCITY. INSTRUMENT D.

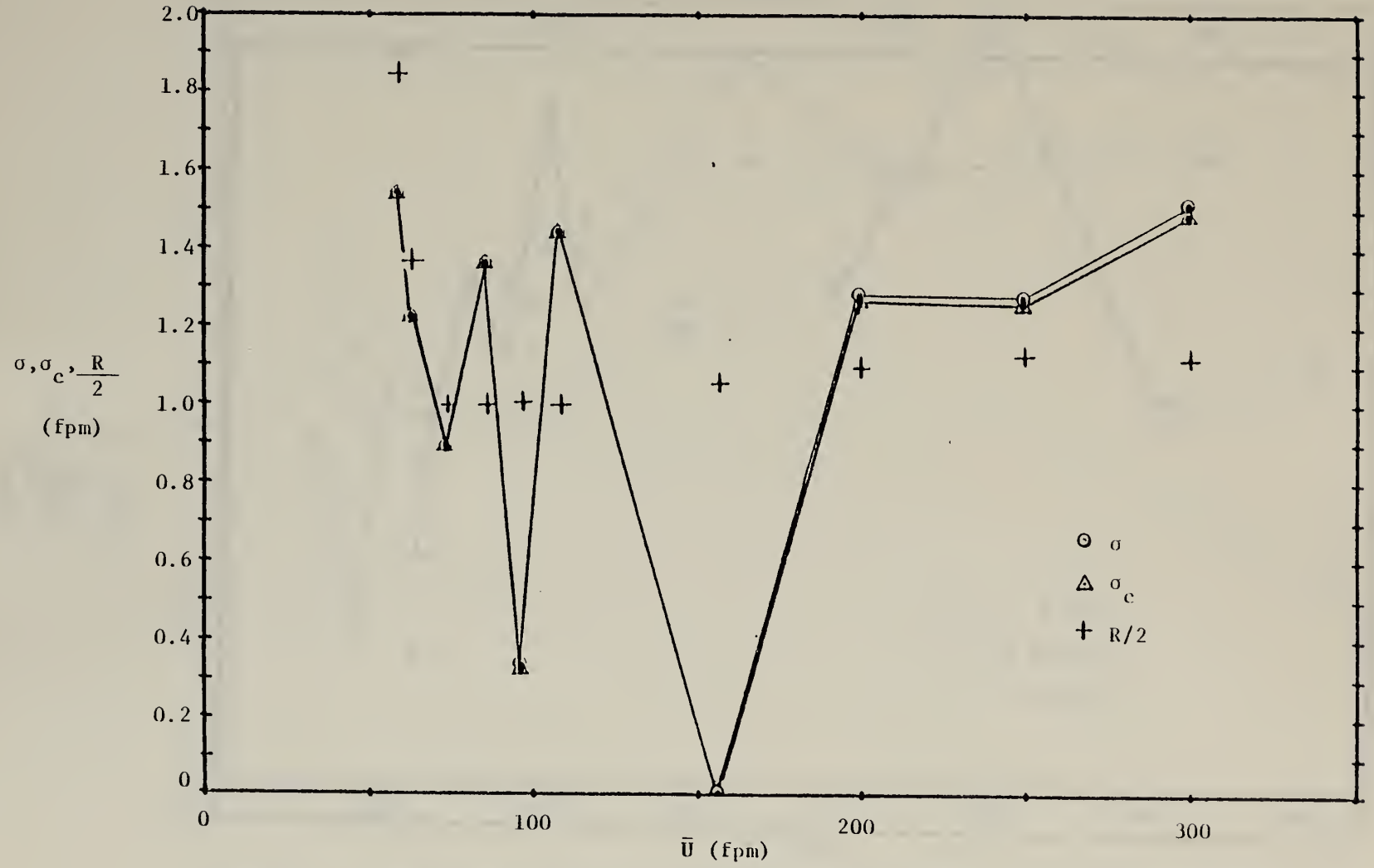

FIGURE 69. σ AND σ_c IN TERMS OF TRUE VELOCITY, LOW RANGE. R/2 NOTED. INSTRUMENT E.

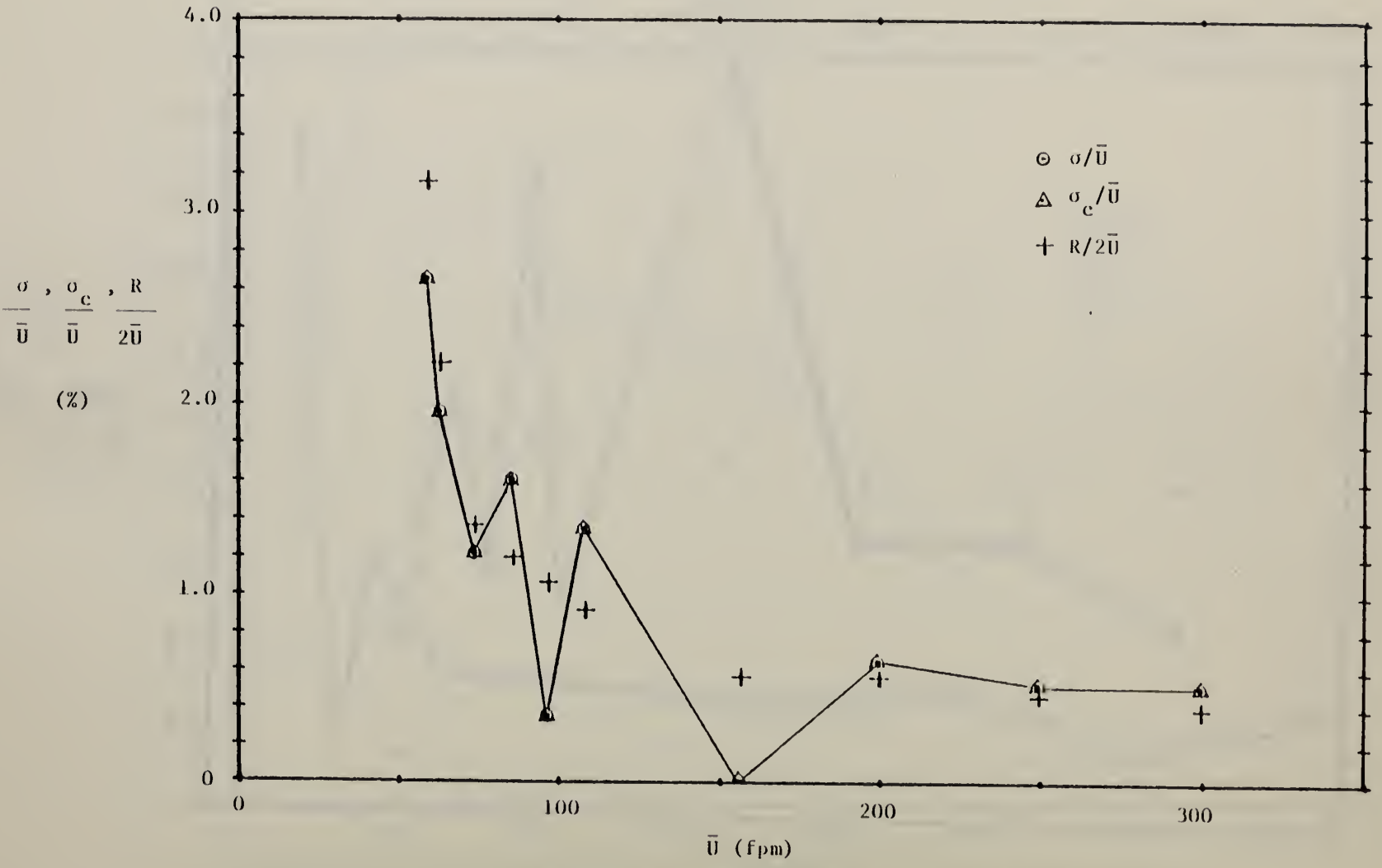

FIGURE 70. σ AND σ_c AS PERCENT OF GROUP MEAN VELOCITY, LOW RANGE. R/2Ū NOTED. INSTRUMENT E.

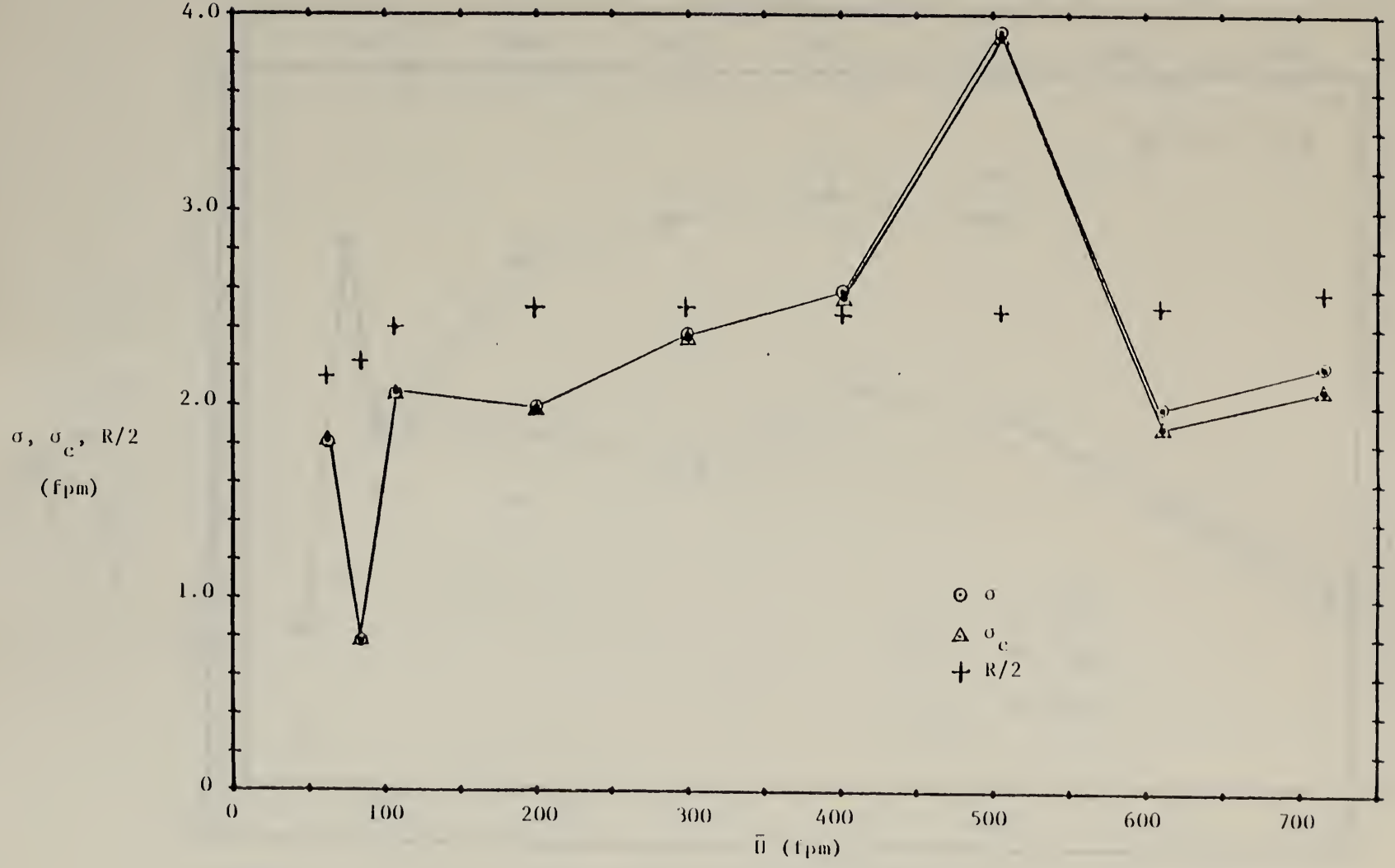

FIGURE 71. σ AND σ_c IN TERMS OF TRUE VELOCITY, MEDIUM RANGE. R/2 NOTED. INSTRUMENT E.

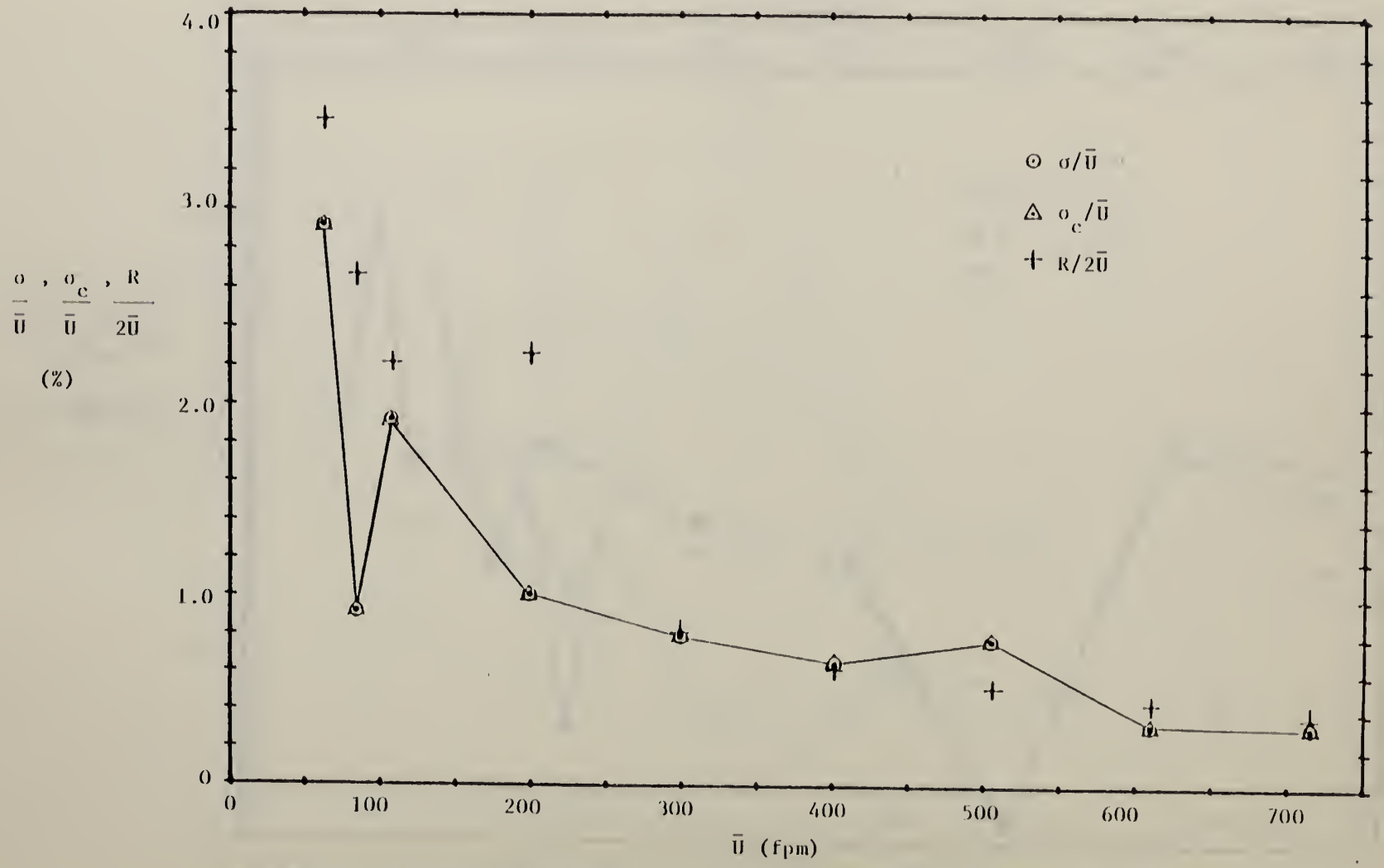

FIGURE 72. σ AND σ_c AS PERCENT OF GROUP MEAN VELOCITY, MEDIUM RANGE. $R/2\bar{U}$ NOTED. INSTRUMENT E.

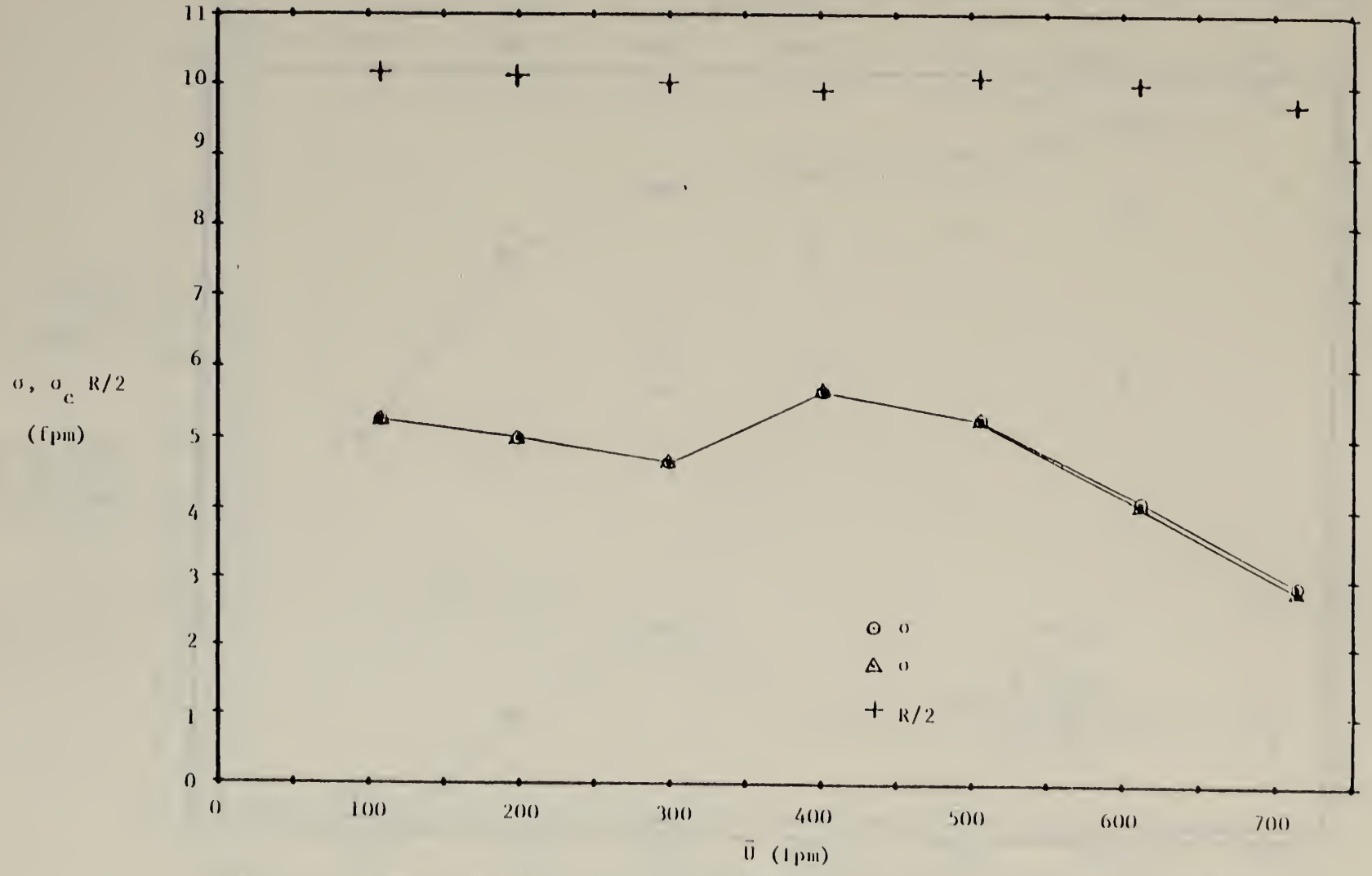

FIGURE 73. σ AND σ_c IN TERMS OF TRUE VELOCITY, HIGH RANGE. R/2 NOTED. INSTRUMENT E.

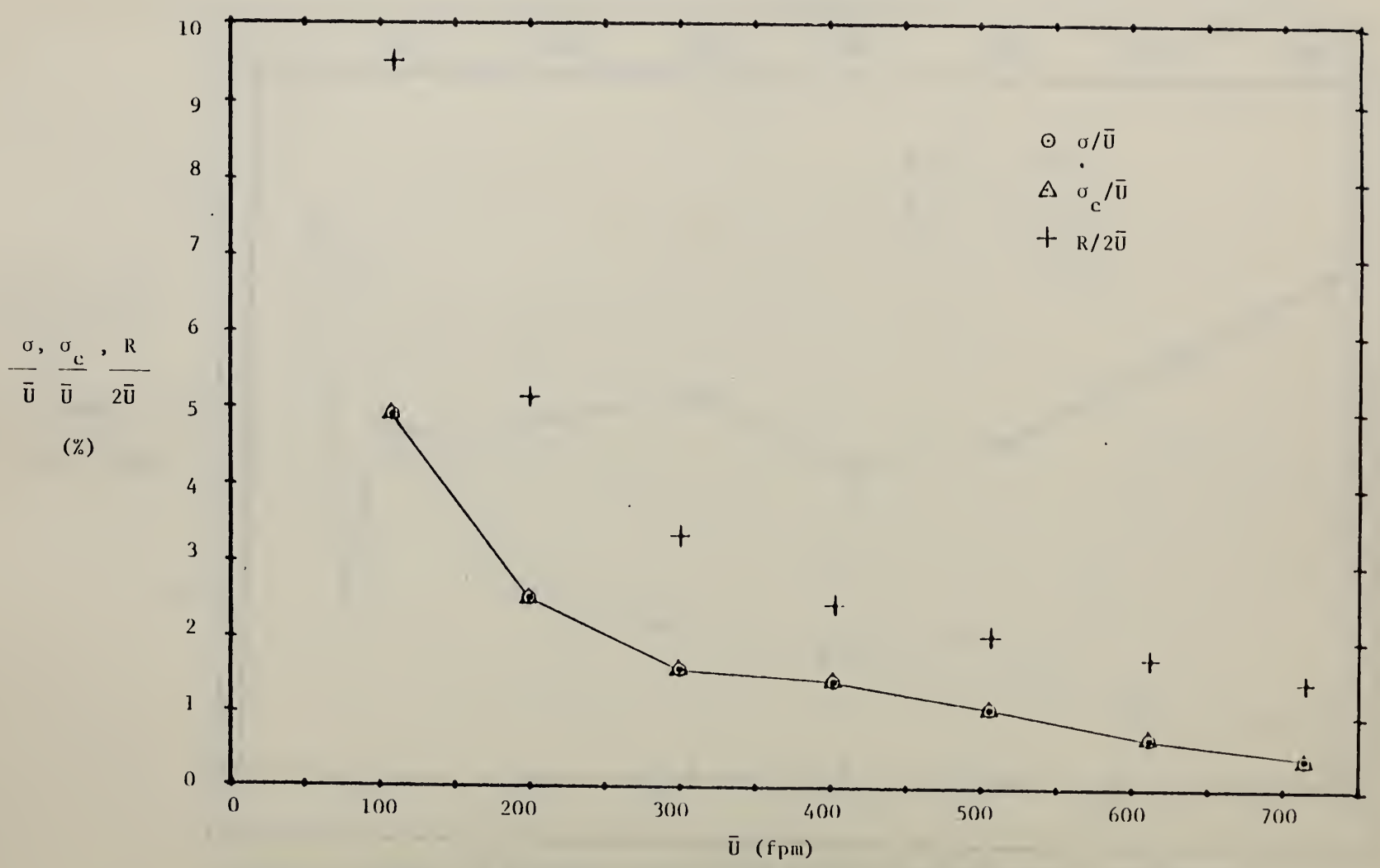

FIGURE 74. σ_c AND σ AS PERCENT OF GROUP MEAN VELOCITY, HIGH RANGE. $R/2\bar{U}$ NOTED. INSTRUMENT E.

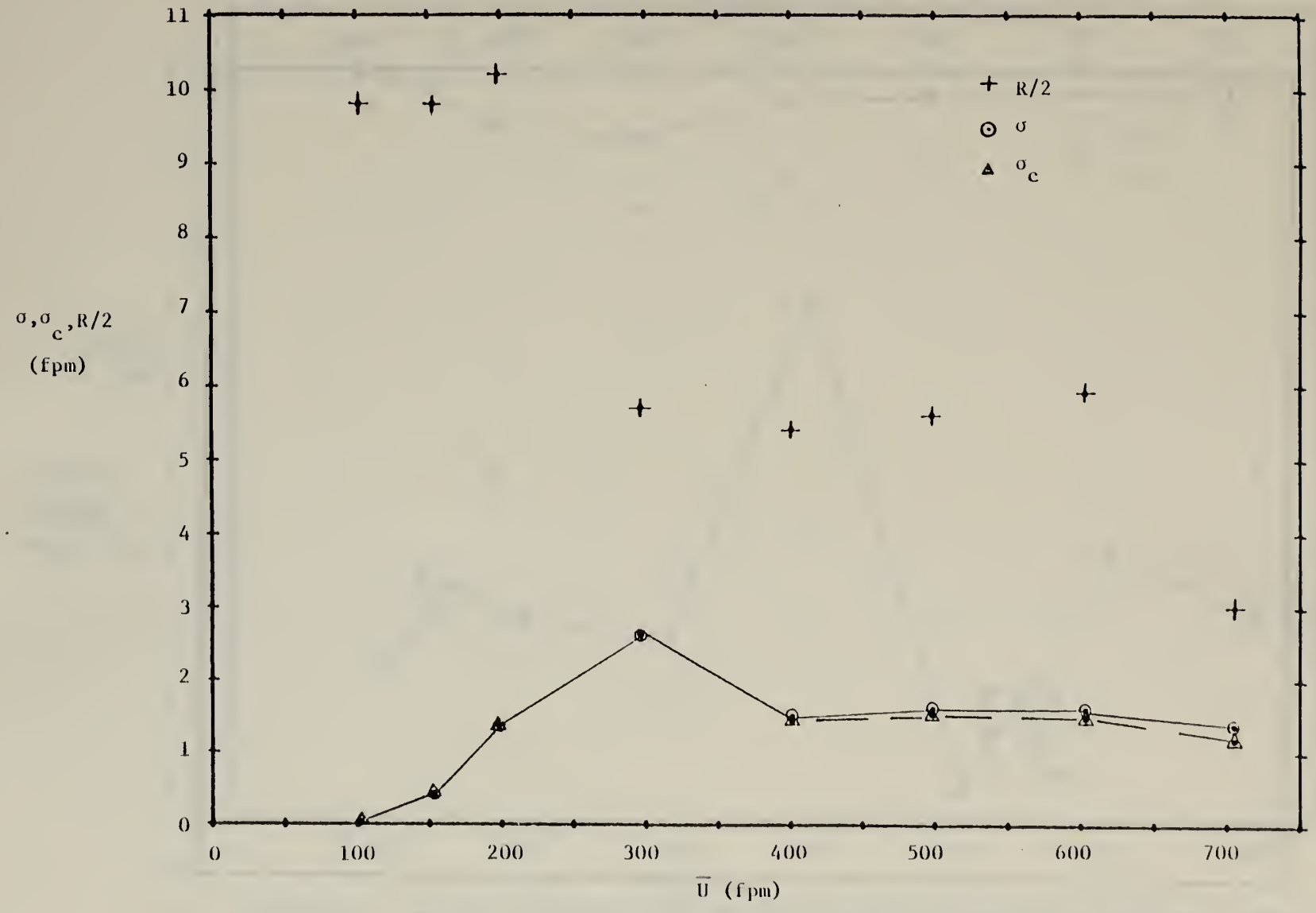

FIGURE 75. σ AND σ_c IN TERMS OF TRUE VELOCITY FOR PITOT PROBE, LOW RANGE. R/2 NOTED. INSTRUMENT F.

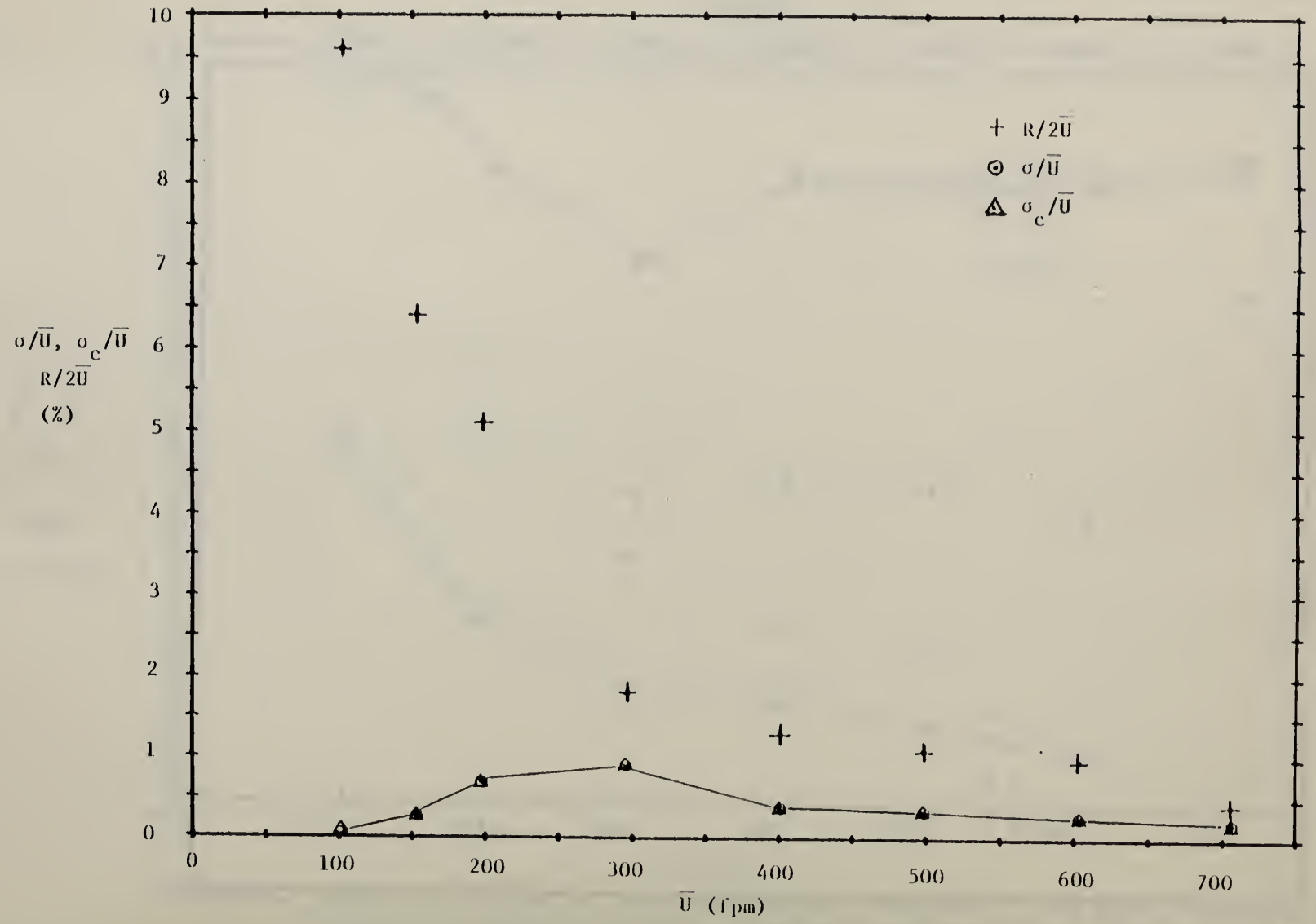

FIGURE 76. σ AND σ_c AS PERCENT OF GROUP MEAN VELOCITY FOR PITOT PROBE, LOW RANGE. R/2 $\bar{U}$ NOTED. INSTRUMENT F.

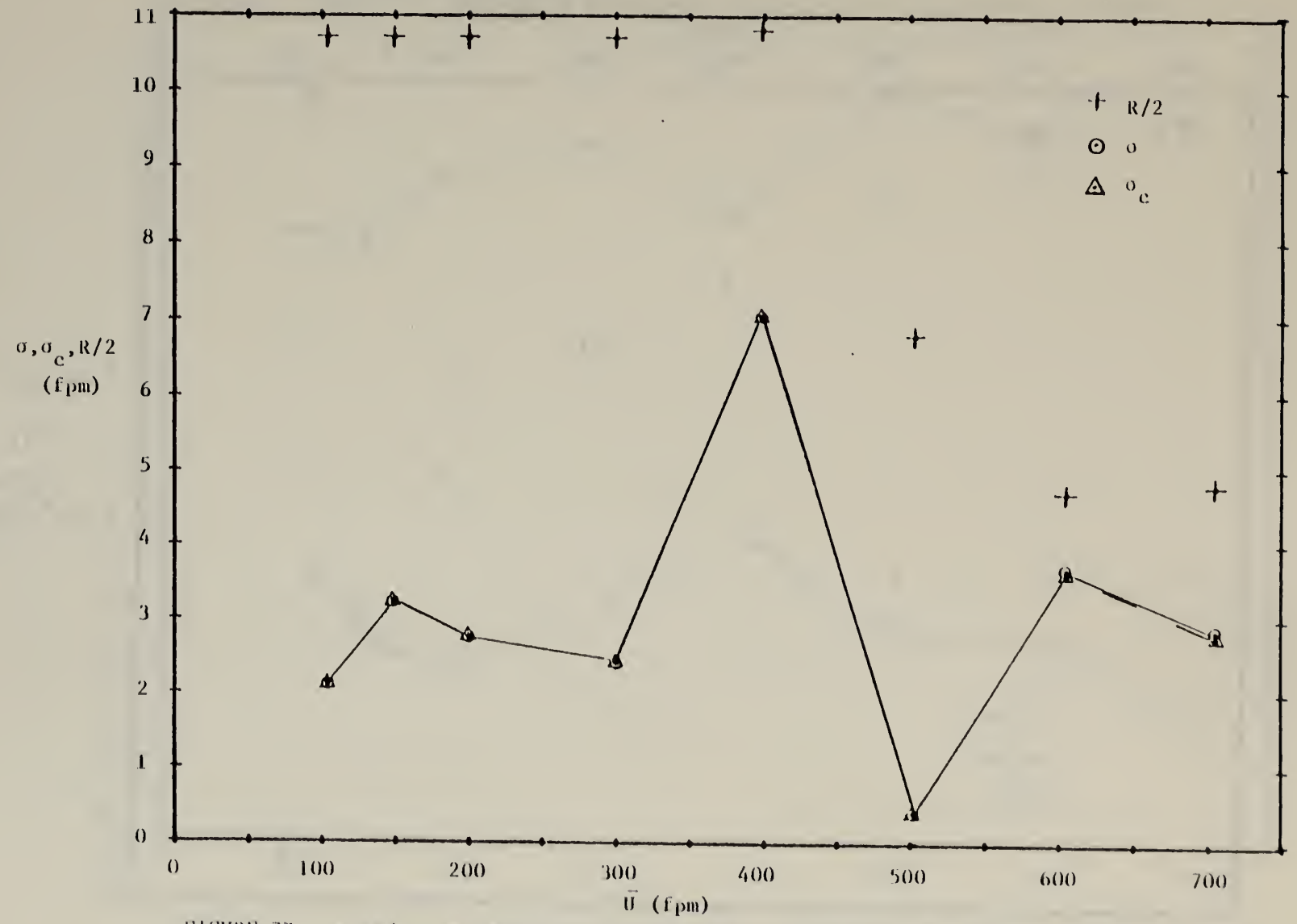

FIGURE 77. σ and σ_c IN TERMS OF TRUE VELOCITY FOR PITOT PROBE, HIGH RANGE. R/2 NOTED. INSTRUMENT F.

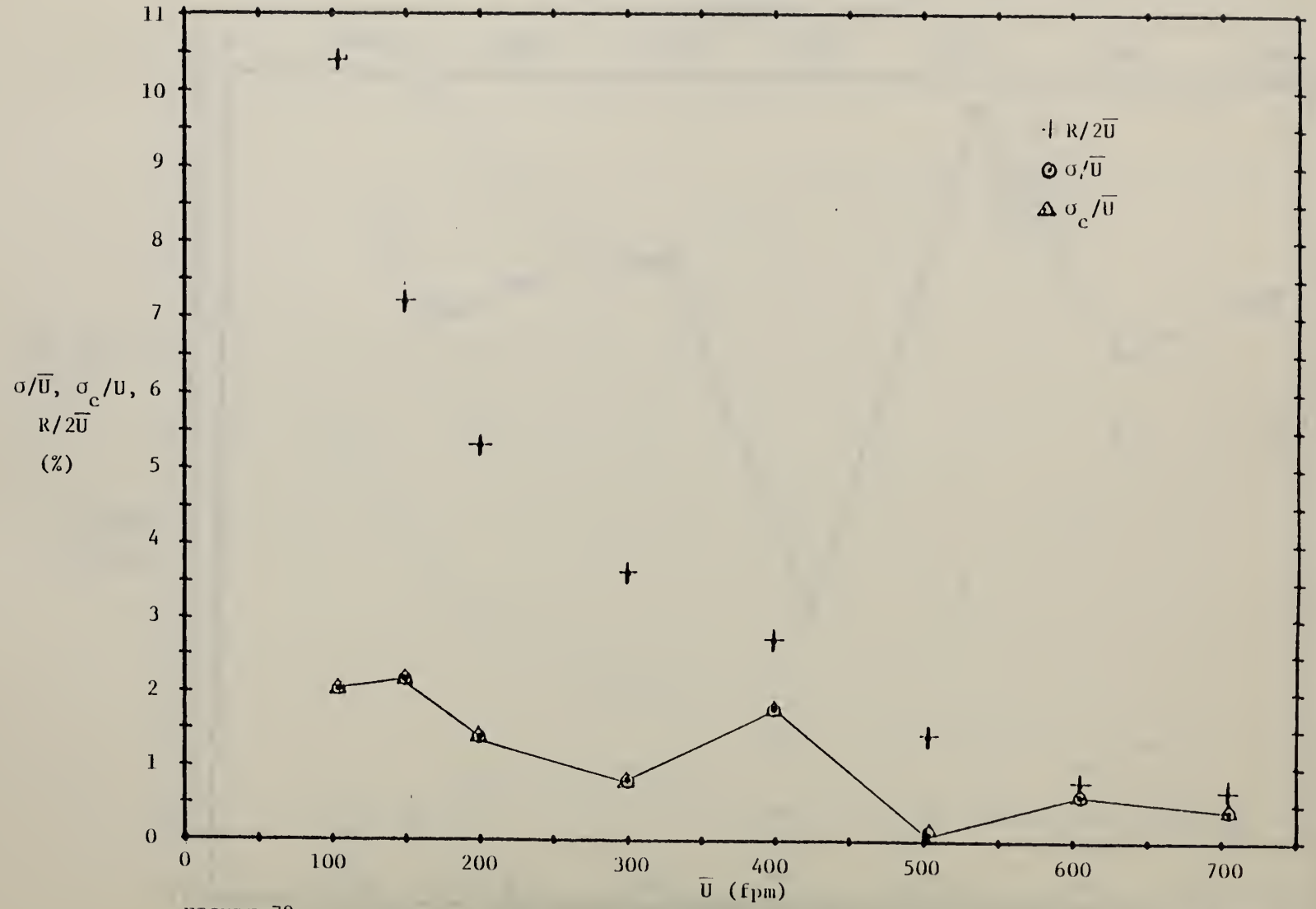

FIGURE 78. σ AND σ_c AS PERCENT OF GROUP MEAN VELOCITY FOR PITOT PROBE, HIGH RANGE. $R/2\bar{U}$ NOTED. INSTRUMENT F.

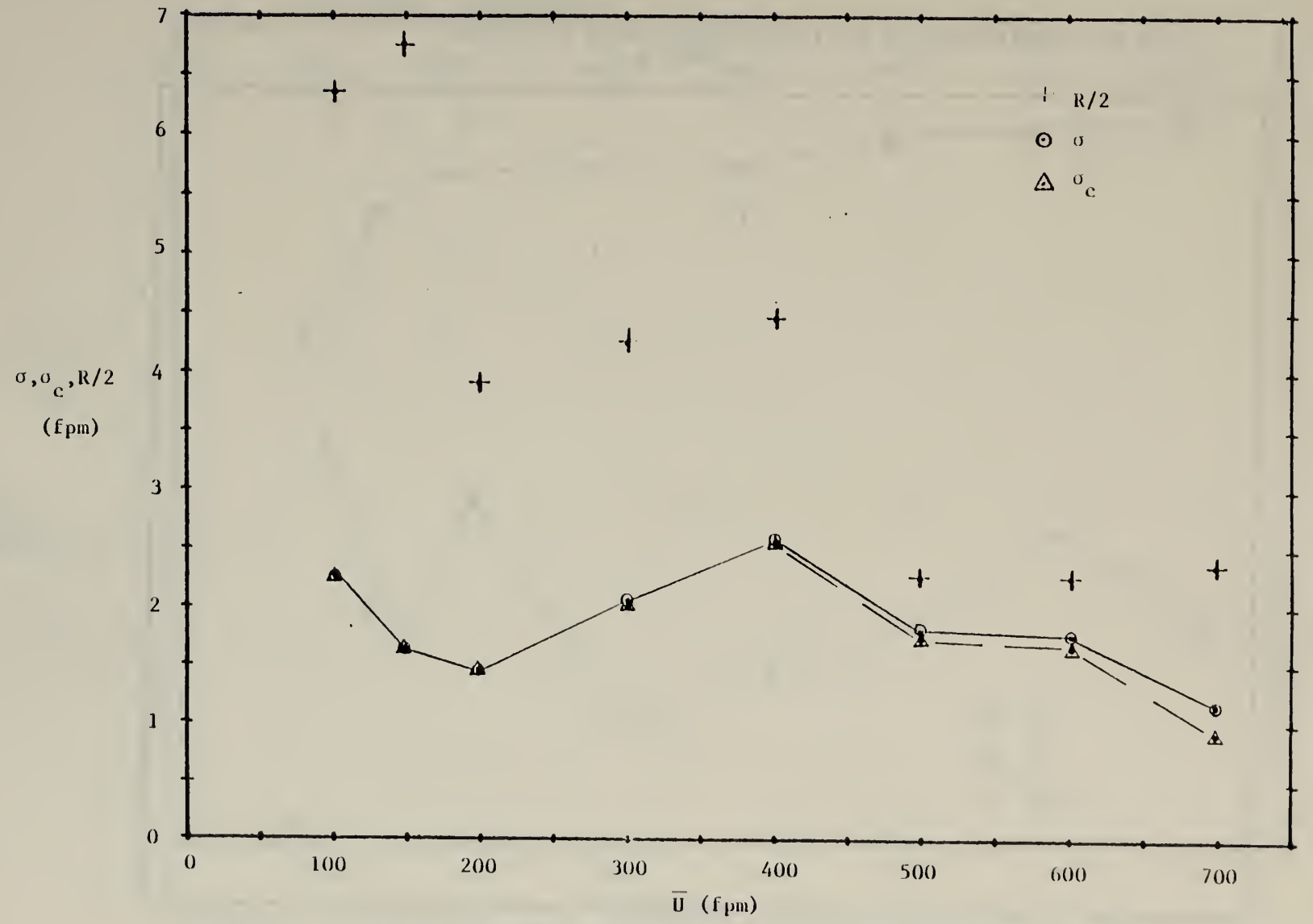

FIGURE 79. σ AND σ_c IN TERMS OF TRUE VELOCITY FOR DIFFUSER PROBE, LOW RANGE. R/2 NOTED. INSTRUMENT F.

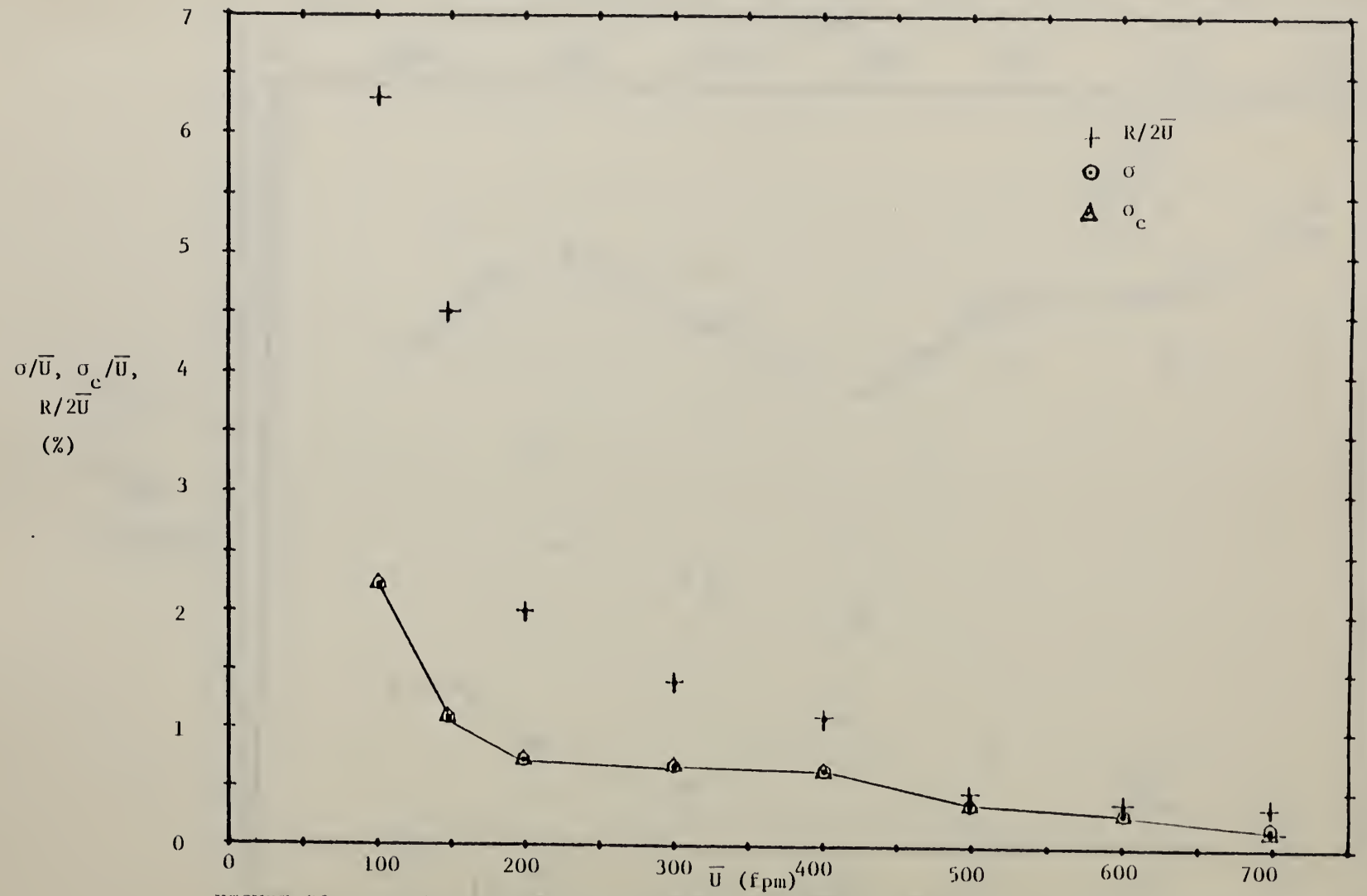

FIGURE 80. σ and σ_c AS PERCENT OF GROUP MEAN VELOCITY FOR DIFFUSER PROBE, LOW RANGE. $R/2\overline{U}$ NOTED. INSTRUMENT F.

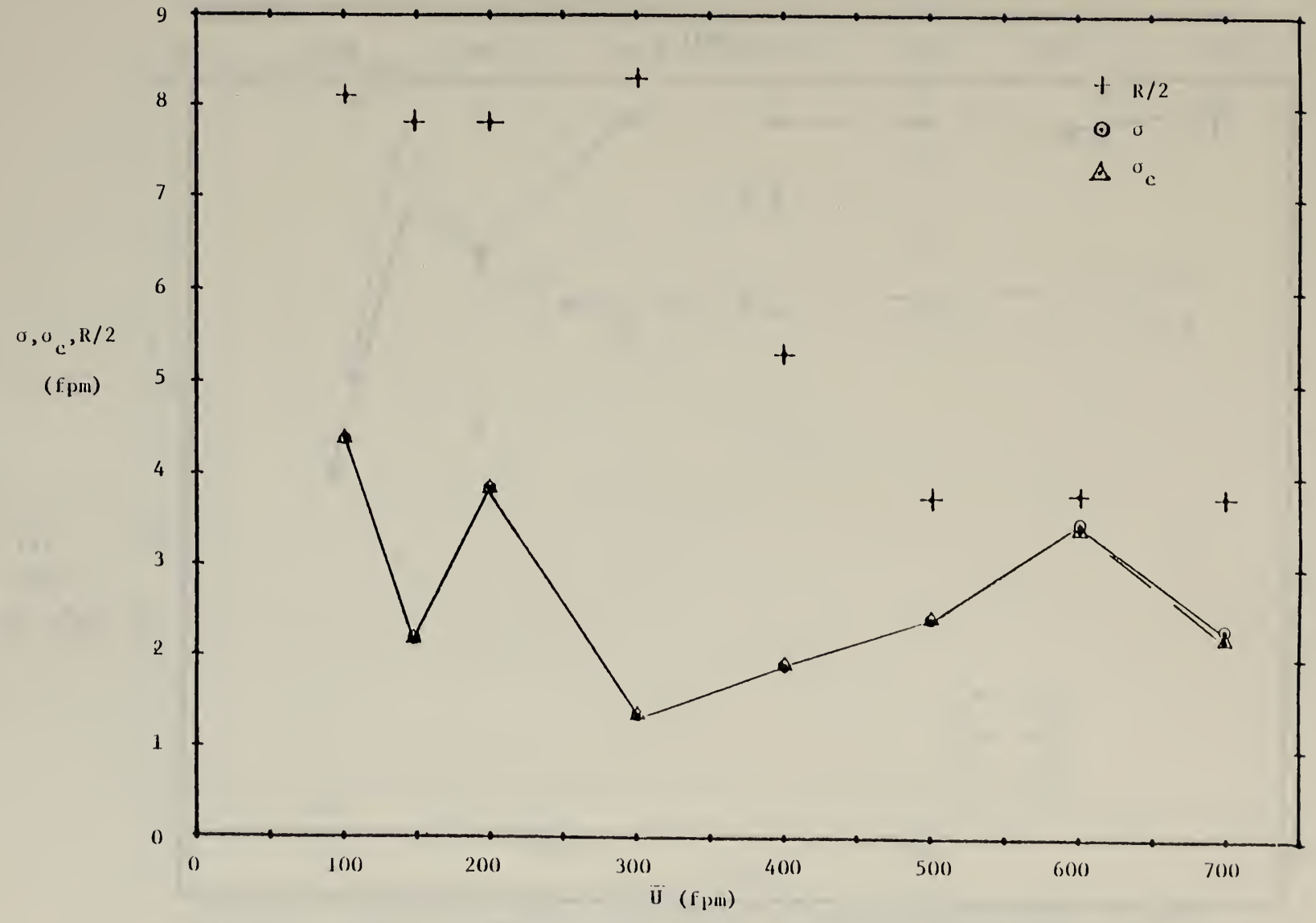

FIGURE 81. σ AND σ_c IN TERMS OF TRUE VELOCITY FOR DIFFUSER PROBE, HIGH RANGE. R/2 NOTED. INSTRUMENT F.

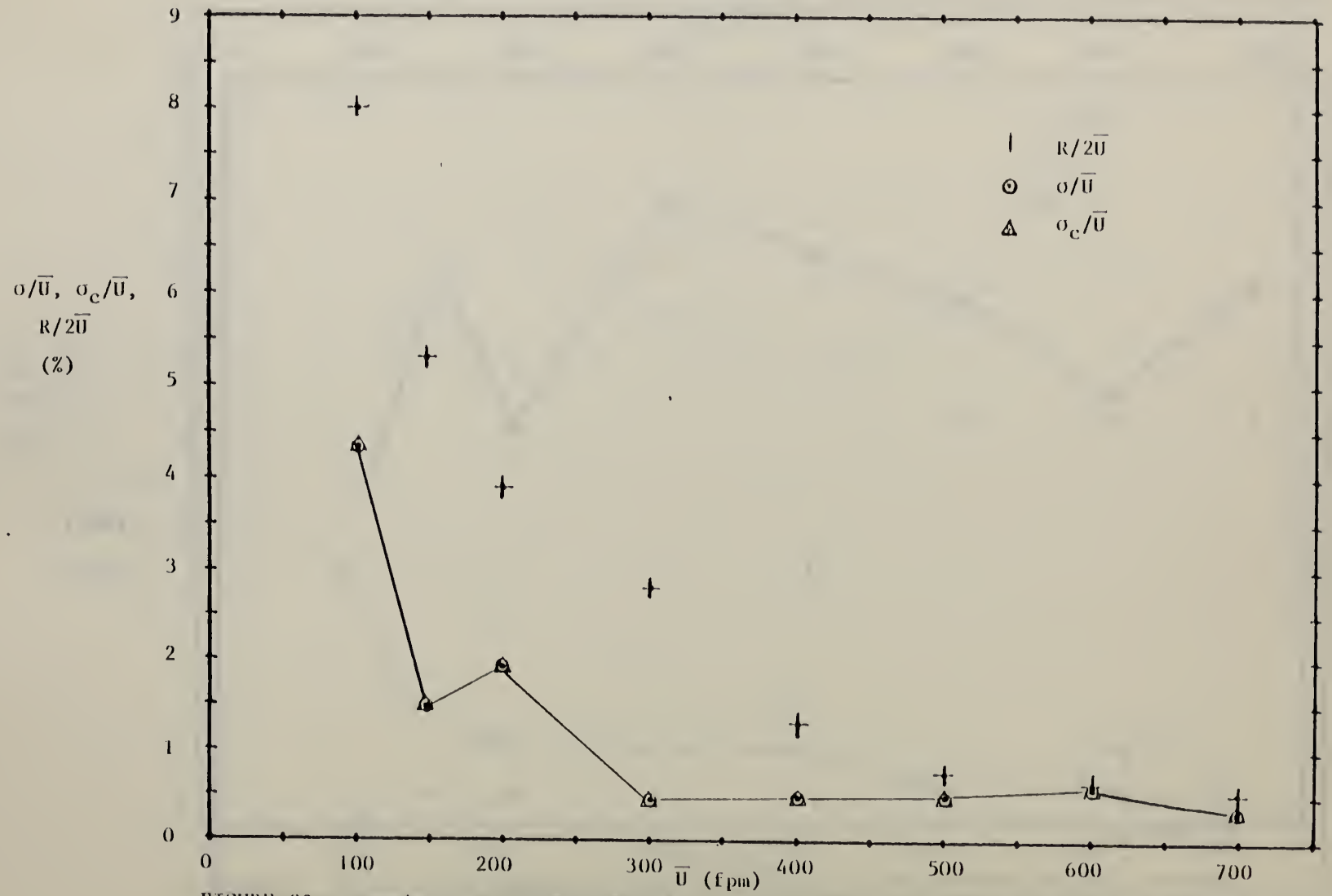

FIGURE 82. σ and σ_c AS PERCENT OF GROUP MEAN VELOCITY FOR DIFFUSER PROBE, HIGH RANGE. R/2U NOTED. INSTRUMENT F.

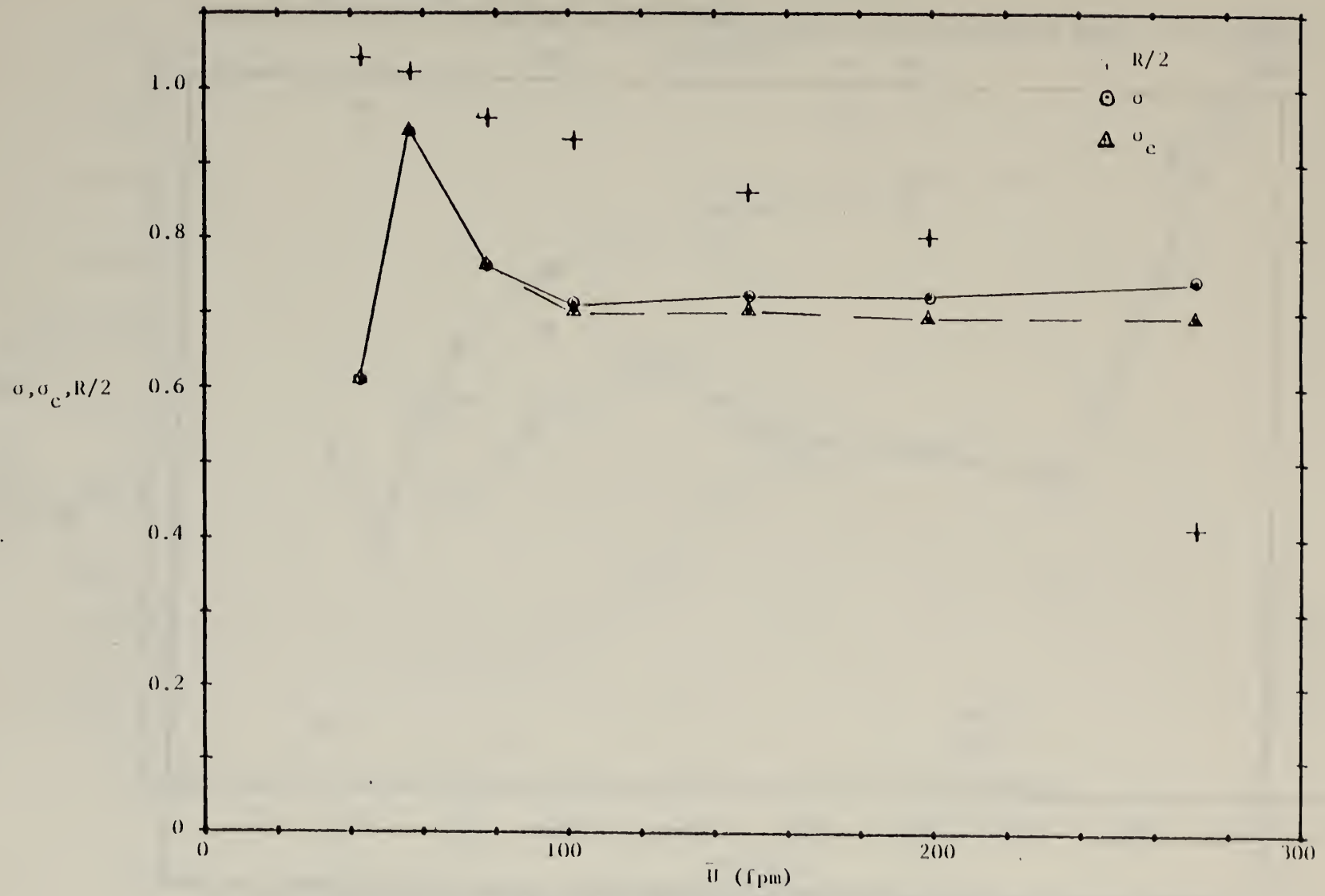

FIGURE 83. σ AND σ_c IN TERMS OF TRUE VELOCITY FOR LOW VELOCITY PROBE. R/2 NOTED. INSTRUMENT F.

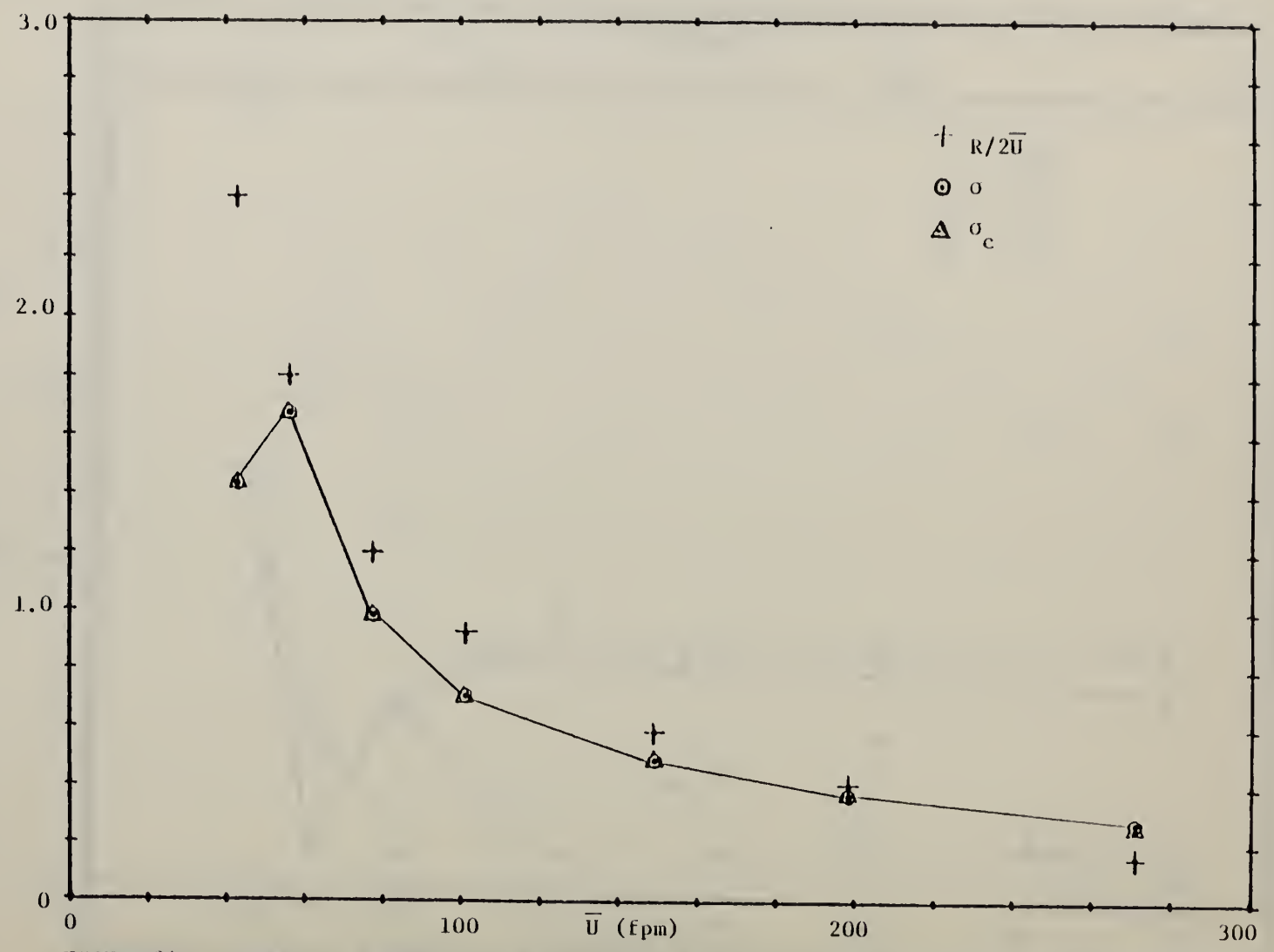

FIGURE 84. σ AND σ_c AS PERCENT OF GROUP MEAN VELOCITY FOR LOW VELOCITY PROBE. $R/2\overline{U}$ NOTED. INSTRUMENT F.

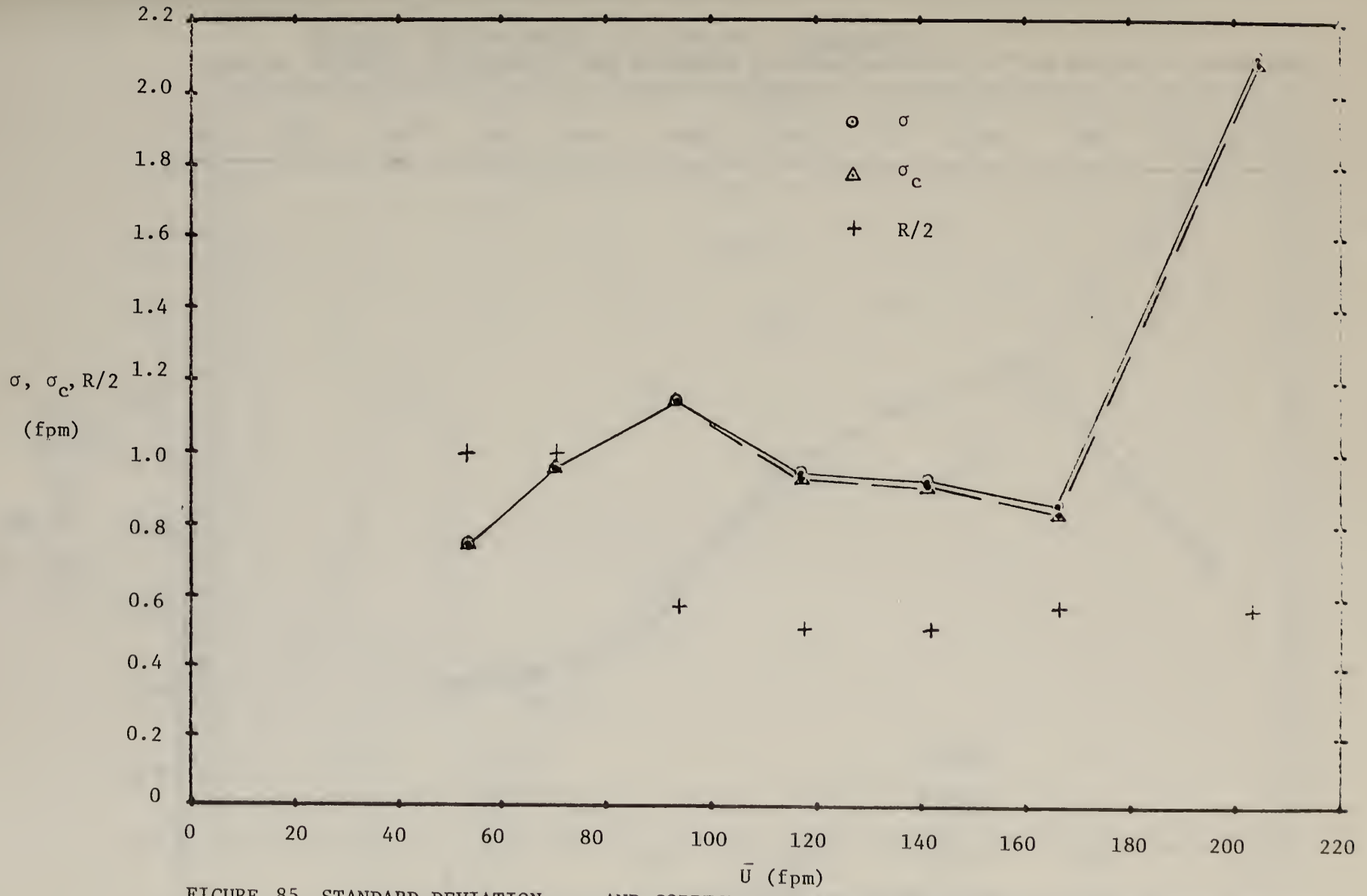

FIGURE 85. STANDARD DEVIATION, σ, AND CORRECTED STANDARD DEVIATION, σ_c, OF INDICATED VELOCITY IN TERMS OF TRUE VELOCITY, LOW RANGE. R/2 NOTED. INSTRUMENT G.

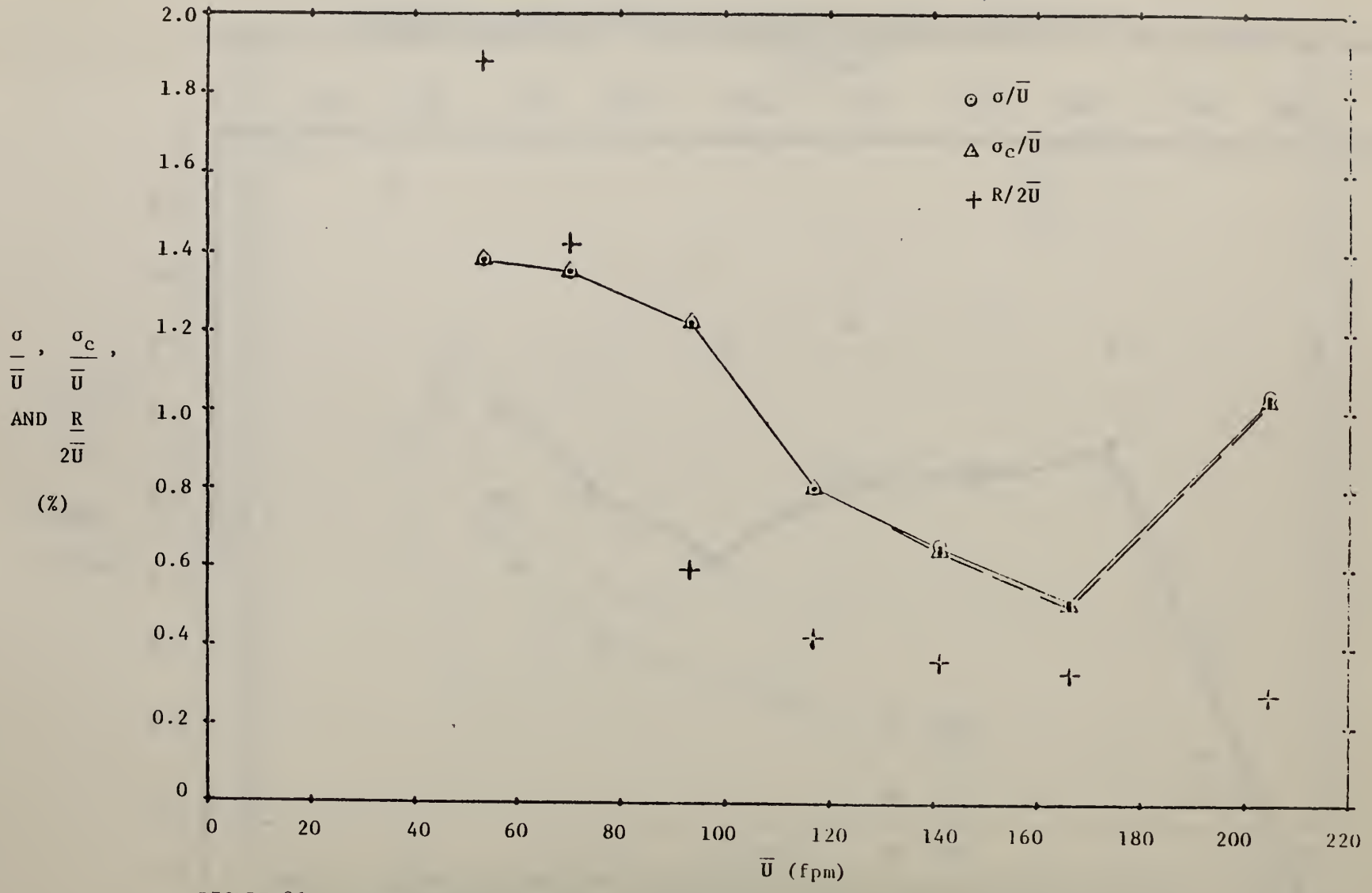

FIGURE 86. STANDARD DEVIATION, σ, AND CORRECTED STANDARD DEVIATION, σ_c, AS PERCENT OF GROUP MEAN VELOCITY, FOR LOW RANGE. R/2 Ū NOTED. INSTRUMENT G.

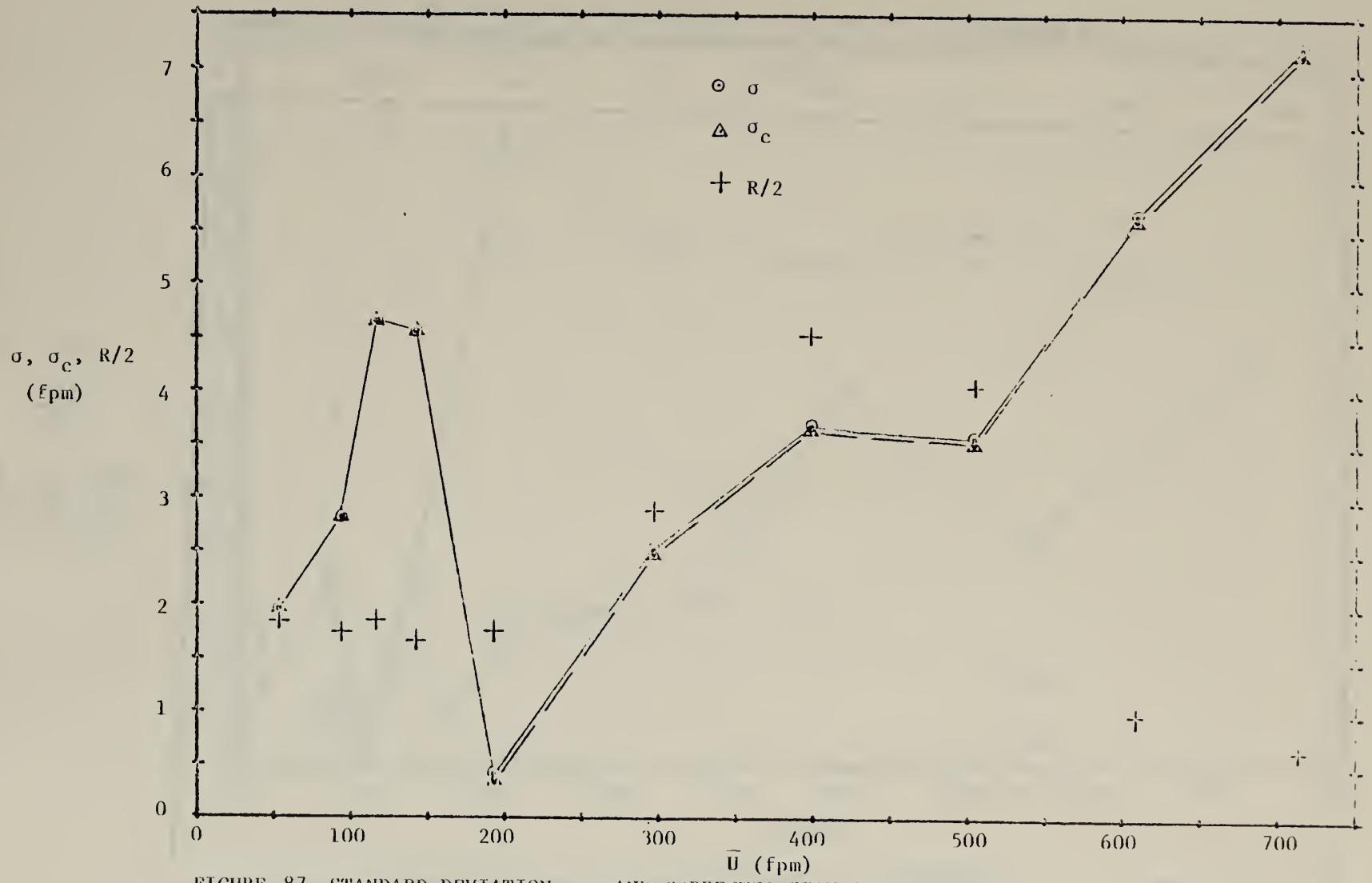

FIGURE 87. STANDARD DEVIATION, σ, AND CORRECTED STANDARD DEVIATION, σ_c, OF INDICATED VELOCITY IN TERMS OF TRUE VELOCITY, HIGH RANGE. R/2 NOTED. INSTRUMENT C.

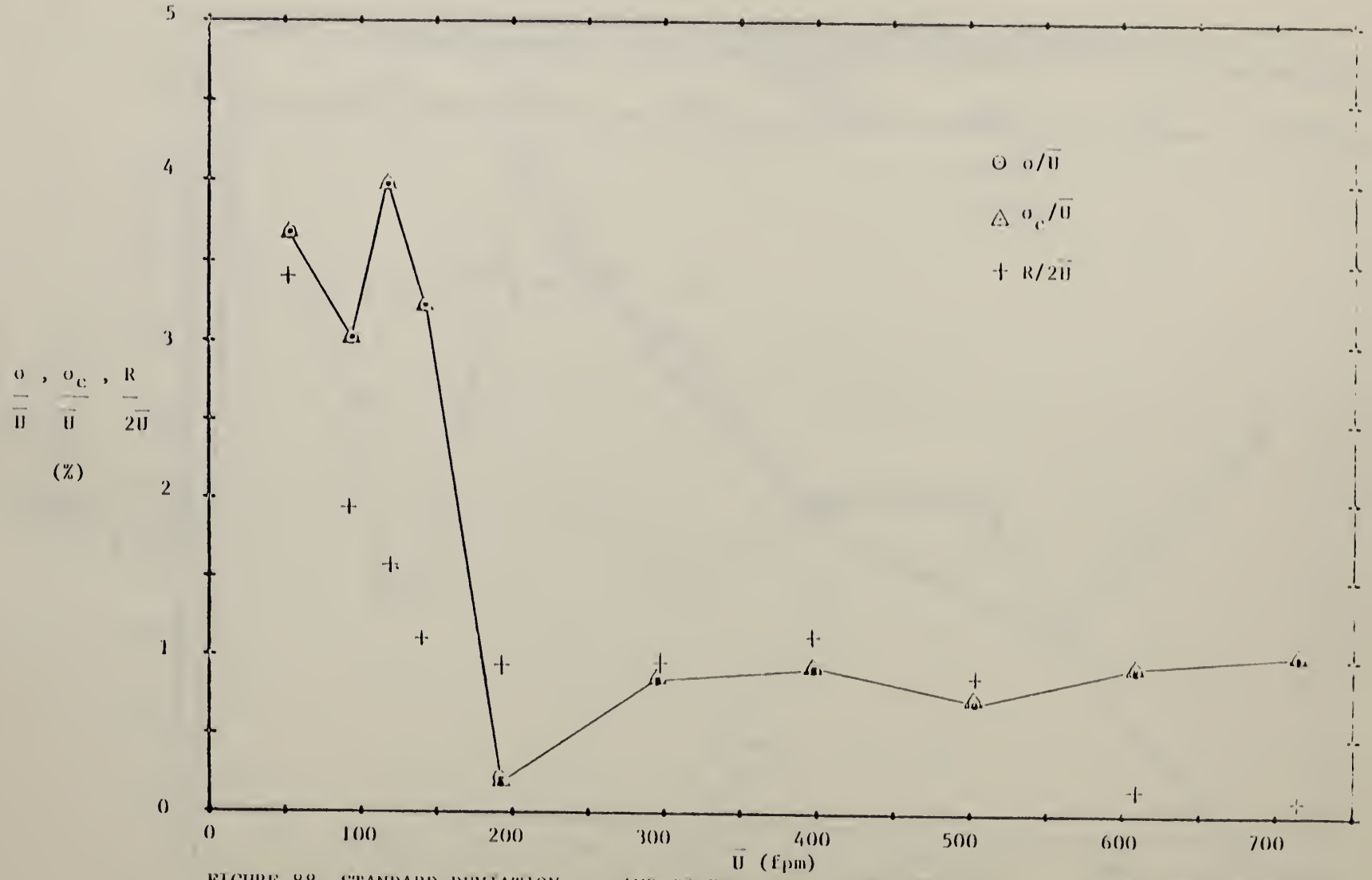

FIGURE 88. STANDARD DEVIATION, σ, AND CORRECTED STANDARD DEVIATION, σ_c, AS PERCENT OF GROUP MEAN VELOCITY, $\bar{U}$, FOR HIGH RANGE. R/2U NOTED. INSTRUMENT G.

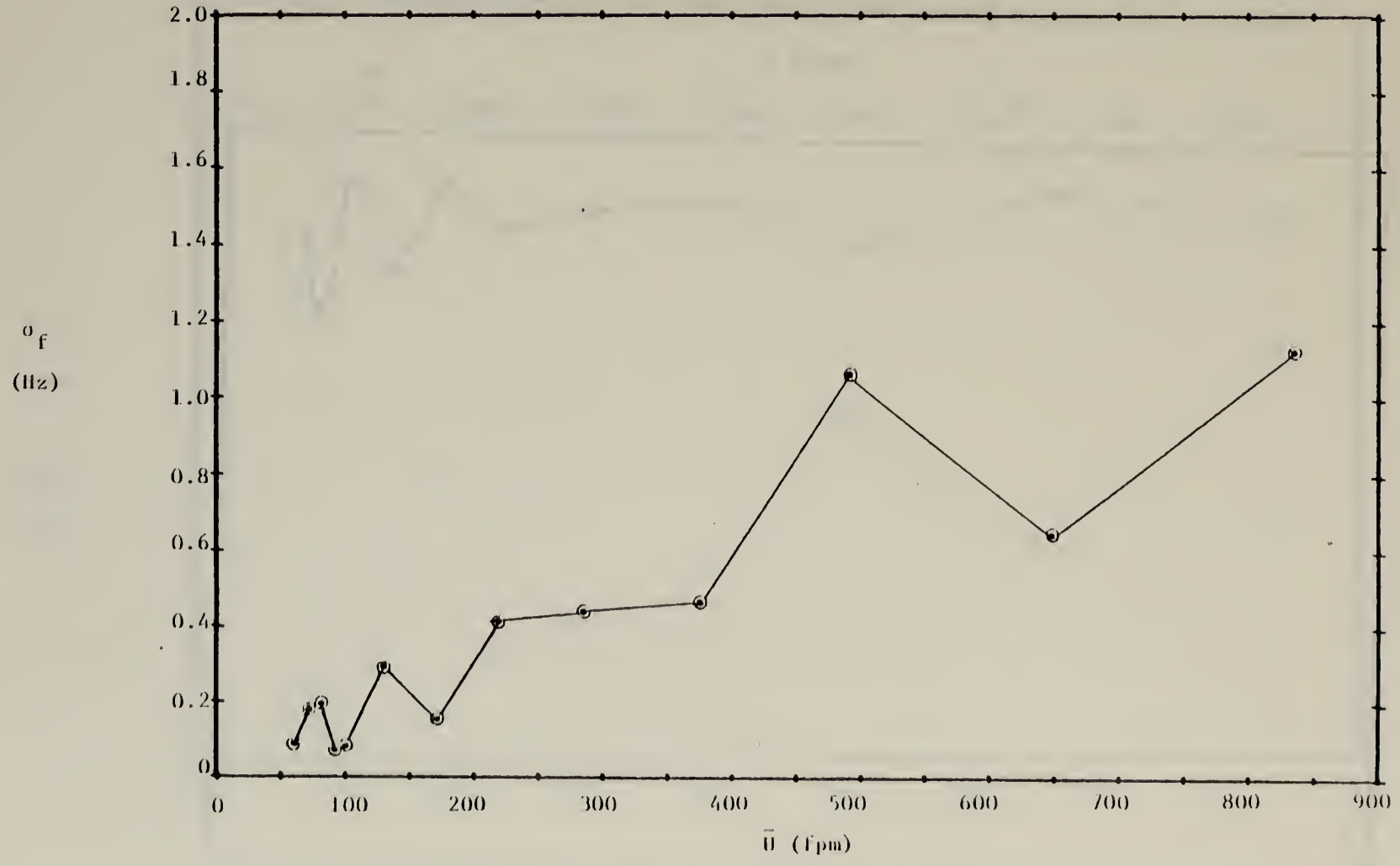

FIGURE 89. STANDARD DEVIATION OF PULSE FREQUENCY. INSTRUMENT H.

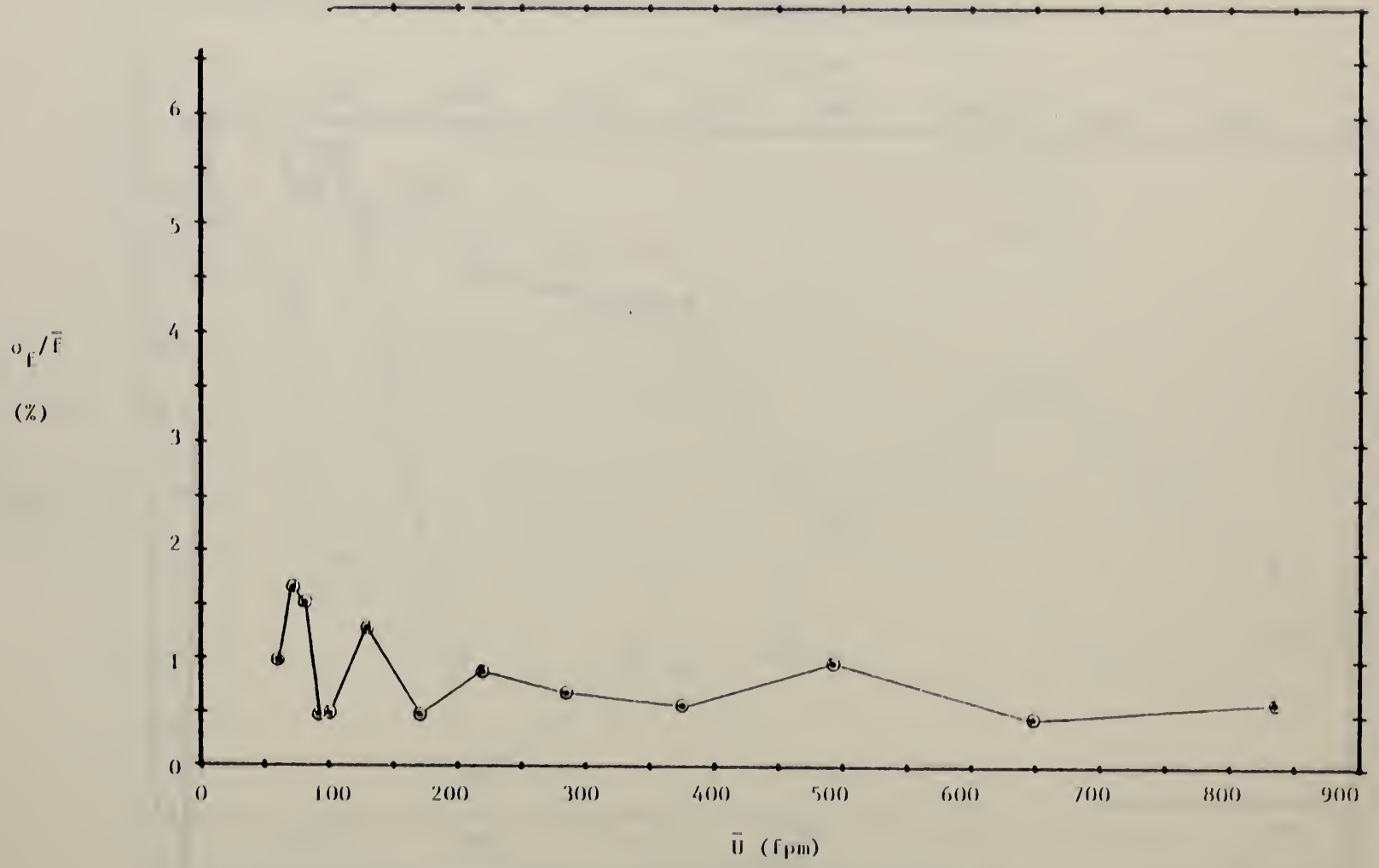

FIGURE 90. STANDARD DEVIATION OF PULSE FREQUENCY AS PERCENT OF GROUP MEAN FREQUENCY. INSTRUMENT II.

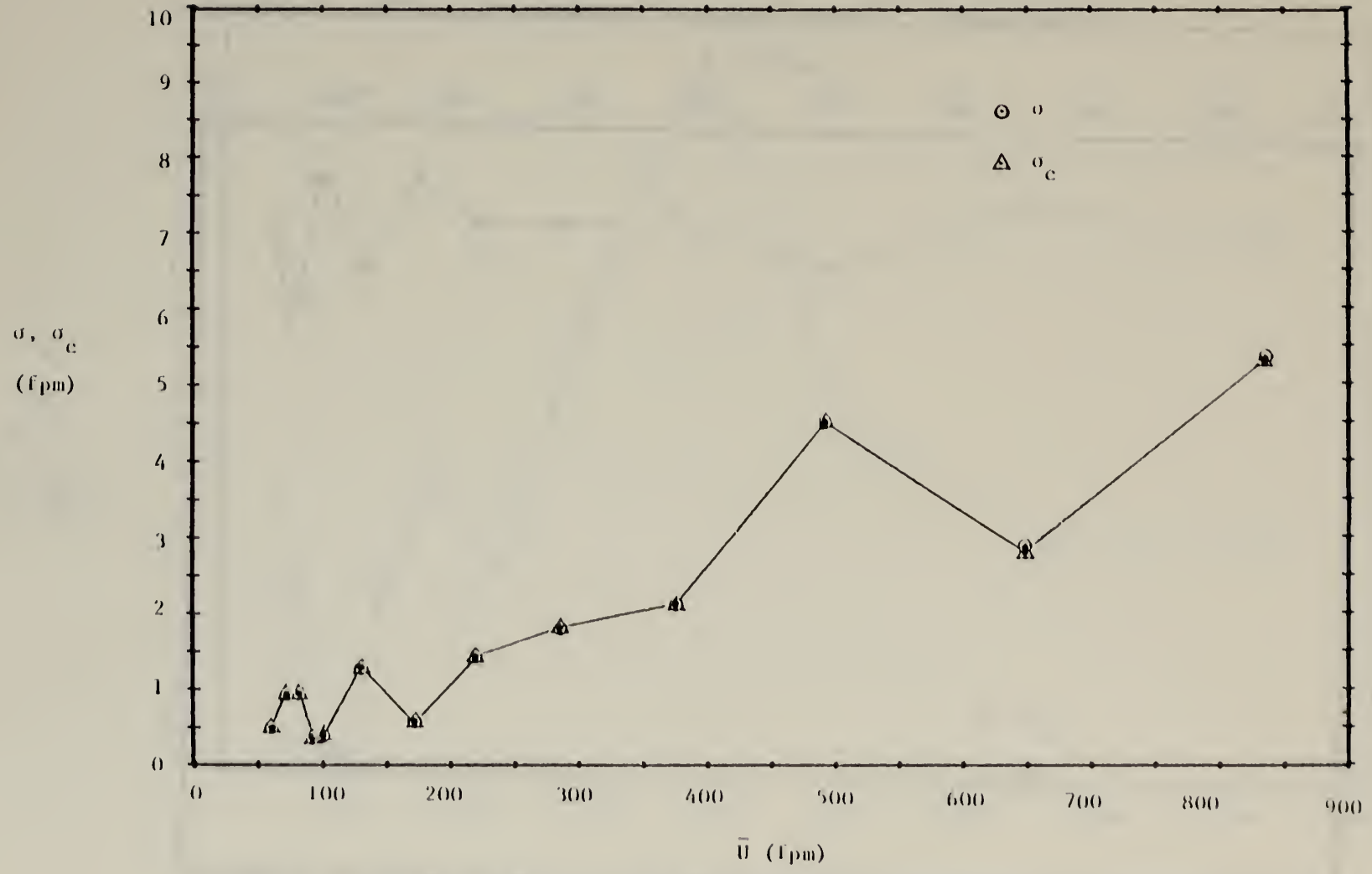

FIGURE 91. STANDARD DEVIATION, σ, AND CORRECTED STANDARD DEVIATION, σ_c, EXPRESSED AS EQUIVALENT TRUE VELOCITY. INSTRUMENT H.

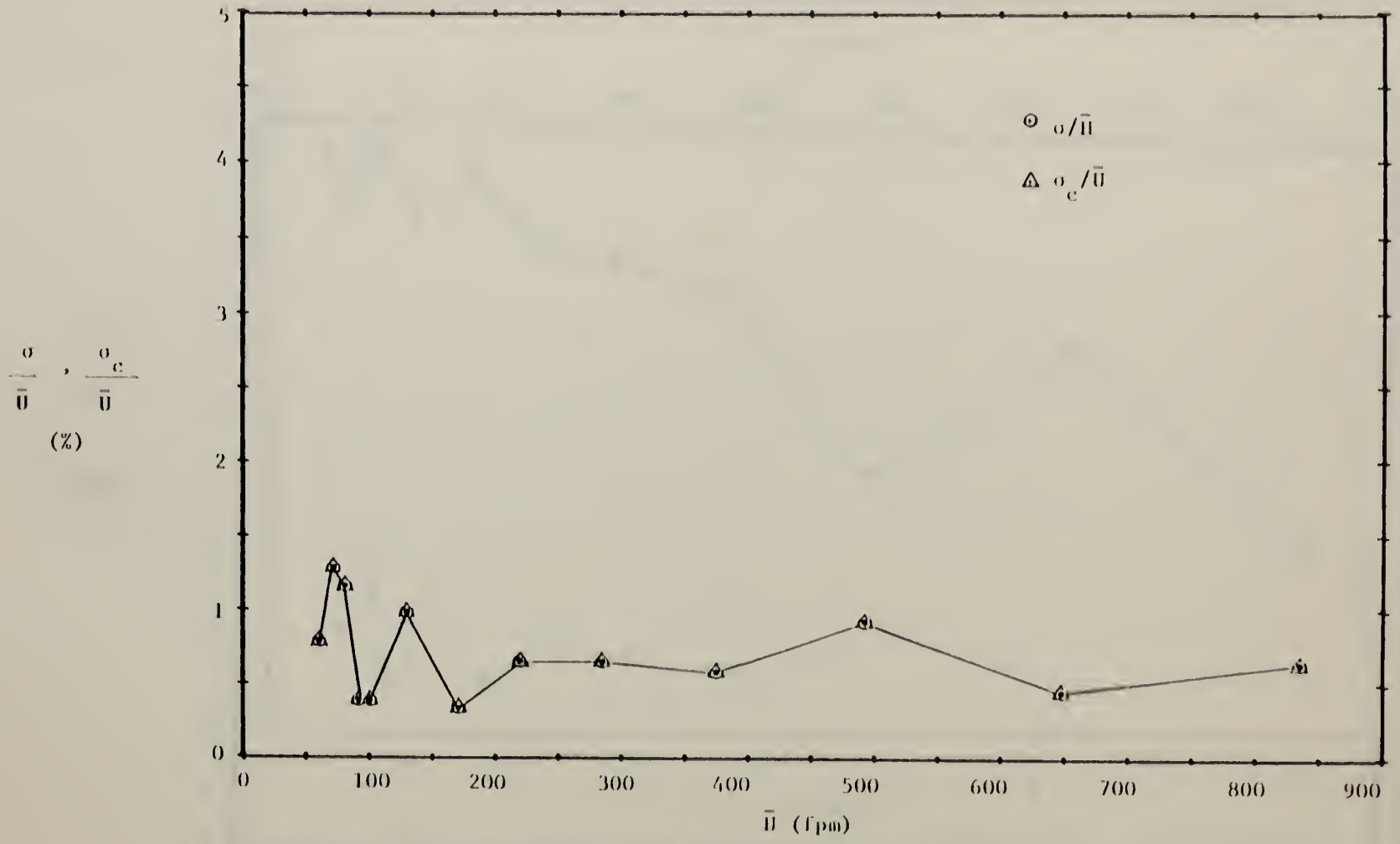

FIGURE 92. σ AND σ_c AS PERCENT OF GROUP MEAN VELOCITY. INSTRUMENT H.

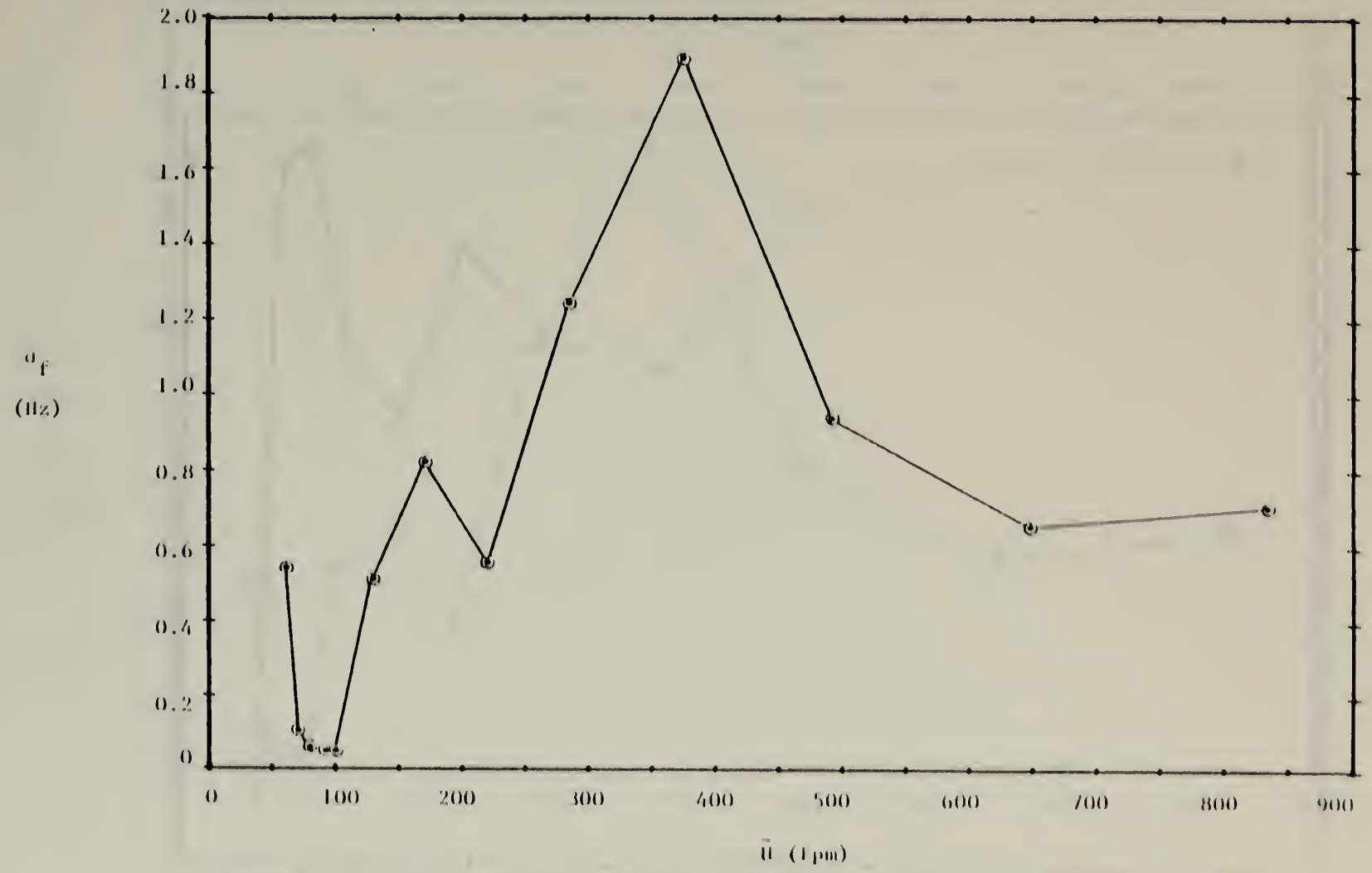

FIGURE 93. STANDARD DEVIATION OF PULSE FREQUENCY. INSTRUMENT 1.

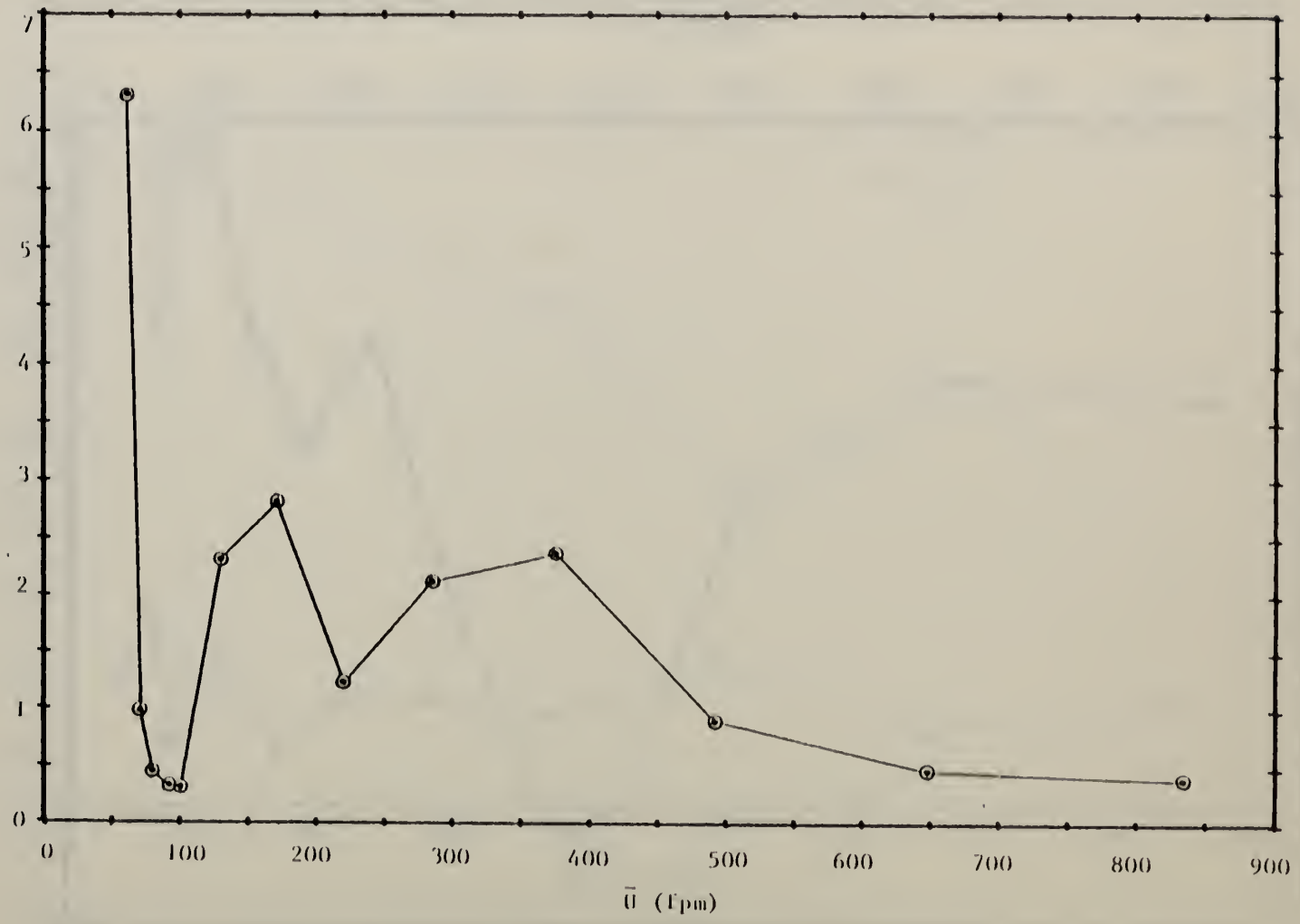

FIGURE 94. STANDARD DEVIATION OF PULSE FREQUENCY AS PERCENT OF GROUP MEAN FREQUENCY. INSTRUMENT I.

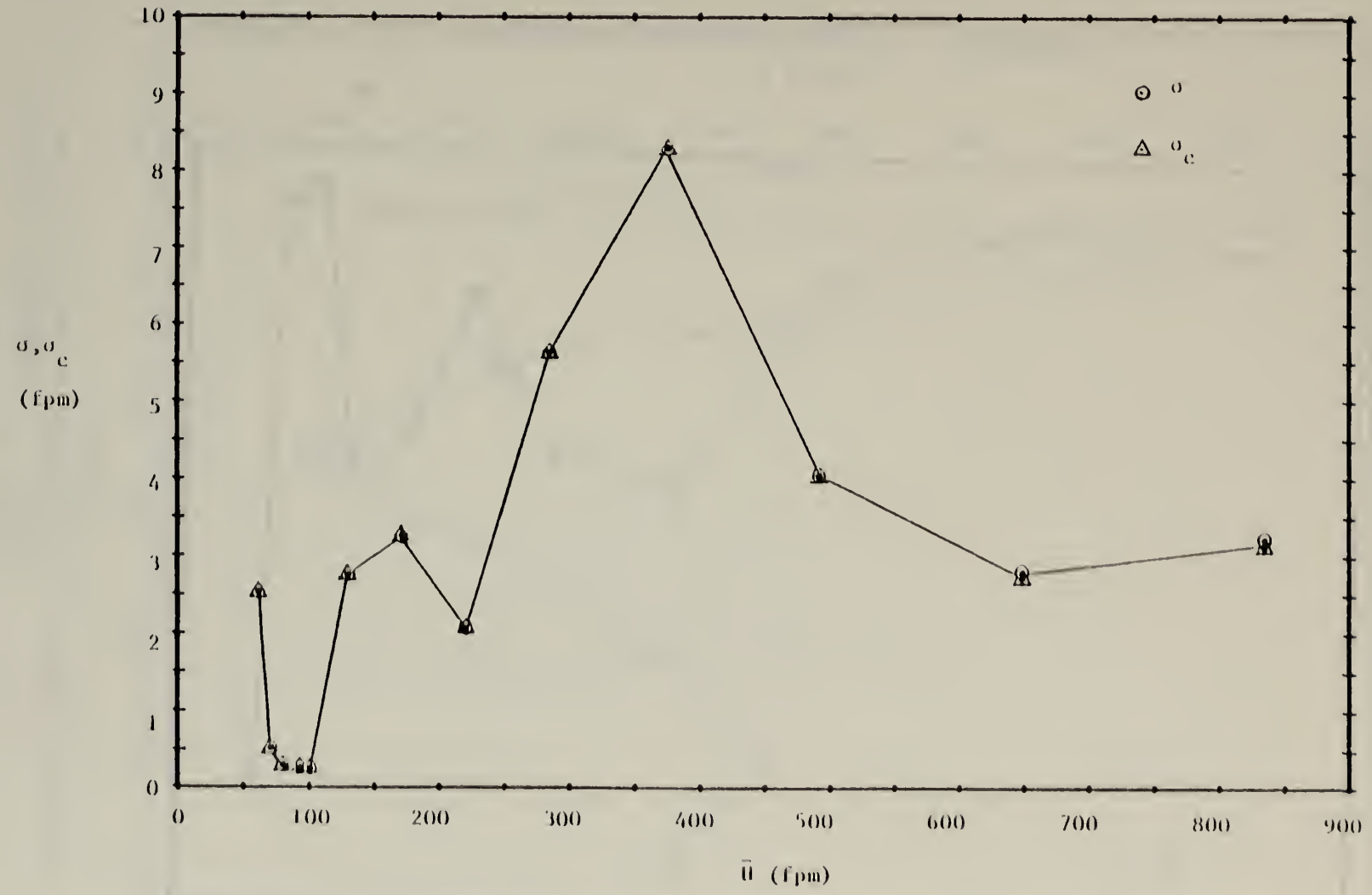

FIGURE 95. STANDARD DEVIATION, σ, AND CORRECTED STANDARD DEVIATION, σ_c, EXPRESSED AS EQUIVALENT TRUE VELOCITY. INSTRUMENT 1.

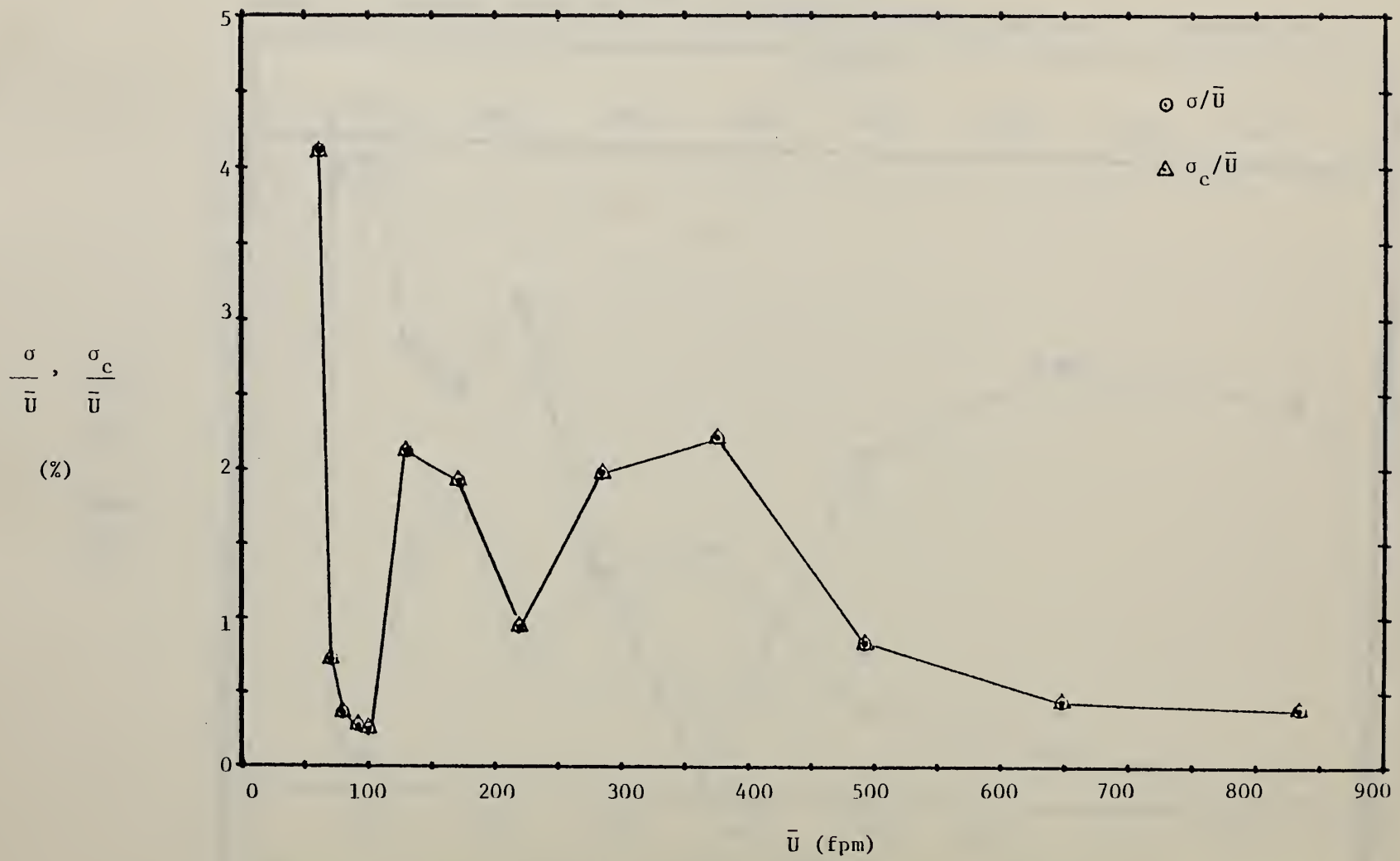

FIGURE 96. σ AND σ_c AS PERCENT OF GROUP MEAN VELOCITY. INSTRUMENT I.

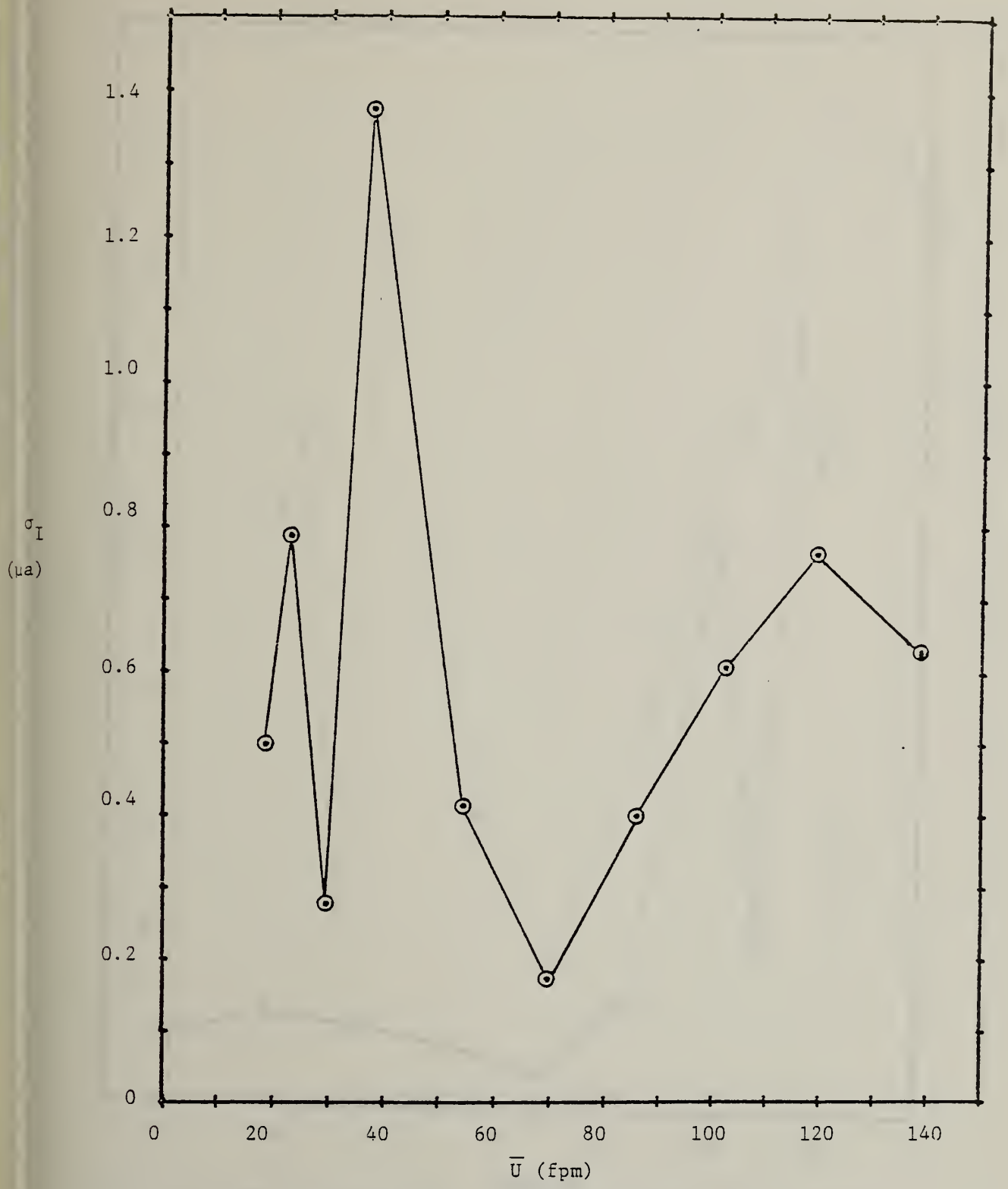

FIGURE 97. STANDARD DEVIATION OF INSTRUMENT OUTPUT AGAINST GROUP MEAN VELOCITY. INSTRUMENT J.

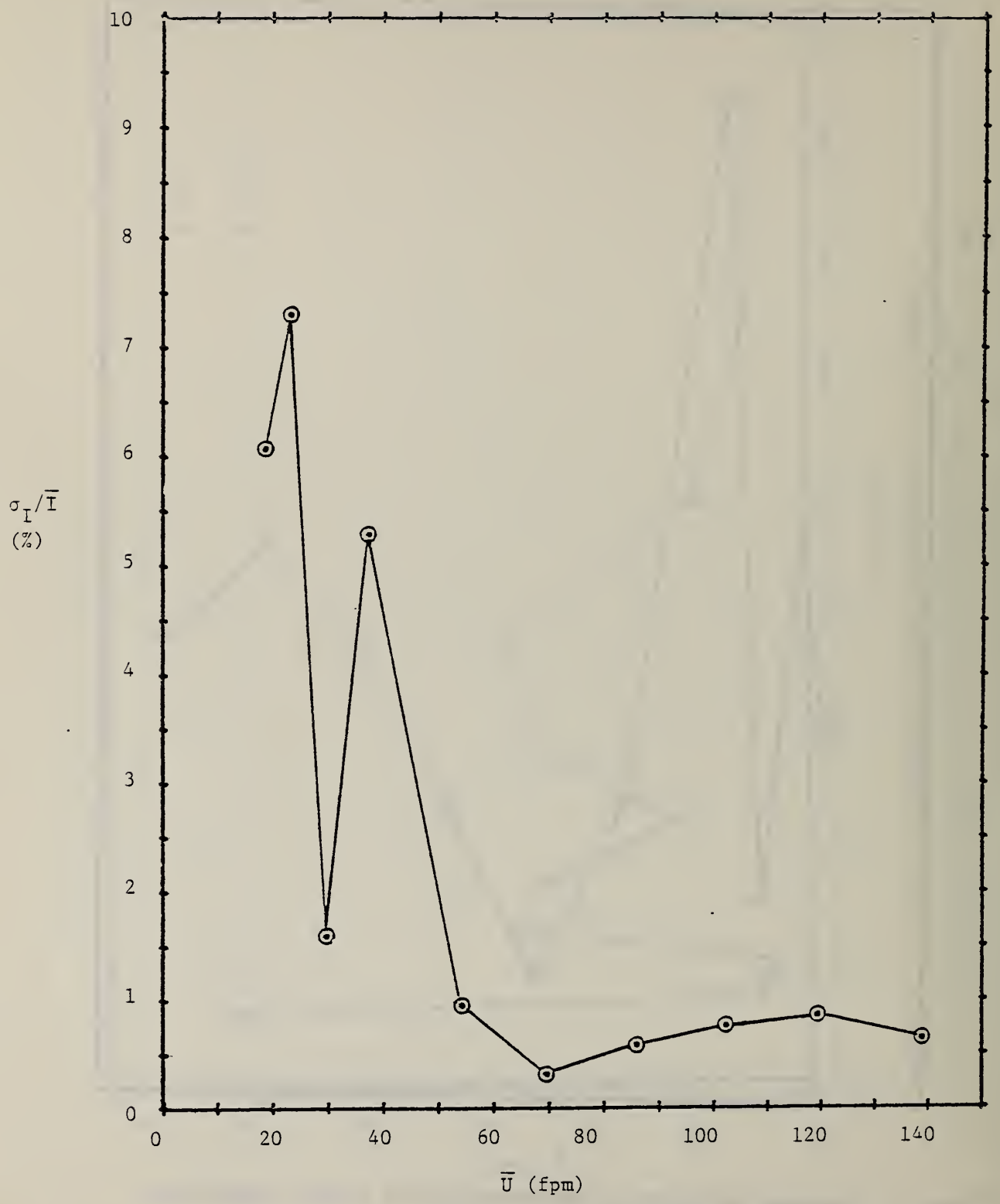

FIGURE 98. STANDARD DEVIATION OF INSTRUMENT OUTPUT AS PERCENT OF INSTRUMENT OUTPUT. INSTRUMENT J.

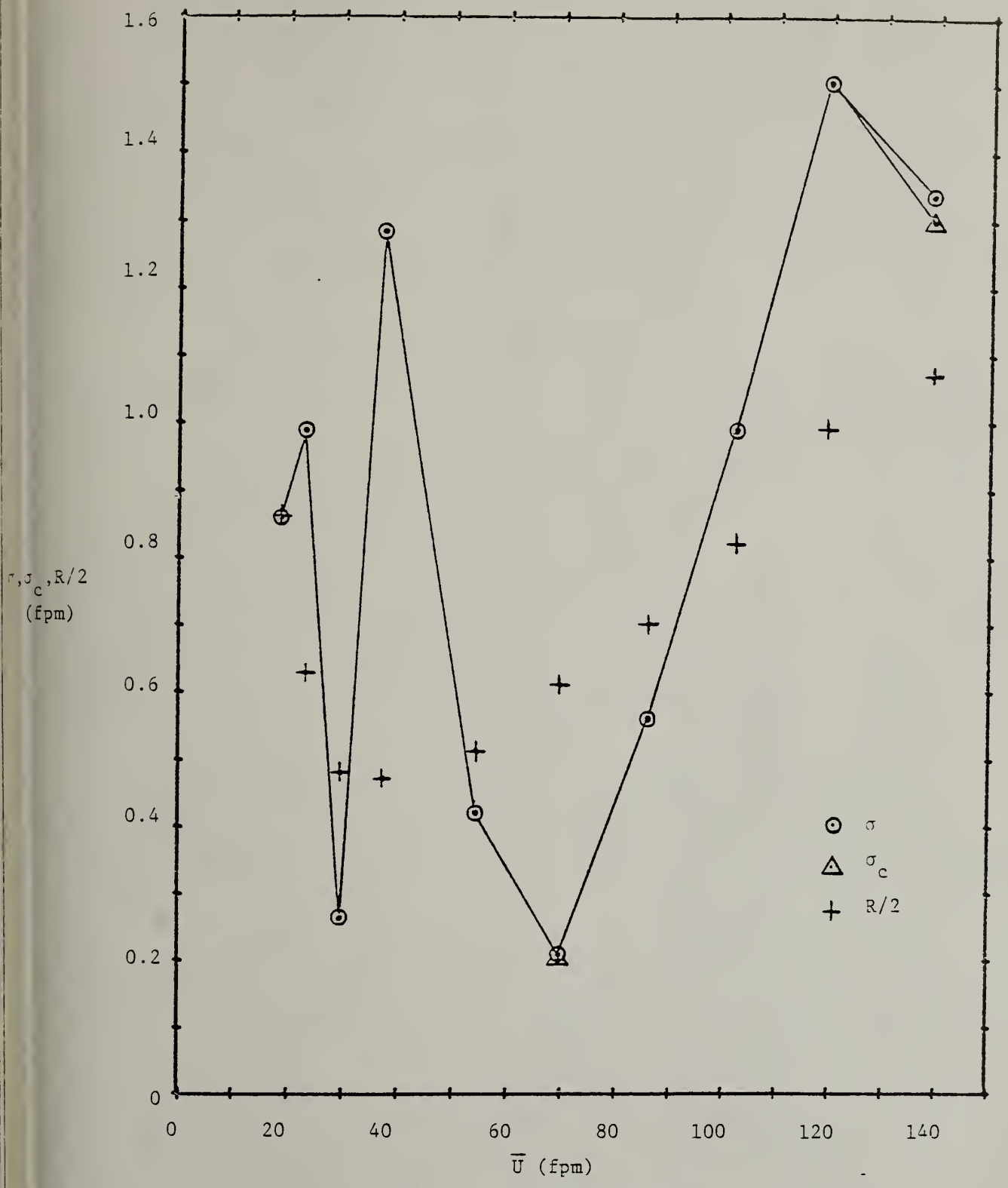

FIGURE 99. STANDARD DEVIATION AND CORRECTED STANDARD DEVIATION IN TERMS OF VELOCITY. R/2 NOTED. INSTRUMENT J.

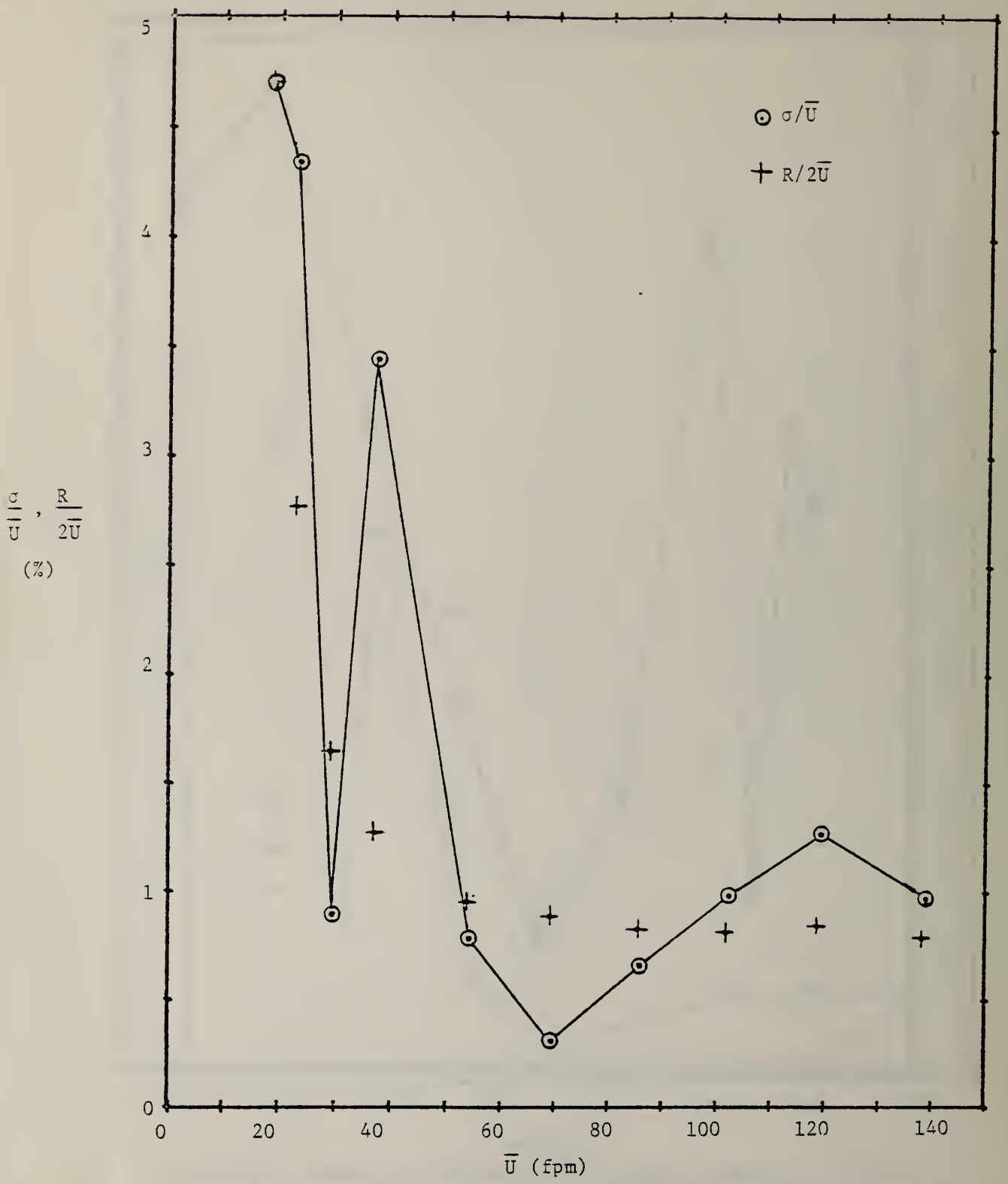

FIGURE 100. STANDARD DEVIATION IN TERMS OF VELOCITY AS PERCENT OF GROUP MEAN VELOCITY. $R/2\bar{U}$ NOTED. INSTRUMENT J.